2020-01-01

Development And Assesment Of Local Scaled Self-Interaction Corrected Density Functional Method With Simple Scaling Factor

Selim Romero
University of Texas at El Paso

DEVELOPMENT AND ASSESMENT OF LOCAL SCALED SELF-INTERACTION CORRECTED DENSITY FUNCTIONAL METHOD WITH SIMPLE SCALING FACTOR

SELIM SABAG ROMERO GONZALEZ

Master's Program in Computational Science

APPROVED:

Rajendra R. Zope, Ph.D., Chair

Tunna Baruah, Ph.D.

Ramon Ravelo, Ph.D.

Mahesh Narayan, Ph.D.

Stephen L. Crites, Jr., Ph.D.
Dean of the Graduate School

DEDICATION

I dedicate this thesis to my uncle Omar Gonzalez (2002) who helped me to follow my path in physics and mathematics. I also dedicate this writing to my sensei Hugo Tello (2019) who taught me strength in discipline and constant work, and to my family and close friends.

DEVELOPMENT AND ASSESMENT OF LOCAL SCALED SELF-INTERACTION CORRECTED DENSITY FUNCTIONAL METHOD WITH SIMPLE SCALING FACTOR

by

SELIM SABAG ROMERO GONZALEZ

THESIS

Presented to the Faculty of the Graduate School of

The University of Texas at El Paso

in Partial Fulfillment

of the Requirements

for the Degree of

MASTER OF SCIENCE

Computational Science Program

THE UNIVERSITY OF TEXAS AT EL PASO

August 2020

ACKNOWLEDGEMENTS

I am pleased to acknowledge my advisor Dr. Rajendra Zope for his faith in me and his constant reminder of keep obtaining knowledge, Dr. Tunna Baruah as my co-advisor for her patience and sharing her knowledge, Dr. Yoh Yamamoto who helped me in coding and from whom I learned about self-interaction correction, Dr. Luis Basurto for introducing me into electronic structure lab and helping me learn about C/C++, Dr. Jorge Vargas for helping me understand density functional theory, Carlos Diaz for his help in the last steps of this writing and finally to my lab mates for their help when I needed them. This work was supported by the US Department of Energy, Office of Science, Office of Basic Energy Sciences, as part of the Computational Chemical Sciences Program under Award No. DE-SC0018331. Support for computational time at the Texas Advanced Computing Center through NSF Grant No. TG-DMR090071 and at NERSC is gratefully acknowledged. I also sincerely acknowledge Gobierno de Mexico, CONACyT.

ABSTRACT

The Hohenberg-Kohn-Sham (HKS) density functional theory (DFT) is widely used to compute electronic structures of atoms, molecules, and solids. It is an exact theory in which ground state electron density plays the role of basic variable, same as the wavefunction does in quantum mechanics. The total ground state energy is a functional of electron density. The practical application of HKS DFT require approximation to the exchange-correlation energy functional. Many density functional approximations (DFAs) with various degree of sophistication and complexities have been developed. Depending on the complexity, these functionals include electron density, density gradients, density Laplacian, kinetic energy densities, Hartree-Fock exchange etc. Some examples of widely used non-empirical functionals are local density approximation (LDA), Perdew-Burke-Ernzerhof (PBE) generalized-gradient approximation (GGA), and strongly constrained and appropriately normalized (SCAN) meta-GGA.

Practically all DFAs suffer from a systematic error known as self-interaction error (SIE) where an electron incorrectly interacts with itself. These DFAs can fail dramatically for cases such as systems with a stretched bond where SIE is pronounced. The SIE arises from an improper cancellation of the self-Coulomb energy with the approximated self-exchange-correlation energy for the one-electron limit. Perdew and Zunger self-interaction correction (PZSIC) provides the exact cancellation for one- and two-electron self-interaction, but it does not necessarily eliminate many-electron self-interaction. The present work uses Fermi-Lowdin orbitals (FLOS) which are Fermi orbitals orthogonalized via Löwdin scheme. FLOs are localized orbitals through Fermi orbital descriptors (FODs) which are special positions to capture the electronic density of a system. The PZSIC implementation using FLOs, called FLOSIC, results in size-extensive implementation of the PZSIC. The PZSIC calculations provide more accurate results for stretched bond and anionic states but worsen properties where DFA performs well, this is known as the PZSIC paradox.

The present thesis deals with development and assessments of methods to overcome the paradoxical behavior of PZSIC. We compare PZSIC against the new local scaling SIC (LSIC) with two different approaches. The first approach uses ratio of kinetic energy densities referred to as LSIC(z) hereafter. It showed impressive results by keeping the correct behavior PZSIC and

improving it where PZSIC fails. LSIC(w), the second method that uses orbital and total densities as scaling factor is proposed in this work. We compare the methods against orbital scaling SIC (OSIC). The comparison is done with an extensive test of different properties such as total energies, ionization potentials and electron affinities for atoms, atomization energies, dissociation and reaction energies, and reaction barrier heights of molecules. We also show that unlike LSIZ(z) the simple scaling factor in LSIC(w) can describe binding of hydrogen bonded water well. This work also presents an extensive study of OSIC applied to SCAN functional for different forms of scaling factors to identify one-electron regions, OSIC-SCAN provides better results than the previously reported OSIC-LSDA, -PBE and -TPSS results. Furthermore, we propose a new method of selective scaling of OSIC to remove the major shortcoming of OSIC that destroys the $-1/r$ asymptotic behavior of the potential shape. The SOSIC gives the HOMO eigenvalues practically identical to PZSIC, unlikely to OSIC. Overall, the thesis presents new methods for self-interaction free density functional calculations.

TABLE OF CONTENTS

LIST OF TABLES

LIST OF FIGURES

CHAPTER 1: DENSITY FUNCTIONAL THEORY

This chapter aims to provide the background theory. Starting with the Schrödinger equation, followed by brief discussion of methods that simplify the many-body problem, we introduce density functional theory. A brief discussion of exchange-correlation functionals is also given.

1.1 SCHRÖDINGER EQUATION

The Schrödinger equation plays fundamental role in quantum mechanics like the Newton equations do in classical mechanics. Newton equations or classical mechanics describe the position, velocity, momentum, kinetic energy, potential energy, total energy, and force of a specific system, to achieve it, we must solve a differential equation given by Newton's second law.
To obtain properties of a quantum system one needs to solve the Schrodinger equation, solution of which provides a wavefunction (WF) of a particle. The wavefunction is used to calculate properties such as total energy, kinetic energy and another set of properties [131]. The Schrödinger equation for one particle is:

$$i\,\hbar\frac{\partial\Psi(\vec{r},t)}{\partial t} = -\frac{\hbar^2}{2m}\nabla^2\,\Psi(\vec{r}) + V(\vec{r})\,\Psi(\vec{r},t) \tag{1.1.1}$$

here $\hbar$ is the Planck's constant, m is the particle mass, $V(\vec{r})$ is the potential and Ψ is the time-dependent wavefunction of a particle (e.g. electron). When the potential does not depend explicitly on time, one can write the solution as $\Psi(\vec{r},t) = \phi(\vec{r})\psi(t)$. Dividing both sides of above equation by Ψ, we get the following equation:

$$i\,\hbar\frac{1}{\psi(t)}\frac{\partial\psi(t)}{\partial t} = -\frac{\hbar^2}{2m}\nabla^2\phi(\vec{r})\frac{1}{\phi(\vec{r})} + V(\vec{r}) = E \tag{1.1.2}$$

Eq. (1.1.2) is an eigenvalue problem, where E is a constant number and it represents the equilibrium energy of a system:

$$-\frac{\hbar^2}{2m}\,\nabla^2\phi(\vec{r})\; + V(\vec{r})\,\phi(\vec{r})\; =\; E\phi(\vec{r}) \tag{1.1.3}$$

the Hamiltonian operator is known as:

$$\widehat{H} =\; -\frac{\hbar^2}{2m}\,\nabla^2 + V(\vec{r}) \tag{1.1.4}$$

the components of Eq (1.1.4) are the kinetic energy operator ($\widehat{T}$) and potential (V), and $\widehat{H}$ provides the total energy of the system, in this case, of the wavefunction. The next set of equations are the definitions of the operators and the operational form of the Hamiltonian.

$$\hat{p} = -i\hbar\nabla \tag{1.1.5}$$

$$\widehat{T} =\; \frac{\hat{p}^2}{2m} =\; -\frac{\hbar^2}{2m}\,\nabla^2 \tag{1.1.6}$$

$$V(\vec{r}) = \frac{q_1 q_2}{4\pi\epsilon_0}\frac{1}{\left|\vec{r} - \overrightarrow{r'}\right|} \tag{1.1.7}$$

$$\widehat{H}\phi(\vec{r}) = E\phi(\vec{r}) \tag{1.1.8}$$

$\hat{p}$ is the momentum operator, V is defined as the Coulomb potential, where $|\vec{r} - \vec{r}'|$ is the distance between two charged particles (e.g. electron charge or proton charge) with charges q_1 and q_2.The interpretation of quantum mechanics is probabilistic. A normalized wavefunction can be obtained by

$$\int_{-\infty}^{\infty}\; (\,\phi'(\vec{r})\,)^*\,\phi(\vec{r})\,d\vec{r}\; = 1 \tag{1.1.9}$$

here ϕ^* is the complex conjugate of the wavefunction. This integration is related to the number of electrons, also the inner terms of the integral are related to the electronic density, whose definition is:

$$\rho(\vec{r}) = \left(\phi'(\vec{r})\right)^* \phi(\vec{r}) = |\phi(\vec{r})|^2 \tag{1.1.10}$$

in quantum mechanics, the physical properties are obtained by taking the expectation value of the corresponding Hermitian operator $\hat{O}$. The total energy of a quantum system is obtained by taking expectation value of the Hamiltonian operator.

$$\int_{-\infty}^{\infty} \left(\phi'(\vec{r})\right)^* \hat{H}\, \phi(\vec{r}) d\vec{r} = E \tag{1.1.11}$$

Eq. (1.1.11) can be written compactly using Dirac notation:

$$\langle \phi' |\, \hat{H}\, | \phi \rangle \;=\; E \tag{1.1.12}$$

this notation has the introduction to bra $\langle \phi |$ as complex conjugate ϕ and ket $|\phi\rangle$ as just ϕ, this set forms the bracket notation.

1.1.1 MANY-BODY SCHRÖDINGER EQUATION

The description of a quantum system depends on the number of nuclei and electrons [130]. An example of the simplest real system is the hydrogen atom that has one electron and one proton, using the Eq. (1.1.4), leads to the next equation:

$$\hat{H} = -\frac{\hbar^2}{2m_n} \nabla_n^2 - \frac{\hbar^2}{2m_e} \nabla_e^2 - \frac{e^2}{4\pi\epsilon_0} \frac{1}{|\vec{r_n} - \vec{r_e}|} \tag{1.1.13}$$

the last term of the Eq. (1.1.13) is the attractive potential between proton-electron ($V_{ep}(\vec{r}) = -\frac{e^2}{4\pi\epsilon_0}\frac{1}{|\vec{r_p}-\vec{r_e}|}$). In a similar fashion for a system containing M nuclei with mass M_I at position $\vec{R}_I$, and N electrons with mass m_e , the Hamiltonian can be expressed as:

$$\hat{T} = -\sum_I^N \frac{\hbar^2}{2M_I}\nabla_I{}^2 - \sum_i^N \frac{\hbar^2}{2m_e}\nabla_i{}^2 \tag{1.1.14}$$

$$V(\vec{r}) = V_{ee} + V_{nn} + V_{en} \tag{1.1.15}$$

here V_{ee} is the Coulomb interaction between electrons, $V_{en}$is the Coulomb interaction between electron and nuclei, and V_{nn} is the Coulomb interaction between nuclei. Their definitions are:

$$V_{ee} = \frac{1}{2}\sum_{i\neq j}^N \frac{e^2}{4\pi\epsilon_0}\frac{1}{|\vec{r_i}-\vec{r_j}|} \tag{1.1.16}$$

$$V_{nn} = \frac{1}{2}\sum_{I\neq J}^M \frac{e^2}{4\pi\epsilon_0}\frac{Z_I Z_J}{|\vec{R_I}-\vec{R_J}|} \tag{1.1.17}$$

$$V_{en} = -\sum_{i,I}^{N,M} \frac{e^2}{4\pi\epsilon_0}\frac{Z_I}{|\vec{r_i}-\vec{R_I}|} \tag{1.1.18}$$

V_{ee} and V_{nn} are repulsive potentials, and V_{en} is an attractive potential. Putting all the pieces together in the Hamiltonian, we can rewrite the Eq. (1.1.13) as:

$$\left[-\sum_I^M \frac{\hbar^2}{2M_I}\nabla_I{}^2 - \sum_i^N \frac{\hbar^2}{2m_e}\nabla_i{}^2 + \frac{1}{2}\sum_{i\neq j}^N \frac{e^2}{4\pi\epsilon_0}\frac{1}{|\vec{r_i}-\vec{r_j}|} + \frac{1}{2}\sum_{I\neq J}^M \frac{e^2}{4\pi\epsilon_0}\frac{Z_I Z_J}{|\vec{R_I}-\vec{R_J}|} + \sum_{i,I}^{N,M} \frac{e^2}{4\pi\epsilon_0}\frac{Z_I}{|\vec{r_i}-\vec{R_I}|}\right]\Psi = E_{total}\,\Psi \tag{1.1.19}$$

Eq. (1.1.19) is the Schrödinger equation for the i-th electron and I-th nuclei with Z_I protons, this provides the total energy of the system. The wavefunction depends on the position of each electron and nuclei, it is as follows:

$$\Psi = \Psi(\vec{r}_1, \dots, \vec{r}_N, \vec{R}_1, \dots, \vec{R}_M) \tag{1.1.20}$$

the probability of a finding an electron at $\vec{r}_1$ is given by

$$P(\vec{r}_1 = \vec{r}) = \int \Psi^*(\vec{r}, \vec{r}_2 \dots, \vec{r}_N, \vec{R}_1, \dots, \vec{R}_M)\Psi(\vec{r}, \vec{r}_2 \dots, \vec{r}_N, \vec{R}_1, \dots, \vec{R}_M)d\vec{r} \quad (1.1.21)$$

it is useful to remember that in QM the electrons are indistinguishable particles, so Eq. (1.1.21) is N times the same probability distribution, or simply speaking, N electrons by the integral, leading to the following description for the electronic density:

$$\rho(\vec{r}) = \sum_{i=1}^{N} P(\vec{r}_i = \vec{r}) = N\, P(\vec{r}) \quad (1.1.22)$$

$$\rho(\vec{r}) = N \int \Psi^*(\vec{r}, \vec{r}_2 \dots, \vec{r}_N, \vec{R}_1, \dots, \vec{R}_M)\Psi(\vec{r}, \vec{r}_2 \dots, \vec{r}_N, \vec{R}_1, \dots, \vec{R}_M)d\vec{r} \quad (1.1.23)$$

the integral of the total electronic density is the number of electrons in the system.

$$\int \rho(\vec{r})d\vec{r} = N \quad (1.1.24)$$

1.1.3 ATOMIC UNITS

The Schrödinger equation contains fundamental constants [130] like electron mass m_e, proton mass m_p, electron charge e, reduced Plank's constant $\hbar$ and the permittivity of vacuum ϵ_0. The official values retrieved from (https://physics.nist.gov/cuu/Constants/index.html) are:

$$\hbar = 1.05457163 * 10^{-34} J$$
$$m_e = 9.10938291 * 10^{-31} kg$$
$$m_p = 1.67262164 * 10^{-27} kg$$
$$e = 1.60217649 * 10^{-19} C$$
$$\epsilon_0 = 8.85418782 * 10^{-12} F/m$$

the hydrogen at its ground state has an average orbital radius of $a_0 \cong 0.529\ \dot{A}$ for the electron, if we use this value in the Coulomb formula (Eq. (1.1.18)), it gives the average Coulomb energy for a proton-electron pair.

$$E_{ep} = -\frac{e^2}{4\pi\epsilon_0 d_{ep}} = -\frac{e^2}{4\pi\epsilon_0 a_0} = 27.2114\ eV \tag{1.1.25}$$

the previous value is known as the Hartree energy (E_{Ha}), which is the typical unit of energy. In atomic units, $a_0 = 1, m_e = 1, E_{Ha} = 1$ and $e = 1$ numerically. Thus, the many-body Schrödinger equation in atomic units can be expressed as

$$\left[-\sum_{I}^{M}\frac{1}{2M_I}\nabla_I^2 - \sum_{i}^{N}\frac{1}{2}\nabla_i^2 + \frac{1}{2}\sum_{i\neq j}^{N}\frac{1}{|\vec{r_i}-\vec{r_j}|} + \frac{1}{2}\sum_{I\neq J}^{M}\frac{Z_I Z_J}{|\vec{R_I}-\vec{R_J}|} + \sum_{i,I}^{N,M}\frac{Z_I}{|\vec{r_i}-\vec{R_I}|}\right]\Psi = E_{total}\Psi \tag{1.1.31}$$

here E_{total} is measured in Hartree energy units, and M_I in atomic mass units.

1.1.4 BORN-OPPENHEIMER APPROXIMATION

The Born-Oppenheimer approximation allows separation of nuclear and electronic degrees of freedom based on the observation that the nuclei being much heavier than electrons move much slower compared to the electrons. Consequently, the wavefunction of a system can be separated into nuclear and electron wavefunctions [115]. Within this consideration in Eq (1.1.31) for the kinetic energy contribution, the nuclei do not add much change compared to the electron contribution, therefore, we can take out the nuclei contribution of kinetic energy. The potential given by the nuclei-nuclei interaction is also frozen and it can be taken as constant. Any constant value added to the Hamiltonian operator will not affect the eigenvalues of the eigenfunctions or

wavefunctions, and the remaining pieces of the Hamiltonian take the name of electronic Hamiltonian or the Hamiltonian description of N electrons in a field presence of M point charges.

$$\widehat{H}_{elec} = -\sum_i^N \frac{1}{2}\nabla_i^{\,2} + \frac{1}{2}\sum_{i\neq j}^N \frac{1}{|\vec{r_i}-\vec{r_j}|} + \sum_{i,I}^{N,M} \frac{Z_I}{|\vec{r_i}-\vec{R_I}|} \tag{1.1.32}$$

the application of this Hamiltonian is:

$$\widehat{H}_{elec}|\phi_{elec}\rangle = E_{\text{elec}}\,|\phi_{elec}\rangle \tag{1.1.33}$$

then, the electronic wavefunction has the next description:

$$\phi_{elec} = \phi_{elec}(\{\vec{r}_i\},\{\vec{R}_I\}) \tag{1.1.34}$$

ϕ_{elec} depends explicitly on the position of the electrons and parametrically on nuclei coordinates, Eq. (1.1.34) also describes the motion of the electrons. When we get the energy of an electronic system through this approach, it still has a parametric dependence on the nuclei coordinates, this theory is known as clamped nuclei approximation.

$$\widehat{H}_{elec}\,\left|\phi_{elec}(\{\vec{r}_i\},\{\vec{R}_I\})\right\rangle = \mathrm{E}_{\text{elec}}(\{\vec{R}_I\})\,\left|\phi_{elec}(\{\vec{r}_i\},\{\vec{R}_I\})\right\rangle \tag{1.1.35}$$

to get the total energy of the system, one needs to add the constant nuclear repulsion.

$$E_{tot}(\{\vec{R}_I\}) = E_{elec} + + \frac{1}{2}\sum_{I\neq J}^M \frac{Z_I Z_J}{|\vec{R_I}-\vec{R_J}|} \tag{1.1.36}$$

if we apply Eq. (1.1.32) to the electronic wavefunction, and measure the energy through Eq. (1.1.11), which is the expectation value, we can approximate the total nuclei Hamiltonian with the next expression:

$$\widehat{H}_{nuc} = -\sum_I^M \frac{1}{2M_I} \nabla_I^2 + E_{tot}(\{R_I\}) \tag{1.1.37}$$

the Eq. (1.1.36) provides a potential (surface) description for the nuclear dynamics. To get the energy of the nuclear Schrödinger equation, one has to the solve the following equation.

$$\widehat{H}_{nuc}|\phi_{nuc}\rangle = E|\phi_{nuc}\rangle \tag{1.1.38}$$

here $\phi_{nuc} \equiv \phi_{nuc}(\{\vec{R}_I\})$. The nuclear Hamiltonian describes the vibration, rotation, and translation of a molecule, and this is the Born-Oppenheimer approximation for the total energy of the molecule. The approximation for the total wavefunction (molecular orbital) of this method is:

$$\phi(\{\vec{r}_i\},\{\vec{R}_I\}) = \phi_{elec}(\{\vec{r}_i\},\{\vec{R}_I\})\,\phi_{nuc}(\{\vec{R}_I\}) \tag{1.1.39}$$

we will focus on just the electronic problem and drop the "elec" suffix of every equation, so the energy is going to be the electronic energy unless otherwise indicated.

1.1.5 ANTISYMMETRY PRINCIPLE

The description of the electron wavefunction is not yet complete given that ϕ only depends on the positions of electrons and nuclei, this means that we have a lack of description of the spin in our wavefunction. To include such description, we need to introduce two spin functions [115] in the context of nonrelativistic theory, these are $\alpha(\omega)$ for spin up and $\beta(\omega)$ for spin down. The variable ω can be α or β, and must meet the following conditions of orthogonality for a complete set.

$$\langle\alpha|\alpha\rangle = \langle\beta|\beta\rangle = 1 \tag{1.1.40}$$

$$\langle\alpha|\beta\rangle = \langle\beta|\alpha\rangle = 0 \tag{1.1.41}$$

within this formalism, one electron is described by position coordinates $\vec{r}$ and one spin coordinate ω, leading to a four (x, y, z, ω) coordinate description:

$$\vec{x} = \{\vec{r}, \omega\} \tag{1.1.42}$$

therefore, the wavefunction for the i-th electron is $\phi(\{\vec{x}_i\}, \{\vec{R}_I\})$, even though we don't have an explicit dependence in the Hamiltonian for this spin variable, it is not worthless to include an extra requirement for the wavefunction such as the antisymmetric interchange of electrons or coordinate exchange as follows:

$$\phi(\vec{x}_1, \vec{x}_2, \dots, \vec{x}_N) = -\phi(\vec{x}_2, \vec{x}_1, \dots, \vec{x}_N) \tag{1.1.43}$$

this requirement is known as the antisymmetry principle, which is a simple and general statement of the Pauli exclusion principle. Thus, our wavefunction has not only to satisfy the Schrödinger equation, but also the antisymmetry principle, which is an independent postulate of the quantum mechanics theory. In following sections will be used this principle.

1.2 HARTREE-FOCK THEORY

This chapter has the goal of presenting the electronic orbitals and molecular orbitals within Hartree products to construct the Slater determinant, which is a type of orbital that obeys the antisymmetry principle. Following this, basic definitions of Hartree-Fock equations will be presented. Finally present the self-consistency field approximation of Hartree-Fock, which gives the approximation of the Hartree-Fock method [115,116].

1.2.1 TYPES OF ORBITALS

This section introduces notations for further usage in the Hartree-Fock theory [116]. In the following, we will define what a Slater determinant is, and use many-electron wavefunctions that are either single Slater determinant or a linear combination of Slater determinants. To achieve this, we need to consider the nature of an orbital wavefunction and the single electron wavefunction. For a molecule, a wavefunctions will be molecular orbital (MO) for an electronic structure. A spatial orbital $\psi_i(\vec{r})$ is just a function of spatial coordinates, and it describes the electron distribution in space, in a molecule, these orbitals are taken as an orthonormal set:

$$\int \psi_i^*(\vec{r})\psi_j(\vec{r})d\vec{r} = \delta_{ij} \tag{1.2.1}$$

if the spatial orbitals form a complete set, we must be able to describe any arbitrary function $f(\vec{r})$ in terms of this complete set, therefore, it can be described as follows:

$$f(\vec{r}) = \sum_{i=1}^{\infty} a_i\psi_i(\vec{r}) \tag{1.2.2}$$

where a_i are constant coefficients. This kind of expansion is only possible if the set is complete, and that completeness is only reached when the set is infinite. In practice we have finite sets, this means that it only spans a certain region of the complete space, thus, the results can be approximated to the exact description through a spanned subspace.

Once again, there is a lack of spin description, so we will define a wavefunction that not only depends on the position $\vec{r}$, but also its spin, that is an electron wavefunction containing both spatial and spin parts as $\chi(\vec{x})$. One can build an electron wavefunction according to the spin-state functions $\alpha(\omega)$ (up) and $\beta(\omega)$ (down), and the spatial electron distribution $\psi(\vec{r})$. A simple and useful description for one-electron wavefunction including position and spin is:

$$\chi(\vec{x}) = \begin{cases} \alpha(\omega)\psi(\vec{r}) \\ \beta(\omega)\psi(\vec{r}) \end{cases} \tag{1.2.3}$$

two different orbitals obey the orthonormality principle when the spatial orbitals are orthonormal.

$$\int \chi_i^*(\vec{x})\chi_j^*(\vec{x})d\vec{x} = \delta_{ij} \tag{1.2.4}$$

1.2.2 INDEPENDENT ELECTRON APPROXIMATION AND HARTREE PRODUCTS

Once we observed the electron-orbital wavefunction $\chi(\vec{x})$, which is the chosen description for this subchapter, we continue with the consideration of N electrons. But before we get a definition of a wavefunction that describes an interacting system for the electrons, let us consider a simpler system of noninteracting electrons [115]. For such a system, the electron-electron contribution of the Hamiltonian will not be considered ($\hat{V}_{ee} = 0$), therefore we define the one-electron Hamiltonian as:

$$\hat{h}(\vec{x}_i) = -\frac{1}{2}\nabla_i^2 - \sum_A^M \frac{Z_A}{r_{iA}} \tag{1.2.5}$$

the r_{iA} is $\left|\vec{r}_i - \vec{R}_A\right|$, $\vec{x}_i$ are the electron coordinates $(x_i, y_i, z_i, \omega_i)$, the Laplacian applied to the i-th electron and h_i is the Hamiltonian for a noninteracting electron. Then the whole Hamiltonian for a set of noninteracting electrons will be:

$$\hat{H} = \sum_i^N \hat{h}\,(\vec{x}_i) \tag{1.2.6}$$

Eq. (1.2.6) is a dramatic simplification, but it allows us to handle the equations separately and solve electron by electron with h_i operator. The operator is applied to a set of eigenfunctions χ_j and provides the eigenvalues corresponding to the energy of each orbital (ε_j).

$$\hat{h}(\vec{x}_i)\chi_j(\vec{x}_i) = \varepsilon_j\chi_j(\vec{x}_i) \tag{1.2.7}$$

Our interest resides in the wavefunction of the whole Hamiltonian, which a collection of all the one-electron Hamiltonians. A one-electron Hamiltonian is independent of any other orbital. We can invoke a wavefunction that is a product of all the orbitals χ, we get:

$$\Psi^{HP}(\vec{x}_1, \vec{x}_2, \dots, \vec{x}_N) = \chi_i(\vec{x}_1)\chi_j(\vec{x}_2)\cdots\chi_k(\vec{x}_N) \tag{1.2.8}$$

this wavefunction placed in $\hat{H}$ will provide:

$$\sum_i^N h_i \Psi^{HP}(\vec{x}_1, .., \vec{x}_i, \dots, \vec{x}_N) = (\varepsilon_i + \varepsilon_j + \cdots + \varepsilon_k)\Psi^{HP}(\vec{x}_1, .., \vec{x}_i, \dots, \vec{x}_N) \tag{1.2.9}$$

Eq. (1.2.9) is an eigenvalue equation, whose eigenvalue is the summation of all the wavefunction energies in the form ($E = \varepsilon_i + \varepsilon_j + \cdots + \varepsilon_k$).

$$\hat{H}\Psi^{HP} = E\Psi^{HP} \tag{1.2.10}$$

a many-electron wavefunction with this behavior is called Hartree product, where the description of electron i-th is given by χ_i, electron two is described by χ_j and consequently. The product of wavefunctions has the meaning of the intersection of probabilities, which is the product of independent events. On the other hand, the electrons interact with each other and they will repel, so the motion of the electrons will be explicitly correlated. This model has a deficiency of distinguishing electrons, but it is needed to have an indistinguishable system of electrons to describe the antisymmetry principle.

1.2.3 SLATER DETERMINANTS

The Hartree product does not satisfy the antisymmetry principle. But it is possible to get a wavefunction that describes the antisymmetry principle and the indistinguishability of electrons. This can be done by a suitable linear combination of two Hartree products [115]. The distinguishability of a Hartree product comes out from describing two different electrons:

$$\Psi_{12}^{HP}(\vec{x}_1,\vec{x}_2) = \chi_i(\vec{x}_1)\chi_j(\vec{x}_2)$$
$$\Psi_{21}^{HP}(\vec{x}_1,\vec{x}_2) = \chi_i(\vec{x}_2)\chi_j(\vec{x}_1) \tag{1.2.11}$$

these wavefunctions show that electrons $\vec{x}_1$ and $\vec{x}_2$ swap in different orbitals and make a distinction between those two electrons. The convenient wavefunction is as follows:

$$\Psi(\vec{x}_1,\vec{x}_2) = \frac{1}{\sqrt{2}}\Big(\chi_i(\vec{x}_1)\chi_j(\vec{x}_2) - \chi_j(\vec{x}_1)\chi_i(\vec{x}_2)\Big) \tag{1.2.12}$$

where $1/\sqrt{2}$ is a normalization factor, if we look at the interchange of electrons $\vec{x}_1$ and $\vec{x}_2$, the antisymmetry principle is included ($\Psi(\vec{x}_2,\vec{x}_1) = -\Psi(\vec{x}_1,\vec{x}_2)$) and describes the Pauli exclusion principle, which says that two electrons cannot be in the same occupied orbital. The Eq. (1.2.12) can be written as a determinant:

$$\Psi(\vec{x}_1,\vec{x}_2) = \frac{1}{\sqrt{2}}\begin{vmatrix}\chi_i(\vec{x}_1) & \chi_j(\vec{x}_1)\\ \chi_i(\vec{x}_2) & \chi_j(\vec{x}_2)\end{vmatrix} \tag{1.2.13}$$

the Eq. (1.2.13) is the famous Slater determinant, and its general form for N electrons is:

$$\Psi(\vec{x}_1,\vec{x}_2,\dots,\vec{x}_N) = \frac{1}{\sqrt{N!}}\begin{vmatrix}\chi_i(\vec{x}_1) & \chi_j(\vec{x}_1) & \cdots & \chi_k(\vec{x}_1)\\ \chi_i(\vec{x}_2) & \chi_j(\vec{x}_2) & \cdots & \chi_k(\vec{x}_2)\\ \vdots & \vdots & \ddots & \vdots\\ \chi_i(\vec{x}_N) & \chi_j(\vec{x}_N) & \cdots & \chi_k(\vec{x}_N)\end{vmatrix} \tag{1.2.14}$$

again $\frac{1}{\sqrt{N!}}$ is the normalization factor, the electrons are the rows with $\vec{x}_i$ positions and the columns are the orbitals from χ_i to χ_k. This clever idea carries the concept of swapping electrons or orbitals, to create a change of sign. The change of sign is made by determinant properties to fit the antisymmetry principle. A sort hand notation for the Slater determinant is:

$$\Psi(\vec{x}_1,\vec{x}_2,\dots,\vec{x}_N) = \big|\chi_i(\vec{x}_1)\chi_j(\vec{x}_2)\cdots\chi_k(\vec{x}_N)\big\rangle \tag{1.2.15}$$

if we have the same order of electrons as $\vec{x}_1, \vec{x}_2, \ldots, \vec{x}_N$, the Eq. (1.2.15) can be further reduced to the next expression:

$$\Psi(\vec{x}_1, \vec{x}_2, \ldots, \vec{x}_N) = |\chi_i \chi_j \cdots \chi_k\rangle = |i\, j \ldots\, k\rangle \tag{1.2.16}$$

realize that χ_i becomes i to avoid long notation. We will discuss this wavefunction and some usage in the preceding sections.

1.2.4 NOTATION FOR HARTREE-FOCK THEORY

Before continuing with the Hartree-Fock approximation, we need to introduce the necessary notation [116]. In section 1.2.2 we defined the Hamiltonian for one electron, now it is necessary to specify the rest of the pieces for the Hamiltonian. The one-electron Hamiltonian contains the kinetic energy of the electron and the Coulomb attraction with nuclei, but to completely describe the electronic Hamiltonian, we need to add the nuclei-nuclei interaction ($\hat{V}_{nn}$) which is parametric (or functional) and the electron-electron Coulomb interaction ($\hat{V}_{ee}$). The Coulomb repulsion of two electrons will be simplified as:

$$V(\vec{r}_i, \vec{r}_j) = \frac{1}{|\vec{r}_i - \vec{r}_j|} = \frac{1}{r_{ij}} \tag{1.2.17}$$

r_{ij} is the distance between the electron positions and will be for simplicity $V_{ij} = 1/r_{ij}$. The Hamiltonian for this notation is as follows:

$$\hat{H}_e = \sum_{i=1}^{N} \hat{h}(\vec{x}_i) + \frac{1}{2}\sum_{i,j}^{N} V_{ij} + V_{nn} \tag{1.2.18}$$

applying $\langle\Psi|\widehat{H}_e|\Psi\rangle$, we get the total energy of the electronic system, also looking at the nature of V_{ij}, which only operates on pairs of electrons and it will generate many Kronecker deltas for the Hamiltonian, depending on the orbitals and their orthonormality.

$$\langle\Psi|\widehat{H}_e|\Psi\rangle = \sum_{i=1}^{N}\langle\Psi|\hat{h}(\vec{x}_i)|\Psi\rangle + \frac{1}{2}\sum_{i,j}^{N}\langle\Psi|\mathrm{V_{ij}}|\Psi\rangle + \langle\Psi|V_{nn}|\Psi\rangle \tag{1.2.19}$$

for each of these ingredients, it will generate a matrix element that corresponds to H_{IJ}, each of these elements contains multiplications of their corresponding I-th and J-th orbitals, which will invoke the orthonormality property of Eq.(1.2.4), and if any pair of orbitals are not the same index, it will vanish. This leads to the next equation:

$$E^{HF} = \sum_{i=1}^{N}\langle i|\hat{h}|i\rangle + \frac{1}{2}\sum_{i,j}^{N}\langle ij||ij\rangle \tag{1.2.20}$$

the Eq. (1.2.20) is the Hartree-Fock energy equation that uses the Slater determinant wavefunction. Since the nuclei-nuclei term is constant, it will be taken out for now. The first component of the Hartree-Fock energy is:

$$\langle i|\,\hat{h}\,|j\rangle = \int \chi_i^*(\vec{x}_1)\; h_i\,(\vec{x}_1)\chi_j(\vec{x}_1)d\vec{x}_1 \tag{1.2.21}$$

the Eq. (1.2.21) includes the kinetic energy of one electron and the nuclei-electron attraction, $h_i(\vec{x}_1)$ is integrated over $\vec{x}_1$ electron coordinates that sweep overall space, and since the electrons are indistinguishable, this $\vec{x}_1$ electron position will describe any other electron as well. Also, the integral carry the overlap of the orbitals χ_i^* and χ_j, which is the probability density of the electron $\vec{x}_1$ to be in the orbital i and j. The second integral is known as the double bar integral. Required notation and Its generic form are as follow:

$$\langle ij||kl\rangle = \langle ij|kl\rangle - \langle ij|lk\rangle \tag{1.2.22}$$

$$\langle ij|kl\rangle \equiv \int d\vec{x}_1 \int d\vec{x}_2 \ \chi_i^*(\vec{x}_1)\chi_j^*(\vec{x}_2) r_{12}^{-1} \chi_k(\vec{x}_1)\chi_l(\vec{x}_2) \tag{1.2.23}$$

the Eq. (1.2.22) and (1.2.23) are written in physics notation or Dirac notation. Note that $\langle ij|kl\rangle = \langle ij|V_{12}|kl\rangle$ to simplify representation, also that the electrons $\vec{x}_1$ and $\vec{x}_2$ are dummy indexes. This is possible given the indistinguishability of the electrons and that we will always integrate over a pair of electrons. For last, we show the representation of Eq. (1.2.23) in chemist notation [116] to further usage.

$$[ij|kl] \equiv \int d\vec{x}_1 \int d\vec{x}_2 \ \chi_i^*(\vec{x}_1)\chi_j(\vec{x}_1) \ r_{12}^{-1} \ \chi_k^*(\vec{x}_2)\chi_l(\vec{x}_2) \tag{1.2.24}$$

the Hartree-Fock energy expression in both notations are as follows:

$$E^{HF} = \sum_{i=1}^{N} \langle i|\hat{h}|i\rangle + \frac{1}{2}\sum_{i,j}^{N}(\langle ij|ij\rangle - \langle ij|ji\rangle) \tag{1.2.25}$$

$$E^{HF} = \sum_{i=1}^{N} [i|\hat{h}|i] + \frac{1}{2}\sum_{i,j}^{N}([ii|jj] - [ij|ji]) \tag{1.2.26}$$

from Eq. (1.2.26), we observe the Coulomb repulsion of two electrons in the terms $[ii|jj]$ and $[ij|ji]$, which is a quantum mechanical Coulomb description for a pair of electrons.

$$[ii|jj] = \int d\vec{x}_2 \int d\vec{x}_1 \ \chi_i^*(\vec{x}_1)\chi_i(\vec{x}_1) \ r_{12}^{-1} \chi_j^*(\vec{x}_2)\chi_j(\vec{x}_2) \tag{1.2.27}$$

$\chi_i^*(\vec{x}_1)\chi_i(\vec{x}_1)$ is the probability of finding the electron one in orbital i at position $\vec{x}_1$, likewise for electron two in orbital j at position $\vec{x}_2$, the peculiar term is $[ij|ji]$ represented as:

$$[ij|ji] = \int d\vec{x}_2 \int d\vec{x}_1 \ \chi_i^*(\vec{x}_1)\chi_j(\vec{x}_1) \ r_{12}^{-1} \chi_j^*(\vec{x}_2)\chi_i(\vec{x}_2) \tag{1.2.28}$$

it is hard to interpret, Eq. (1.2.28) does not have a straightforward explanation. Eq. (1.2.27) is the "interaction-energies" for a pair of electrons, and Eq. (1.2.28) is an interchange of orbital indexes

of Eq. (1.2.27). In literature, this term is called the exchange term. This term comes from the nature of a Slater determinant wavefunction that accomplishes the antisymmetry principle and the Pauli exclusion principle.

1.2.5 HARTREE-FOCK APPROXIMATION

This section has the Hartree-Fock approximation [115,116], which assumes that the wavefunction can be approximated by a single Slater determinant and this approximation is done with the variational principle (undetermined multipliers to enforce orthonormality of the orbitals), thus it will minimize the Hartree-Fock energy by tweaking the orbitals χ.

$$\mathcal{L}[\{\chi_i\}] = E^{HF}[\{\chi_i\}] - \sum_{i,j}^{N} \varepsilon_{ij}\left(\langle i|j\rangle - \delta_{ij}\right) \tag{1.2.29}$$

ε_{ij} is the Lagrange multiplier.

$$\delta\mathcal{L} = \delta E^{HF}[\{\chi_i\}] - \sum_{i,j}^{N} \varepsilon_{ij}\, \delta\langle i|j\rangle \tag{1.2.30}$$

where $\delta\langle i|j\rangle$ is the variation of the overlap between orbitals i and j.

$$\delta\langle i|j\rangle = \langle \delta\chi_i|\chi_j\rangle + \langle \chi_i|\delta\chi_j\rangle \tag{1.2.31}$$

if we do the variation of the Hartree-Fock energy, and recall that i and j indexes are just dummy indexes, it provides:

$$\delta\mathcal{L} = \sum_{i}^{N}\left[\langle\delta\chi_i|\hat{h}|\chi_i\rangle + \langle\chi_i|\hat{h}|\delta\chi_i\rangle\right] + \sum_{i,j}^{N}\left(\left[\delta\chi_i\chi_i|\chi_j\chi_j\right] + \left[\chi_i\delta\chi_i|\chi_j\chi_j\right]\right)$$
$$- \sum_{i,j}^{N}\left(\left[\delta\chi_i\chi_j|\chi_j\chi_i\right] + \left[\chi_i\delta\chi_j|\chi_j\chi_i\right]\right) - \sum_{i,j}^{N}\varepsilon_{ij}\left(\langle\delta\chi_i|\chi_j\rangle + \langle\chi_i|\delta\chi_j\rangle\right)$$

(1.2.32)

in shorthand, Eq. (1.2.32) can be described in terms of an expression and its complex conjugate, e.g., $\left(\langle\chi_i|\hat{h}|\delta\chi_i\rangle\right)^* = \langle\delta\chi_i|\hat{h}|\chi_i\rangle$, this is helpful given that the Hamiltonian is a Hermitian operator. The Hartree-Fock minimum energy is reached by $\delta\mathcal{L} = 0$.

$$\delta\mathcal{L} = \sum_{i}^{N}\left[< \delta\chi_i|\hat{h}|\chi_i >\right] + \sum_{i,j}^{N}\left(\left[\delta\chi_i\chi_i|\chi_j\chi_j\right]\right) - \sum_{i,j}^{N}\left(\left[\delta\chi_i\chi_j|\chi_j\chi_i\right]\right) - \sum_{i,j}^{N}\varepsilon_{ij}\left(< \delta\chi_i|\chi_j >\right)$$
$$+ complex\ conjugate = 0$$

(1.2.33)

with some algebraic manipulation of Eq. (1.2.33), we get the Hartree-Fock equation that defines the orbitals.

$$\hat{h}(\vec{x}_1)\chi_i(\vec{x}_1) + \sum_{i\neq j}^{N}\chi_i(\vec{x}_1)\left[\int d\vec{x}_2|\chi_j(\vec{x}_2)|^2 r_{12}^{-1}\right] - \sum_{i\neq j}^{N}\chi_j(\vec{x}_1)\left[\int d\vec{x}_2\chi_j^*(\vec{x}_2)\chi_i(\vec{x}_2)r_{12}^{-1}\right]$$
$$= \sum_{j}^{N}\varepsilon_{ij}\chi_j(\vec{x}_1)$$

(1.2.34)

the right side of the Eq. (1.2.34) can be diagonalized by a rotation, becoming $\varepsilon_i\chi_i(\vec{x}_1)$. This equation can minimize a set of guess orbitals. The equations are solved iteratively until self-consistency is obtained.

1.3 KOHN-SHAM THEORY

As in previous sections, the Kohn-Sham (KS) Theory [1] can provide description of many-body electronic structure systems, it is widely used to obtain electronic properties of atoms, molecules and solids. This method leads to Density Functional Theory (DFT), which uses the KS Theory with a functional approximation for the exchange-correlation of electrons.

1.3.1 HOHENBERG-KOHN THEOREM

The energy is a functional of a wavefunction ($E = \mathcal{F}[\psi]$). A functional takes a function as input and returns a number [130]. The main concept of DFT is to describe the properties of system using the electron density. The ground state energy is a functional of the electronic density ($E = F[\rho]$). This is remarkable, given that instead of having $3N$ variables from the wavefunction, now we have a functional $\rho(\vec{r})$ that depends on 3 variables. The Hohenberg-Kohn theorem [132] allows this. In general, if it is not a ground state system, we must use the whole wavefunction to calculate the energy.

$$E = \begin{cases} F[\rho(\vec{r})] & ground\ state \\ \mathcal{F}[\psi(\vec{r}_1, \dots, \vec{r}_n)] & exited\ state \end{cases} \tag{1.3.1}$$

therefore, any operator described before will be in terms of the electronic density $\rho(\vec{r})$.

2.3.2 KOHN-SHAM EQUATION

The Hohenberg-Kohn theorem describes the total energy of many-electrons in their ground state as a functional of the electronic density [130], unfortunately, the exact form of this functional is still unknown and approximations are used.

$$E = F[\rho(\vec{r})] = \int d\vec{r}\rho(\vec{r})V_n(\vec{r}) + \langle\psi[\rho]|\,\hat{T} + \widehat{W}\,|\psi[\rho]\rangle \tag{1.3.2}$$

where $\widehat{W} = \frac{1}{2}\sum_{i\neq j}\frac{1}{|\vec{r}_i - \vec{r}_j|}$ is the Coulomb potential and V_n is the potential shape given by the parametric positions of the nuclei. The Eq. (1.3.2) depends explicitly on ρ in the first term, the second term has an implicit dependence. The main idea of [1] was to break into pieces the kinetic and Coulomb energy terms as independent electrons and include an extra term to describe the exchange and correlation of the electrons.

$$E = F[\rho] = \int d\vec{r}\rho(\vec{r})V_n(\vec{r}) - \sum_i \int d\vec{r}\phi_i^*(\vec{r})\left(\frac{\nabla^2}{2}\right)\phi_i(\vec{r}) + \frac{1}{2}\int d\vec{r}\rho(\vec{r})V_H(\vec{r}) + E_{xc}[\rho] \tag{1.3.3}$$

$$V_H(\vec{r}) = \int d\vec{r}'\frac{\rho(\vec{r}')}{|\vec{r} - \vec{r}'|} \tag{1.3.4}$$

the summation of all the terms correspond to the total energy of the independent electron approximation, except for E_{xc}, which is the exchange-correlation energy, and V_H is the Hartree potential. If we knew E_{xc}, then we would be able to calculate the total energy of a system in its ground state with just the electron density (ρ).

2.3.2 VARIATIONAL PRINCIPLE IN KS-EQUATION

The ground state density (ρ_0) is obtained by minimizing the total energy $E[\rho]$, and this property is stated in Hohenberg-Kohn variational principle [130] as follows:

$$\frac{\delta F[\rho]}{\delta\rho}\Big|_{\rho_0} = 0 \tag{1.3.5}$$

this description is equivalent to the variational principle in the Hartree-Fock equation. The variational principle applied to the functional will lead to an equation for the KS orbitals $\phi_i(\vec{r})$, that is used to construct the electronic density. Minimizing the energy functional by enforcing the orthogonality of orbitals, leads to the following set of equations:

$$\left[-\frac{1}{2}\nabla^2 + V_n(\vec{r}) + V_H(\vec{r}) + V_{xc}(\vec{r})\right]\phi_i(\vec{r}) = \epsilon_i\phi_i(\vec{r}) \tag{1.3.6}$$

where V_n is the nuclear potential, V_H is the Hartree potential, the squared gradient contains the kinetic energy and V_{xc} is an extra term that describes the exchange-correlation potential, defined as:

$$V_{xc}(\vec{r}) = \frac{\delta E_{xc}[\rho]}{\delta\rho}\Big|_{\rho(\vec{r})} \tag{1.3.7}$$

Eq. (1.3.6) is called Kohn-Sham equations, which is a very powerful tool to calculate the electronic properties of molecules. The approximation of $E_{xc}[\rho]$ introduce errors or inaccuracies. Therefore, search for more sophisticated and accurate approximation is an active area of research.

1.3.3 LOCAL DENSITY APPROXIMATION

The search for approximations of exchange-correlation functionals $E_{xc}[\rho]$ has led to large number of approximation, the simplest functional being the Local Density Approximation (LDA) [9,128]. This functional is based on the homogeneous electron gas. The free electron gas model assumes that electrons do not interact with each other, nuclear potential is constant and that there are N electrons within a box of volume V [129].

$$\phi_{\vec{k}}(\vec{r}) = \frac{1}{\sqrt{V}}\exp(i\vec{k}\cdot\vec{r}) \tag{1.3.8}$$

$$\epsilon_k = \frac{|\vec{k}|^2}{2} \tag{1.3.9}$$

here, Eq. (1.3.8) is the stationary wavefunction with $\vec{k}$ as wavevector and Eq. (1.3.9) are the eigenvalue of this wavefunction. The highest occupied state is the Fermi level that corresponds to the Fermi energy ϵ_F and wavevector $\vec{k}_F$. The usefulness of this method comes from the unique dependence on the electron density.

$$\vec{k}_F = (3\pi\rho)^{\frac{1}{3}} \tag{1.3.10}$$

knowing all these considerations, we can approximate the exchange energy using plane waves $\phi_{\vec{k}}$ in the Hartree-Fock exchange energy. We then get the next expression:

$$E_x[\rho] = -\frac{3}{4}\left(\frac{3}{\pi}\right)^{\frac{1}{3}} \rho^{\frac{4}{3}} V \tag{1.3.11}$$

this ignores the correlation, but it was possible to get the correlation energy by solving directly from the many-body Schrödinger equation with stochastic numerical methods [128]. The generated data from this approach led to the correlation energy approximation for electron gas frame, such approximation was developed by Perdew and Zunger (1981) [9], resulting in the following expression:

$$E_C[\rho] = \rho V \begin{cases} -0.048 + 0.0311 \ln r_s + 0.002 r_s \ln r_s - 0.0116 r_s & if\ r_s < 1 \\ -\dfrac{0.1423}{1 + 1.0529\sqrt{r_s} + 0.3334 r_s} & if\ r_s \geq 1 \end{cases} \tag{1.3.12}$$

r_s it the Wigner-Seitz radius, this is the radius of an average occupied sphere by an electron.

1.3.4 GENERALIZED GRADIENT APPROXIMATION

The LDA functional is too simple to lack of description for inhomogeneous systems. A step to account for inhomogeneity is to include reduced gradient [5,125-127]. This has led to the development of semilocal approximation.

$$E_{XC}^{GGA}[\rho_\uparrow, \rho_\downarrow] = \int d\vec{r}\, f(\rho_\uparrow, \rho_\downarrow, \vec{\nabla}\rho_\uparrow, \vec{\nabla}\rho_\downarrow) \tag{1.3.13}$$

this semilocal functional recovers the second-order gradient approximation for slowly varying density and fits extra exact constraints of exchange-correlation energy. A widely used semilocal functional is the Perdew-Burke-Ernzerhof (PBE) functional [5,6]. The exchange energy for spin unpolarized is as follows:

$$E_x^{PBE}[\rho] = \int d\vec{r}\, \rho(\vec{r})\, \epsilon_x^{unif}[\rho]\, F_x(s) \tag{1.3.14}$$

where $\epsilon_x^{unif}[\rho] = -\frac{3}{4\pi}(3\pi^2\rho)^{1/3}$ is the exchange energy density of LDA, $F_x(s)$ is the enhancement factor, and $s = |\vec{\nabla}\rho|/(2\rho(3\pi^2\rho)^{1/3})$ is the dimensionless density gradient. The enhancement factor of PBE is:

$$F_X(s) = 1 + \kappa - \frac{\kappa}{1+\mu\, s^2/\kappa} \tag{1.3.15}$$

where the constant values are $\kappa = 0.804$, and $\mu = 0.21951$. The enhancement factor obeys the uniform electron gas density limit $F_X(0) = 1$, and Lieb-Oxford lower bound given by $F_x(s) \leq 1.804$. The correlation energy is expressed as:

$$E_C^{PBE}[\rho_\uparrow, \rho_\downarrow] = \int d\vec{r}\, \rho(\vec{r}) \left[\epsilon_c^{unif}(r_s, \zeta, \mathrm{t}) + H(r_s, \zeta, \mathrm{t})\right] \tag{1.3.16}$$

where $t = |\vec{\nabla}\rho|/(2\phi k_s \rho)$ is another dimensionless density gradient, $k_s = \sqrt{4k_F/\pi a_0}$ is the Thomas-Fermi screening wave vector, $\zeta = \frac{\rho_\uparrow + \rho_\downarrow}{\rho}$ is the relative spin polarization, and $\phi(\zeta) = [(1+\zeta)^{\frac{2}{3}} + (1-\zeta)^{\frac{2}{3}}]/2$ is the spin scaling factor. The H function is defined as follows:

$$H(r_s, \zeta, t) = \gamma\phi^3 \ln\left[1 + \frac{\beta}{\gamma}t^2 \cdot \frac{1+At^2}{1+At^2+A^2t^4}\right] \tag{1.3.17}$$

where the constant values are $\beta = 0.066725$, $\gamma = 0.031091$, and A is defined as:

$$A = \frac{\beta}{\gamma}\left(\exp\left[-\frac{\epsilon_c^{unif}}{\gamma\phi^3}\right] - 1\right)^{-1} \tag{1.3.18}$$

if $t \to 0$ then the function $H \to \beta\phi^3 t^2$, then this is the slow varying limit that is described by a second-order gradient expansion. The opposite case is the rapidly varying limit, which uses $t \to \infty$ to reach the limit $H \to -\epsilon_c^{unif}$, this makes correlation vanish. In the high-density case, the correlation energy reaches a constant value when $r_s \to 0$.

1.3.5 META-GENERALIZED GRADIENT APPROXIMATION

Meta-generalized approximation (meta-GGA) [75] is a further improvement that includes kinetic energy or density Laplacian to describe improve chemical properties compared to LDA of GGAs functionals. The exchange-correlation energy is defined as:

$$E_{XC}^{MGGA}[\rho_\uparrow, \rho_\downarrow] = \int d\vec{r}\, \rho(\vec{r})\epsilon_{xc}(\rho_\uparrow, \rho_\downarrow, \vec{\nabla}\rho_\uparrow, \vec{\nabla}\rho_\downarrow, \tau_\uparrow, \tau_\downarrow) \tag{1.3.19}$$

where $\tau_\sigma = \frac{1}{2}\sum_i^{OCCU}\left|\vec{\nabla}\psi_{i\sigma}\right|^2$ is the kinetic energy density of Kohn-Sham orbital with spin σ. The inclusion of τ_σ in meta-GGA functional enables the recovery of the description of fourth-order gradient expansion at a slowly-varying density limit. Nowadays, there are many meta-GGAs [71,117-122]. Our work aims for studies with Strongly Constrained and Appropriately Normed (SCAN) functional [75]. The unpolarized exchange energy in SCAN is as follows:

$$E_x[\rho] = \int d\vec{r}\, \rho(\vec{r})\epsilon_x^{unif} F_x(s, \alpha) \tag{1.3.20}$$

where $\alpha = \frac{\tau - \tau^w}{\tau^{unif}}$ is a dimensionless variable, $\tau^w = \frac{\left|\vec{\nabla}\rho\right|^2}{8\rho}$ is the Von-Weizsäcker kinetic energy density, which is exactly τ for single orbital density limit, and $\tau^{unif} = \frac{3}{10}(3\pi^2)^{2/3}\rho^{5/3}$ is the Thomas-Fermi kinetic energy density or uniform kinetic energy density limit. The quantity α can

describe nicely the chemical bonding, α near to zero describes a covalent single bond, near to one describes a metallic bond, and $\alpha \gg 1$ is a weak interaction. The enhancement factor is defined as:

$$F_x(s,\alpha) = (h_x^1(s,\alpha) + f_x(\alpha)[h_x^0 - h_x^1(s,\alpha)])g_x(s) \tag{1.3.21}$$

with

$$f_x(\alpha) = \exp\left[-\frac{c_{1x}\alpha}{1-\alpha}\right]\theta(1-\alpha) - d_x \exp\left[\frac{c_{2x}}{1-\alpha}\right]\theta(\alpha-1) \tag{1.3.22}$$

$$g_x(s) = 1 - \exp\left[-a_1 s^{-1/2}\right] \tag{1.3.23}$$

where $h_x^0 = 1.174$, and $a_1 = 1.4979$. The other parameters are $c_{1x} = 0.667$, $c_{2x} = 0.8$ and $d_x = 1.24$. θ(x) is a step function of x. When $\alpha \approx 1$, the enhancement factor becomes $F_x(s,\alpha) = h_x^1(s,\alpha)$, which is similar to the PBE enhancement factor that recovers the slow-varying limit, but this satisfies the fourth-order gradient approximation.

$$h_x^1(s) = 1 + \kappa_1 - \frac{\kappa_1}{1+\mu x^2/\kappa_1} \tag{1.3.24}$$

and x is defined as:

$$x = \mu_{AK} s^2 \left[1 + \left(\frac{b_4 s^2}{\mu_{AK}}\right)\exp\left(-\frac{|b_4|s^2}{\mu_{AK}}\right)\right] + [b_1 s^2 + b_2(1-\alpha)\exp(-b_3(1-\alpha)^2)]^2 \tag{1.3.25}$$

the constant values are $\mu_{AK} = 10/11$, $b_2 = (5913/405000)^{1/2}$, $b_1 = (511/13500)/(2b_2)$, $b_3 = 0.5$, and $b_4 = \mu_{AK}/\kappa_1 \ -1606/18225 - b_1^2$, and $\kappa_1 = 0.065$. SCAN satisfies a tight bound condition $F_x \leq 1.174$ [73], this condition is also satisfied by LDA. The correlation energy is:

$$E_C[\rho_\uparrow, \rho_\downarrow] = \int d\vec{r}\, \rho(\vec{r})\left(\epsilon_c^{unif}(r_s,\zeta,s,\alpha)\right) \tag{1.3.26}$$

the components of Eq. (1.3.26) are:

$$\epsilon_c = \epsilon_c^1 + f_c^1(\alpha)[\epsilon_c^0 - \epsilon_c^1] \tag{1.3.27}$$

$$f_c(\alpha) = \exp\left[-\frac{c_{1c}\alpha}{1-\alpha}\right]\theta(1-\alpha) - d_c \exp\left[\frac{c_{2c}}{1-\alpha}\right]\theta(\alpha-1) \tag{1.3.28}$$

Eqs (1.3.26-28) are analogous to exchange energy terms. Therefore, the coefficients are $c_{1c} = 0.64$, $c_{2c} = 1.5$, and $d_c = 0.7$. SCAN has proven to be superior to many GGAs and meta-GGAs, some of this are for liquid water [152], metal surface [153] and many others referred in [154].

1.4 BASIS FUNCTIONS AND GAUSSIAN BASIS SET

The Kohn-Sham equations are often solved using the basis sets. The Kohn-Sham orbitals are often expressed as a linear combination of plane waves [114] or Gaussians [115]. This thesis will use gaussian basis sets and the molecular orbitals are constructed as follows:

$$\psi_i(\vec{r}) = \sum_{\mu=1}^{N_{BF}} C_{\mu i} G_\mu(\vec{r}) \tag{1.4.1}$$

from Eq. (1.4.1), ψ_i is the molecular orbital (MO), G_μ is the Gaussian basis function which is fixed, and $C_{\mu i}$ is the coefficient which is determined by the SCF calculation.

The gaussian basis functions are commonly used by chemists; besides, it is efficient computationally speaking given the simplicity of a gaussian integral. The used version of Gaussians for this document is the primitive Gaussian functions or primitive GTO (Gaussian Type Orbital) [115], in cartesian coordinates.

$$g_\mu(\vec{r}) = x^k y^m z^n e^{-\zeta_\mu(x^2+y^2+z^2)} \tag{1.4.2}$$

nowadays, there are many data sets for the description of the atoms in terms of Gaussians, the minimal set is STO-2G, but there is a lot of choices such as 4-31G that is denser in basis functions

and 6-31G* contains the description of d-type functions of heavy atoms. Our calculations are done with the default basis set of NRLMOL-UTEP program [93], it will be indicated if this is not used.

1.5 SELF-INTERACTION CORRECTION

Self-interaction has its origins in the approximation of the exchange-correlation functional. Recalling the Hartree-Fock type exchange energy for a pair of orbitals is:

$$E_x = \frac{1}{2}\sum_\sigma \sum_{i,j} \int d\vec{r} \int d\vec{r'} \frac{\psi_{i\sigma}(\vec{r})\psi_{j\sigma}(\vec{r'})\psi_{j\sigma}(\vec{r})\psi_{i\sigma}(\vec{r'})}{|\vec{r}-\vec{r'}|} \tag{1.5.1}$$

when the coefficients $i = j$, the expression in Eq. (1.5.1) becomes the self-exchange energy. This is an incorrect behavior of the electron that can see itself in density functional approximations (DFAs) and produces a dramatic failure in cases such as stretched bond system. This misbehavior is addressed as self-interaction error (SIE). SIE arises from an improper cancellation of the self-Coulomb energy with the approximate self-exchange energy for the one-electron density limit in DFA. The self-Coulomb energy ($U[\rho_{i\sigma}]$) is the integration of Eq. (1.3.4), described as:

$$U[\rho_{i\sigma}] = \frac{1}{2}\int d\vec{r}\rho_{i\sigma}(\vec{r}) \int d\vec{r'} \frac{\rho_{i\sigma}(\vec{r'})}{|\vec{r}-\vec{r'}|} \tag{1.5.2}$$

Perdew and Zunger [9] in 1981 proposed a method to correct SIE known as self-interaction correction (PZSIC), this method removes the SIE from a DFA calculation in an orbital by orbital basis from the total DFA energy.

$$E^{PZSIC-DFA}[\rho_\uparrow, \rho_\downarrow] = E^{DFA}[\rho_\uparrow, \rho_\downarrow] - \sum_{i\sigma}(U[\rho_{i\sigma}] + E_{XC}^{DFA}[\rho_{i\sigma}, 0]) \tag{1.5.3}$$

in a traditional PZSIC approach, the orbitals used in Eq. (1.5.3) must satisfy the localization equation (LE) [16,17] to find the minimum energy of the variational method. The LE is a pairwise condition for orbitals $\phi_{i\sigma}$ as follows:

$$\langle \phi_{i\sigma} | V_{i\sigma}^{SIC} - V_{j\sigma}^{SIC} | \phi_{j\sigma} \rangle = 0 \tag{1.5.4}$$

an alternative to solve the PZSIC Eq. (1.5.3) is using the Fermi-Löwdin orbitals, introduced by Pederson, Perdew and Ruzsinszky, this implementation is called FLO-SIC [80,140]. FLOs are Löwdin orthogonalized set of Fermi orbitals (FOs) whose advantage is to be local orbitals, providing a total energy which is unitary invariant. FOs (ϕ^{FO}) are constructed from Fermi orbital descriptors (FODs), which are parameters in space.

$$\phi_i^{FO}(\vec{r}) = \sum_j^{N_{occu}} \frac{\psi_j(\vec{a_i})\psi_j(\vec{r})}{\sqrt{\rho_i(\vec{a_i})}} \tag{1.5.5}$$

here, i and j are the orbital indexes, ψ is the KS orbital, ρ_i is the electron spin density, and $\vec{a_i}$ is the FOD position. FLOSIC method has computational advantage over the traditional PZSIC because it requires the optimization of $3N$ parameters coming from the FODs, compared to the LE (Eq. 1.5.4) that needs to optimize N^2 parameters. The FOD optimization is analogous to the optimization process of geometry for $3N$ parameters.

CHAPTER 2: PERFORMANCE OF LOCAL SELF-INTERACTION CORRECTION METHOD WITH SIMPLE SCALING FACTOR

2.1 ABSTRACT

A recently proposed local self-interaction correction (LSIC) showed improved performance over PZSIC and gave a step toward in resolving the paradox of SIC. In LSIC, an iso-orbital indicator, quantity to identify chemical properties, is used to apply SIC locally in space. LSIC showed remarkable performance when applied to LSDA. In the original LSIC work, the ratio of von Weizsäcker and total kinetic energy densities was used, but that is not the only choice for the iso-orbital indicator. In 2006, Vydrov *et al*. proposed a simpler orbital scaling factor, consisting in orbital and total densities in place of the kinetic energy densities and showed some success when applied to their orbital scaling scheme. In this work, we examine the performance of LSIC when used with the said ratio of orbital and total densities. We compare LSIC(w) vs LSIC(z) performance and show LSIC(w) can be a good alternative to LSIC(z). We compare LSIC(w) vs OSIC(w) performance to show how this iso-orbital indicator perform differently for interior and exterior scaling. We found that....

If we want, we can also include cases where LSIC(z) fails in this paper e.g. binding energy of water and LSIC(w) corrects that. It shows limitation and importance of iso-orbital indicator used supporting the motivation of this work.

2.2 INTRODUCTION

Kohn-Sham (KS) formulation of Density functional theory (DFT) [1] is widely used method to study electronic structures of atoms, molecules, and solids because of its inexpensive computational cost and easy to use software packages. Although the KS theory is exact theory for obtaining the ground state energy of many-electron systems, the exact form of exchange-correlation (XC) energy is unknown. Its practical applications require an approximation to the XC

functional. In the quantum chemistry community, there has been effort to develop accurate exchange-correlation functional, and many semi-local and empirical functionals have been proposed and implemented in DFT software. As the functionals improved their chemical accuracy, so did the density functional approximations (DFAs) over the course of decades. The simplest form of the XC functional is local spin density approximation (LSDA) [133,134], which was one of the pioneers functional based on the uniform electron gas model. LSDA depends only on local electron density but showed commendable success in DFA in the early days. Years later, generalized gradient approximations (GGAs) were proposed. GGA incorporates density gradient in addition to electron density and has contributed on improving the predicting power of DFA. One of the notable GGA functional is Perdew–Burke-Ernzerhof (PBE) [5,6], a widely used functional even to date. To further improve the accuracy, scientists have been developing meta-GGA and hyper-GGA functionals in the last two decades. The meta-GGAs include kinetic energy density or density Laplacian to describe chemical properties more accurately than their predecessors. In 2000s, Tao-Perdew-Staroverov-Scuseria (TPSS) [71,118] and Minnesota 06 meta-GGA [135] gained popularity among the meta-GGAs. Hybrid functionals [7,136], which has a certain percentage of Hartree-Fock, were another area of functional development and were able to mitigate the shortcomings in DFAs. In 2015, the meta-GGAs gained further attention from the scientific communities as Strongly Constrained and Appropriately Normed (SCAN) [75] functional showed its appearance. SCAN is a semilocal functional that satisfies all the 17 known exact constraints of the meta-GGA functionals. SCAN showed success in predicting a wide array of properties as accurately as hybrid functionals or in some cases better [137]. Because of those XC functional development, DFAs are able to describe fair amount of electronic structure properties, and its efficient implementation in DFT is available in a vast number of codes.

Despite of its success, DFAs are known to have a systematic error known as self-interaction error (SIE) where an electron can, incorrectly, see itself and can fail drastically for cases such as a system with a stretched bond where the SIEs are pronounced. SIE in DFAs arises from an improper cancellation of the self-Coulomb energy with the approximated self-exchange-correlation energy for the one electron density limit. It has been shown that many failures of DFAs can be traced down to SIE. SIE causes DFAs to predict wrong chemical reaction barriers, not bind anions [9], cause HOMO eigenvalues to be too shallow, give incorrect asymptotic potentials, and is known to

cause electron delocalization errors [138,139].To accurately describe these properties with a DFA theory, a method to correct SIE is needed.

In 1981, Perdew and Zunger (PZ) [9] proposed a method to eliminate the one-electron SIEs from DFA calculations. Their approach is commonly referred as PZ self-interaction correction (PZSIC) where the SIE is removed from a DFA calculation in an orbital by orbital basis. PZSIC provides the exact cancellation for one- and two-electron self-interaction, but not necessarily for many-electron self-interaction [74]. PZSIC treat the self-Hartree correction exactly and leaves residual self-exchange-correlation via approximation given with a DFA. PZSIC provides no correction to the exact functional [9]. PZSIC, when used with the KS orbitals, causes orbital dependent Hamiltonians and size extensivity problem; it is known that PZSIC formalism leads to an orbital dependent theory. In PZSIC, use of local orbitals is desired for the total energy to be invariant under unitary transformations. Traditionally, PZSIC requires solving the so called Pederson or localization equation (LE) [16,17] to find the set of orbitals that minimize the total energy. Solving the LE and finding the optimal orbitals compliant with the condition is computationally expensive since it requires a unitary transformation of N^2 coefficients. A few decades after the appearance of PZSIC, a new way to deal with the computational expensiveness of PZSIC was introduced by Pederson, Perdew, and Ruzsinszky where Fermi-Löwdin orbitals (FLOs) are used to solve the PZSIC equation. This method is known as FLO-SIC [80,140]. FLOs are Löwdin orthogonalized set of Fermi orbitals (FOs). Using FLOs in PZSIC has a formal advantage that they are local orbitals and total energy becomes unitary invariant and that size-consistency is guaranteed for all systems. For construction of FLOs, Fermi orbital descriptor (FOD) positions are needed as $3N$ parameters in space that can be optimized in analogous to the geometrical optimization processes. FLOSIC method has computational advantage over the traditional PZSIC since it requires optimizing only $3N$ parameters instead of N^2 parameters.

In earlier studies, FLO-SIC was applied for LSDA and showed significant improvements in atomic and molecular properties over SI-uncorrected LSDA performance [63,43,141,142]. Naturally, FLOSIC was later also applied to more sophisticated XC functionals, such as PBE and SCAN, to see if SIC improves the performance of those functionals [44,57-60,62,64,65,67,69,79,97, 106,113,143] Unfortunately, when SIC is applied to modern semilocal functionals, PBE and

SCAN, the predictive power of these semilocal functionals are lost where total energies become overestimated and atomization energies worsen, etc.

In literature, it is shown that, although PZSIC provides more accurate descriptions in stretched bond or in an anionic state, PZSIC worsens the performance in properties where uncorrected DFA performs well. Vydrov and Scuseria [28] reported that SIC worsens thermo-chemical properties for GGAs, meta-GGAs, and hybrid functionals. Klüpfel and Jónsson [144] applied complex orbitals to PZSIC, showing an affinity with PBE semilocal functional to improve the total atomic energies. Shahi *et al.* [106] reported that atomization energies worsen in PZSIC approach, some are due nodality in orbital-densities and can be removed with the usage of complex orbitals. This puzzling behavior of PZSIC was referred as the paradox of SIC [145]. In many situations, PZSIC was found to overcorrect the energy. It was not well understood why the paradox occurs, and it has kept the SIC theory away from DFT of al-most everything. In a recent year, Santra and Perdew [107] showed that using SIC for semilocal DFA breaks at least one of the exact constraints that they are designed with – a possible explanation of the paradox.

Several approaches have been proposed to improve the performance of SIC in hope for resolving the paradox. Many methods involve scaling down of the SIC contribution in the many-electron regions. Jónsson's group used a constant scaling factor to reduce the overcorrection (global scaling) [70]. In the similar spirit, Vydrov *et al*. used a method to scale down the SIC by the orbital contribution (orbital scaling) [30] and found some improvement in performance. A lot of effort has been put into alleviating the overcorrection made by PZSIC. Though there were some success and thought to be a solution to resolve the paradox at the time, those methods also tends to deteriorate the good behaviors of PZSIC such as the correct $-1/r$ asymptotic nature of the potential seen by an electron for a localized system. Ruzsinszky *et al*. [146] found that many-electron SIE and fractional-charge dissociation behavior of positively charged dimers reappear with such scaling approach. The real challenge in resolving the paradox is to remove many-body SIEs while maintaining what is correctly described with PZSIC.

Recently, a new scaling-down approach was proposed where scaling of PZSIC is done locally in a pointwise manner using an iso-orbital indicator as a local scaling factor. This local scaling factor identifies the single-orbital regions where full correction is needed and uniform density regions where correction is not needed. The proposed method is known as local-SIC (LSIC) [69], and LSIC has shown remarkable performance for a wide array of properties when applied to LSDA.

On the other hand, the gauge problem needs to be addressed for application of LSIC to a XC functional at higher rungs of Jacob's ladder [147]. Currently, LSIC is an active subject of research in the SIC community. In the original LSIC work, we used a ratio of von-Weiszäcker and total kinetic energy densities as a choice of the local scaling factor. However, there are different choices of local scaling factor available. Itis possible to use the local orbital density and total orbital density to identify single-electron regions and many-electron regions. In this work, we explored the LSIC method using a simpler iso-orbital indicator. The selected iso-orbital indicator in this study is the ratio of the orbital density and the total density. We shall refer this as LSIC(w) for the remainder of this manuscript. We investigated the performance of LSIC(w) for atomic properties: total energy, ionization potentials, and electron affinities. For molecules, we calculated the total energies, atomization energies, the dissociation energies for selected systems. We found that LSIC(w) provides comparable results to LSIC that uses the ratio of kinetic energy densities.

2.3 THEORY AND COMPUTATIONAL METHOD

2.3.1 PERDEW-ZUNGER SELF-INTERACTION CORRECTION

In PZSIC [9], SIE is removed in an orbital by orbital basis from the DFA energy as

$$E^{PZSIC-DFA} = E^{DFA}[\rho_\uparrow, \rho_\downarrow] - \sum_{i\sigma}^{OCC}\{U[\rho_{i\sigma}] + E_{XC}^{DFA}[\rho_{i\sigma}, 0]\} \tag{2.1}$$

where i is the orbital index, σ is the spin index, $U[\rho_{i\sigma}]$ is the exact self-Coulomb energy, and $E_{XC}^{DFA}[\rho_{i\sigma}, 0]$ is the self-exchange-correlation energy for a given DFA XC functional. In a traditional PZSIC approach, the orbital used in the Eq. (2.1) must satisfy LE for variationally minimum energy. The LE for the orbitals $\phi_{i\sigma}$ is a pairwise condition and given as

$$\langle \phi_{i\sigma} | V_{i\sigma}^{SIC} - V_{j\sigma}^{SIC} | \phi_{j\sigma} \rangle = 0 \tag{2.2}$$

in FLOSIC approach, FLOs are used in place of directly solving the Eq. (2.2). First, FOs ϕ^{FO} are constructed with the density matrix and spin density at special positions in space called Fermi

orbital descriptor (FOD) positions. The FODs are used to transform KS orbitals ψ to a set of FOs as follows,

$$\phi_i^{FO}(\vec{r}) = \frac{\sum_j^{Nocc} \psi_j(\overrightarrow{a_i})\psi_j(\vec{r})}{\sqrt{\rho_i(\overrightarrow{a_i})}} \tag{2.3}$$

here, i and j are the orbital indexes, and ψ is the KS orbital, ρ_i is the electron spin density, and $\overrightarrow{a_i}$ is the FOD position. The obtained FOs are then orthogonalized with the Löwdin's scheme to form FLOs. In the FLOSIC method, optimal set of FLOs are found by finding the FODs that minimizes total energy. This optimization process is similar to that for geometry optimization.

2.3.2 OSIC

As mentioned in Sec. I, PZSIC tends to overcorrect the DFA calculations. That is why some studies proposed schemes to scale down the PZSIC correction through applying different schemes. One notable example of this is Vydrov and co-workers' work [30] where they proposed a scaled down scheme according to the local orbitals applied to PZSIC. In their scaling down approach, PZSIC equation [Eq. (2.1)] is modified to

$$E^{OSIC-DFA} = E_{XC}^{DFA}[\rho_\uparrow, \rho_\downarrow] - \sum_{i\sigma}^{OCC} X_{i\sigma}^k (U[\rho_{i\sigma}] + E_{XC}^{DFA}[\rho_{i\sigma}, 0]) \tag{2.4}$$

where each local orbital SIC term has a different scaling factor $X_{i\sigma}^k$ defined as

$$X_{i\sigma}^k = \int z_\sigma^k \rho_{i\sigma}(\vec{r}) d\vec{r} \tag{2.5}$$

here, i indicates the orbital, σ is the spin, z_σ is the iso-orbital indicator, and k is an integer. We will refer to this method as orbital scaling or OSIC. The z_σ is used to interpolate the single-electron regions ($z_\sigma = 1$) and uniform density region ($z_\sigma = 0$). In their original work, Vydrov *et al*. used $z_\sigma = \tau_\sigma^W / \tau_\sigma$ to study the performance of OSIC with various XC functionals where $\tau_\sigma^W(\vec{r}) = \left|\vec{\nabla}\rho_\sigma(\vec{r})\right|^2 / (8\rho_\sigma(\vec{r}))$ is the von Weiszäcker kinetic energy density and $\tau_\sigma(\vec{r}) = \frac{1}{2}\sum_i \left|\vec{\nabla}\psi_{i\sigma}(\vec{r})\right|^2$ is

the non-interacting kinetic energy density. Satisfying the gradient expansion in ρ requires $k \geq 1$ for LSDA, $k \geq 2$, and $k \geq 3$ for meta-GGA. Vydrov *et al*., however, used various values of k to study its effect on OSIC performance.

In their subsequent work, Vydrov *et al*. [148] proposed an alternative choice of the iso-orbital indicator for OSIC as

$$w_{i\sigma}^{k}(\vec{r}) = \left(\frac{\rho_{i\sigma}(\vec{r})}{\rho_{\sigma}(\vec{r})}\right)^{k} \tag{2.6}$$

$w_{i\sigma}$ was used in place of z_σ in Eq. (2.5). Notice that Eq. (2.6) contains a local orbital index. $w_{i\sigma}$ approaches unity at single orbital regions since $\rho_\sigma(\vec{r}) = \rho_{i\sigma}(\vec{r})$ at those regions. Similarly, $w_{i\sigma}$ approaches zero at many-electron region since $\rho_\sigma(\vec{r}) \gg \rho_{i\sigma}(\vec{r})$ at those regions. It was reported that the OSIC with Eq. (2.6) showed comparable performance as $z_\sigma = \tau_\sigma^W/\tau_\sigma$ despite of its simpler form.

2.3.3 LSIC

Though OSIC had some success in improving the performance with SIC, the approach lead to parameter k dependent performance, $-X_{HO}/r$ asymptotic potential instead of $-1/r$ [30], and inaccurate description of dissociation behavior [74]. Recently proposed LSIC applies scaling to PZSIC in a different way than OSIC and showed promising results while keeping many benefits of PZSIC. In LSIC, PZSIC energy density is scaled down locally as follows,

$$E_{XC}^{LSIC-DFA} = E_{XC}^{DFA}[\rho_\uparrow, \rho_\downarrow] - \sum_{i\sigma}^{OCC}(U^{LSIC}[\rho_{i\sigma}] + E_{XC}^{LSIC}[\rho_{i\sigma}, 0]) \tag{2.7}$$

where

$$U^{LSIC}[\rho_{i\sigma}] = \frac{1}{2}\int d\vec{r}\; z_\sigma^k(\vec{r})\,\rho_{i\sigma}(\vec{r}) \int d\vec{r'}\,\frac{\rho_{i\sigma}(\vec{r'})}{|\vec{r}-\vec{r'}|} \tag{2.8}$$

$$E_{XC}^{LSIC}[\rho_{i\sigma}, 0] = \int d\vec{r}\; z_\sigma^k(\vec{r})\,\rho_{i\sigma}(\vec{r})\,\epsilon_{XC}^{DFA}([\rho_{i\sigma}, 0], \vec{r}) \tag{2.9}$$

in this study, we used $w_{i\sigma}(\vec{r}) = \rho_{i\sigma}(\vec{r})/\rho_{\sigma}(\vec{r})$ in place for z_{σ} in Eqs. (8) and (9) and investigated how this quantity would affect the LSIC performance. We refer the LSIC with $z_{\sigma}(\vec{r})$ as LSIC(z) and LSIC with $w_{i\sigma}(\vec{r})$ as LSIC(w) to differentiate the two cases. LSIC incorporates an iso-orbital indicator to apply SIC pointwise in space. LSIC reduces to DFA in uniform gas limit and reduces to PZSIC in pure one-electron limit.

2.3.4 COMPUTATIONAL DETAILS

All of the calculations were performed using the developmental version of FLOSIC code [95,142], a software based on the UTEP-NRLMOL code. This code has an implementation of the FLOSIC, OSIC, and LSIC methods. FLOSIC/NRLMOL code uses Gaussian type orbitals [96] whose default basis sets are in similar quality as quadruple zeta basis sets. We used the NRLMOL default basis sets throughout our calculations. For calculations of atomic anions, long range s, p, and d single Gaussian orbitals are added to give a better description of the extended nature of anions. The exponents β of these added single Gaussians were obtained using the relation, $\beta(N+1) = \beta(N)^2/\beta(N-1)$, where N is the N-th exponent. FLOSIC code uses a variational integration mesh [96] that provides accurate numerical integration. In this work, our focus is on the LSDA functional because LSIC applied to LSDA is free from the gauge problem [147] unlike GGAs and meta-GGAs where a gauge transformation is needed since their XC potentials are not in the Hartree gauge. We used an SCF energy convergence criteria of 10^{-6} Ha for the total energy and an FOD force tolerance of 10^{-3} Ha/bohr for FOD optimizations in FLOSIC calculations. For OSIC and LSIC calculations, we used respective FLOSIC densities and FODs as a starting point and performed a non-self-consistent calculation. The additional computational cost of the scaling factor in OSIC and LSIC is very small compared to a regular FLOSIC calculation.

2.4 RESULTS

In the original LSIC article, the method was evaluated for a wide array of electronic structure properties to account a good picture of how the new methodology performs. Here, we

follow the same set of properties to assess the performance of LSIC(w). The performance of LSIC(w) is compared to LSIC(z) and OSIC(w). We considered total energies, ionization potentials, and electron affinities for atoms and atomization energies, reaction barrier heights, and dissociation energies for molecules.

2.4.1 ATOMS

TOTAL ENERGY OF ATOMS

We compared the total atomic energies of the atoms $Z = 1 - 18$ against the accurate non-relativistic values reported by Chakravorty *et al*. [99]. Various integer values of k were used for LSIC(w) and OSIC(w). The total energy difference is shown in Fig. 2.1. LSIC(w) and OSIC(w) recover PZSIC when $k = 0$. For the other values of $k > 0$ provide different interpolation between $w_{i\sigma}^{k} = 0$ and $w_{i\sigma}^{k} = 1$. We show the mean absolute errors (MAEs)in total energy with respect to the reference in Table 2.1. The MAE of PZSIC is 0.381 Ha whereas LSIC(w) and OSIC(w) have MAEs of 0.061 and 0.074 Ha with $k = 1$, respectively. LSIC(w) shows a better performance than OSIC(w), and LSIC(w) MAE is in the same order of magnitude as the earlier reported MAE of LSIC(z) of 0.041 Ha [69]. Our results show that LSIC(w) indeed reduces the error compared to PZSIC for all four k's we studied in this work. The smallest error of LSIC(w) was obtained for $k = 1$. On the other hand, for $k = 2 - 4$, the total energies start approaching the LSDA energies deviating away from the theoretical energies. Also, we observed that OSIC(w) behaves differently as a function of k than LSIC(w). The smallest error is achieved at $k = 2$ with MAE of 0.070 Ha.

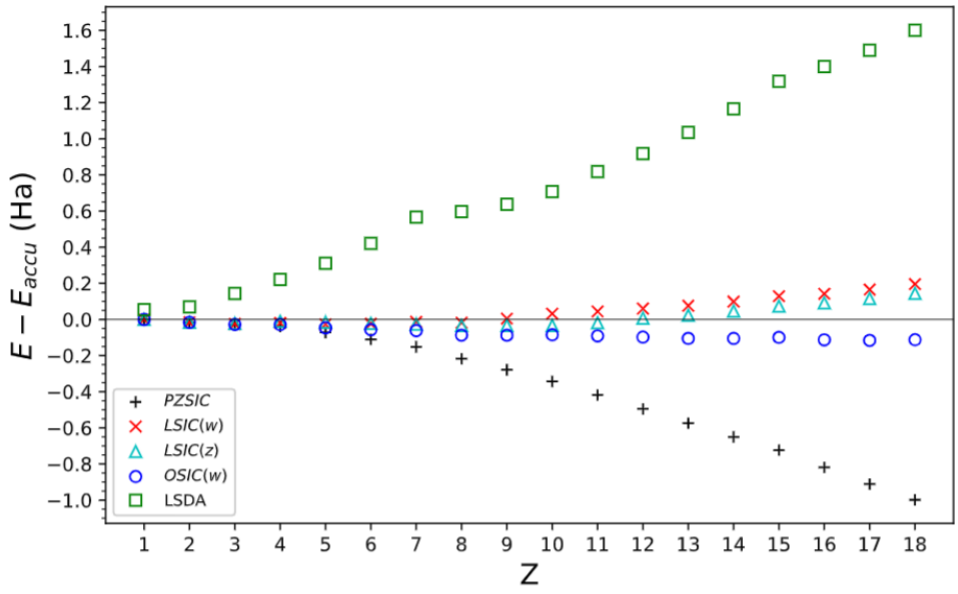

Fig. 2.1. Total energy difference (Ha) of atoms $Z = 1 - 18$ with respect to the theoretical values from Ref. [99].

Table 2.1. Mean absolute error of the total atomic energy (in hartree) for atoms $Z = 1 - 18$ with respect to theoretical accurate energies.

Method	MAE
PZSIC	0.381
LSIC$(z, k = 1)$	0.041
LSIC$(w, k = 1)$	0.061
LSIC$(w, k = 2)$	0.196
LSIC$(w, k = 3)$	0.277
LSIC$(w, k = 4)$	0.332
OSIC$(w, k = 1)$	0.074
OSIC$(w, k = 2)$	0.070
OSIC$(w, k = 3)$	0.135

IONIZATION POTENTIAL

The ionization potential (IP) is the energy required to remove an electron from the outermost orbital. Since electron removal has a relation to the asymptotic shape of potential, one would expect SIC plays an important role in IPs. We calculated the IPs using the ΔSCF method defined as

$$E_{IP} = E_{cat} - E_{neut} \tag{2.10}$$

where E_{cat} is the total energy in the cationic state and E_{neut} is the total energy at the neutral state. The calculations were performed for atoms from helium to krypton, and we compared the computed IPs against the experimental ionization energies [101]. Fig. 2 shows the energy difference of IPs with respect to the reference values. MAEs were also calculated and shown in Table 2. We show MAEs for a subset $Z = 2 - 18$ as well as for the entire set $Z = 2 - 36$ to facilitate a comparison against literature. For the smaller subset, Z= 2−18, we observe that the MAEs are 0.248, 0.206 and 0.223 eV for PZSIC, LSIC(z) and OSIC(w,$k = 1$), respectively. LSIC(w,$k = 1$) show MAE of 0.251 eV, a similar error as PZSIC. MAEs increase for LSIC(w, $k \geq 2$) in comparison to LSIC(w,$k = 1$). Interestingly, however, when we considered the entire set of atoms ($Z = 2 - 36$), LSIC(w) has MAEs of 0.238 and 0.216 eV for $k = 1$ and $k = 2$ respectively showing a smaller error than PZSIC (MAE, 0.364 eV) but fall short to LSIC(z) (MAE, 0.170 eV). For this case, OSIC(w,$k = 1$) (0.267 eV) shows performance worse than LSIC(w,$k = 1$), and this trend remains for all k. Investigating outliers, we observe that Ti for LSIC(w) and LSIC(z) show 12.5 and 3 % of deviation from reference, the difference comes mainly from cation total energy. Likewise, Ni shows 13.6 and 2.2 % of deviation. In contrast, a counter performance is present in K with -0.128 and -4.4 %, and Ca with -1.5 and 4.5 % respectively for LSIC(w) and LSIC(z).

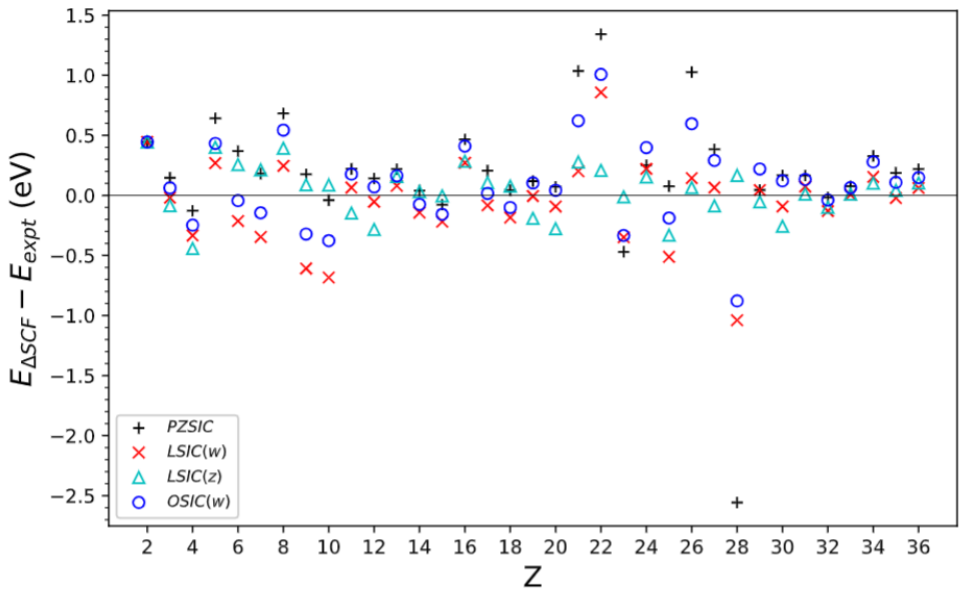

Fig. 2.2. Energy difference in ionization potential (in eV) for a set of atoms $Z = 2 - 36$ with respect to experiment.

Table 2.2. Mean absolute error of ionization potentials (in eV) for set of atoms $Z = 2 - 18$ and $Z = 2 - 36$ with respect to experiment.

Method	Z=2-18 (17-IPs)	Z=2-36(35-IPs)
PZSIC	0.248	0.364
LSIC$(z, k = 1)$	0.206	0.170
LSIC$(w, k = 1)$	0.251	0.238
LSIC$(w, k = 2)$	0.271	0.216
LSIC$(w, k = 3)$	0.297	0.247
LSIC$(w, k = 4)$	0.324	0.284
OSIC$(w, k = 1)$	0.223	0.267
OSIC$(w, k = 2)$	0.247	0.247
OSIC$(w, k = 3)$	0.255	0.259

ELECTRON AFFINITY

The electron affinity (EA) is the energy needed to add an electron to a system. We studied EAs for 20 atoms that are experimentally found to bind an electron [101]. They are H, Li, B, C, O, F, Na, Al, Si, P, S, Cl, K, Ti, Cu, Ga, Ge, As, Se, and Br. The EAs were calculated using the ΔSCF method $E_{EA} = E_{neut} - E_{anion}$ and the values were compared against the experimental EAs [101].

Fig. 2.3 shows the energy difference of EAs with the reference using several methods. MAEs are summarized in Table 2.3. Similarly to IPs, we present the MAEs for smaller subset, hydrogen to chlorine (12 EAs) and for the complete set, hydrogen to bromine (20 EAs). MAEs for PZSIC, LSIC(z), LSIC(w, $k = 1$), and OSIC(w, $k = 1$) are 0.152, 0.097, 0.235, and 0.152 eV, respectively for 12 EAs. MAEs for 20 EAs are 0.190, 0.102, 0.224, and 0.172 eV, in the respective order. The MAEs of 12 EAs and 20 EAs for LSIC(w) and OSIC(w) methods tend to decrease as k increases.

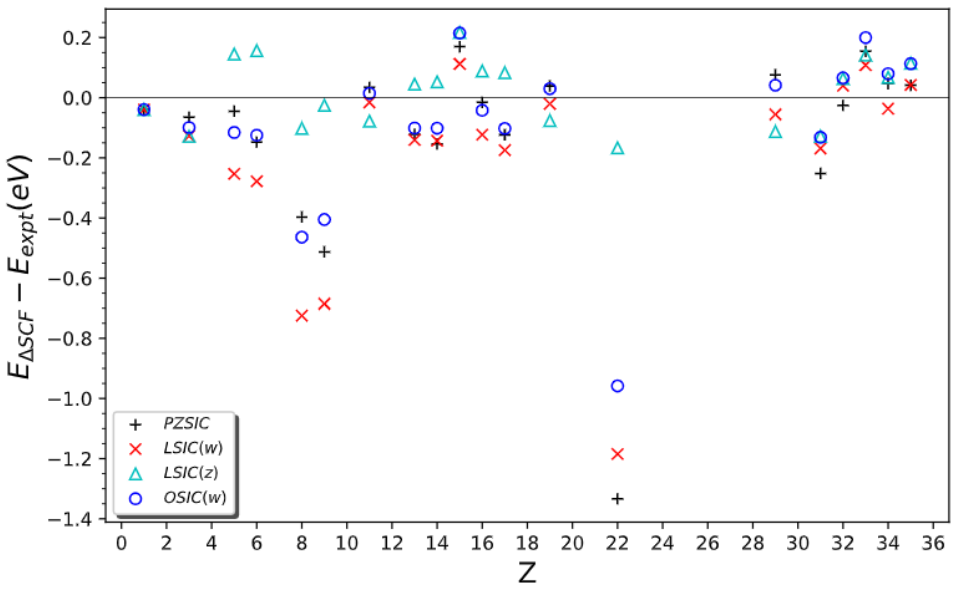

Fig. 2.3. Electron affinity (eV) for atoms Z=2 − 36.

Table 2.3. Mean absolute error in electron affinities (in eV) for 12 EAs and 20 EAs set of atoms with respect to experimental.

Method	(12 EAs) MAE	(20 EAs) MAE
PZSIC	0.152	0.190
LSIC$(z, k = 1)$	0.097	0.102
LSIC$(w, k = 1)$	0.235	0.224
LSIC$(w, k = 2)$	0.229	0.205
LSIC$(w, k = 3)$	0.215	0.189
LSIC$(w, k = 4)$	0.202	0.176
OSIC$(w, k = 1)$	0.152	0.172
OSIC$(w, k = 2)$	0.150	0.164
OSIC$(w, k = 3)$	0.145	0.155

2.4.2 ATOMIZATION ENERGY

To study the performance of LSIC(w) for molecules, first, we calculated the atomization energies (AEs) of 37 selected molecules. Many of these molecules are subset of the G2/97test set [149]. The 37 molecules set includes systems from the AE6 set [102], small but a good representative of the main group atomization energy (MGAE109) set [103]. The AEs were calculated by taking the energy difference of the fragment atoms and the complex as

$$AE = \sum_i^{N_{atom}} E_i - E_{mol} > 0 \tag{2.11}$$

where E_i is the total energy of an atom, E_{mol} is the total energy of the molecule, and N_{atom} is the number of atoms in the molecule. The calculated AEs are compared to the non-spin-orbit coupling values [103] for AE6 set and to the experimental values [101] for the set of 37 molecules. The percentage errors obtained through various methods are shown in Fig. 2.4. The AEs overestimated with PZSIC-LSDA are reduce with the application of LSIC(w). In Table 2.4, we show MAEs and mean absolute percentage errors (MAPEs) of AE6 set and MAPEs of the full set of molecules for

various theories. For AE6 set, MAEs for PZSIC, LSIC(z), LSIC(w, $k = 1$) and OSIC(w, $k = 1$) are 57.9, 10.0, 13.8 and 33.7 kcal/mol respectively. We find that LSIC(z) and LSIC(w, $k = 1$) differ by only a few kcal/mol, and LSIC(w) shows noticeably better performance than PZSIC or OSIC(w). For the larger k in LSIC(w), however, we find the performance starts to degrade. On the contrast, the performance for OSIC improves with larger k. But we expect the OSIC performance to degrade eventually since OSIC recovers DFA in the large k limit. For the full set of 37molecules, PZSIC, LSIC(z), LSIC(w, $k = 1$), and OSIC(w, $k = 1$) show the MAPEs of 13.4, 6.9, 9.5 and 11.9 % respectively against experimentally reported AEs. The other values of k for LSIC(w) tested show MAPE within ± 0.4 % of LSIC(w, $k = 1$). OSIC(w) shows a few percent improvement in MAPE for larger k. Interestingly, in the comparison against the experimental AEs, LSIC(w) consistently shows smaller MAPEs than OSIC(w) for $k = 1 - 3$. All value of k with the LSIC(w) in this study showed better performance than PZSIC for the 37 molecules set.

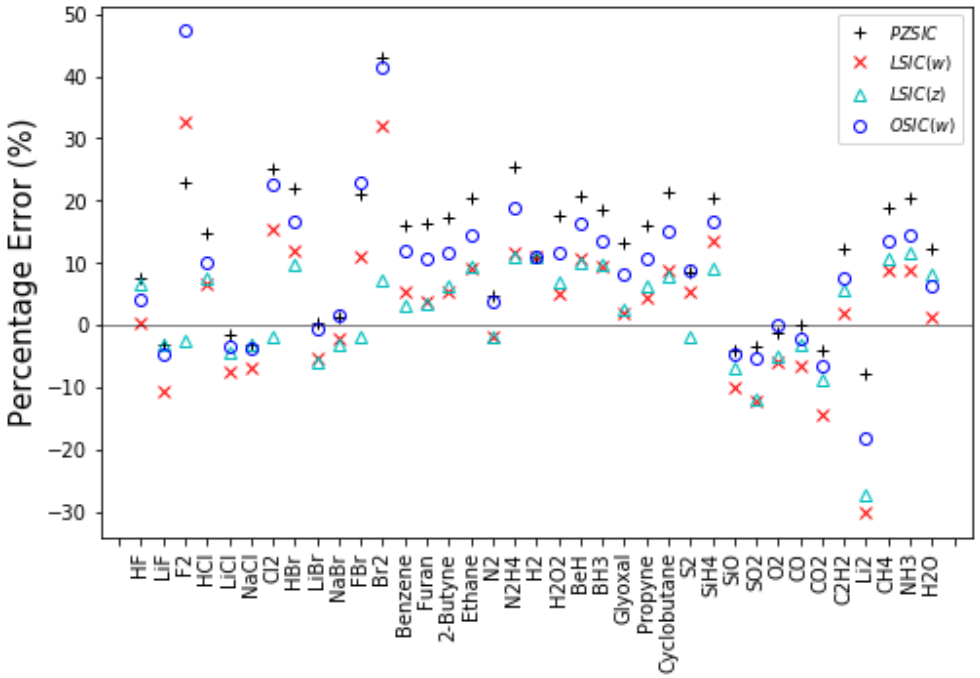

Fig. 2.4. Percentage difference of atomization energy (%) for a set of 37 molecules with respect to experimental reference values for various methods.

Table 2.4. Mean absolute error (in kcal/mol) and mean absolute percentage error (in %) of atomization energy for AE6 set of molecules and a set of 37 molecules.

Method	AE6 MAE (kcal/mol)	AE6 MAPE (%)	37 molecules MAPE (%)
PZSIC	57.9	9.37	13.43
LSIC$(z, k = 1)$	9.9	3.20	6.94
LSIC$(w, k = 1)$	13.8	4.41	9.46
LSIC$(w, k = 2)$	18.6	5.28	9.06
LSIC$(w, k = 3)$	26.9	5.82	9.20
LSIC$(w, k = 4)$	33.5	6.69	9.70
OSIC$(w, k = 1)$	33.7	6.29	11.92
OSIC$(w, k = 2)$	24.1	5.10	11.33
OSIC$(w, k = 3)$	17.8	4.31	10.88

2.4.3 BARRIER HEIGHTS

Accurately describing a chemical reaction barrier is challenging for DFAs. SIC improves providing an accurate picture of reaction barriers. Applying a scaled-down PZSIC to barrier height calculations is a real test whether it retains the benefit of PZSIC. We studied the reaction barriers using the BH6 set of molecules for LSIC(w) method. BH6 is a representative subset of the larger BH24 set consisting of three reactions $OH + CH_4 \rightarrow CH_3 + H_2O$, $H + OH \rightarrow H_2 + O$, and $H + H_2S \rightarrow H_2 + HS$. We calculated the total energies of left- and right-hand side and at the saddle point of these chemical reactions. The barrier heights for the forward (f) and reverse (r) reactions were obtained by taking the energy differences of their corresponding reaction states.

The barrier heights are typically poorly described by DFAs. In most of the cases, the saddle point energies are underestimated since DFAs do not perform well for a non-equilibrium state that involves a stretched bond. This misbehavior of DFAs on a stretched bond arises from SIE; when an electron is shared and stretched out, SIE incorrectly lowers the energy. SIC handles the stretched bond states accurately and provides a correct picture in chemical reaction paths. We computed the barrier heights and compared them against the reference values [102]. Mean errors (MEs) and

MAEs for BH6 set are summarized in Table 2.5 MAEs for PZSIC, LSIC(z), LSIC(w, $k = 1$), and OSIC(w, $k = 1$) are 4.84, 1.30, 3.64, and 3.58 kcal/mol, respectively. PZSIC reduces MAE compared to LSDA, but the barrier heights are still underestimated. This can be seen from its ME and MAE. OSIC(w) shows marginally better performance in barrier heights than PZSIC. There is no dramatic improvement in MEs and MAEs. LSIC(w, $k = 1$) further reduces the error from PZSIC. Its ME and MAE indicate that there is no systematic underestimation or overestimation. LSIC(w, $k = 1$) shows laudable improvement over PZSIC but not as good as LSIC(z). For $k \geq 2$, MAEs increase systematically for LSIC(w, $k \geq 2$) though small MEs are seen for LSIC(w, $k = 2,3$).The performance deteriorates for $k \geq 2$.

Table 2.5. Mean error (in kcal/mol) and mean absolute error (in kcal/mol) of BH6 sets of chemical reactions.

Method	ME (kcal/mol)	MAE (kcal/mol)
PZSIC	-4.84	4.84
LSIC($z, k = 1$)	0.70	1.30
LSIC($w, k = 1$)	-0.99	3.64
LSIC($w, k = 2$)	-0.13	4.55
LSIC($w, k = 3$)	0.33	5.02
LSIC($w, k = 4$)	0.63	5.51
OSIC($w, k = 1$)	-3.38	3.58
OSIC($w, k = 2$)	-3.12	4.12
OSIC($w, k = 3$)	-3.00	4.60

2.4.4 DISSOCIATION AND REACTION ENERGIES

A pronounced SIE effect can be seen by considering dissociation of positively charged dimers X_2^+. SIE causes the system to dissociate into two $X^{+0.5}$ instead of X and X^+. To account for the effect of SIE, it is worthwhile to study a set of chemical reactions that are directly affected by

SIE. In this section, we show our study of the SIE4x4 [58] and SIE11 [59] sets. The SIE4x4 set consists of dissociation energy calculations of four positively charged dimers at varying distances R from their equilibrium distance R_e such that $R/R_e = 1.0, 1.25, 1.5$ and 1.75. The dissociation energy E_D is calculated as

$$E_D = E(X) + E(X^+) - E(X_2^+) \tag{2.12}$$

the SIE11 set consists of eleven reaction energy calculations: six cationic reactions and five neutral reactions. These two sets are commonly used for SIE related problems. The calculated dissociation and reaction energies were compared against the CCSD(T) reference values [104,150], and MAEs were obtained. The MAEs are summarized in Table 2.6. For the SIE4x4 set, PZSIC, LSIC(z), LSIC(w, $k = 1$), and OSIC(w, $k = 1$) show MAEs of 3.0, 2.6, 4.7 and 5.2 kcal/mol. LSIC(z) provides small improvement in equilibrium energies while keeping accurate behavior of PZSIC at the dissociation limit resulting in marginally better performance. LSIC(w) shows errors a few kcal/mol larger than PZSIC. This increase in error arises because LSIC(w) changes the $(NH_3)_2^+$ dissociation curve. OSIC(w) has a slightly larger error than LSIC(w).

Table 2.6. Mean absolute error for dissociation and reaction energies (in kcal/mol) of SIE4x4 and SIE11 sets of chemical reactions.

Reaction	SIE4x4	SIE11	SIE11, 5 cationic	SIE11, 6 neutral
PZSIC	3.0	11.5	14.9	8.7
LSIC(z)	2.6	4.5	2.3	6.3
LSIC(w) (k=1)	4.7	8.3	8.6	8.0
LSIC(w) (k=2)	5.5	8.3	8.3	8.3
LSIC(w) (k=3)	5.8	8.8	8.2	9.3
LSIC(w) (k=4)	5.9	9.3	8.2	10.2
OSIC(w) (k=1)	5.2	11.1	13.7	9.0
OSIC(w) (k=2)	6.0	11.0	13.5	9.0
OSIC(w) (k=3)	6.4	10.9	13.3	8.8

For the SIE11 set, MAEs are 11.5, 4.5, 8.3, and 11.1 kcal/mol for PZSIC, LSIC(z), LSIC(w, $k = 1$), and OSIC(w, $k = 1$), respectively. For both z and w, LSIC showed improvement in performance from PZSIC. LSIC(z) shows the error reduction of 60%, and LSIC(w, $k = 1$) shows 28% compared to PZSIC. OSIC(w)'s MAEs are within 1 kcal/mol of PZSIC. But OSIC performance is expected to deteriorate after an SCF cycle. LSIC method improves more for cationic reactions than neutral reactions with respect to PZSIC. For LSIC(w, $k \geq 2$), there are slight increases in MAEs up to 1.0 kcal/mol. LSIC(w) yielded consistently smaller MAEs than OSIC(w) for SIE11.

Finally, we show the ground-state dissociation curves for H_2^+ and He_2^+ in Fig. 2.5. As previously discussed in literature [60], DFAs at large separation cause the fragment atoms to dissociate into two $H^{+0.5}$ fragments. PZSIC restores the correct dissociation behavior at the large separation distance. When LSIC is applied, the behavior of PZSIC at the dissociation limit is preserved in both LSIC(z) and LSIC(w). For H_2^+, a one-electron system, LSIC reproduces the identical behavior as PZSIC [Fig. 2.5 (a)]. For He_2^+, a three-electron system, LSIC applies the correction only to near equilibrium distance where more than one electron (two in this case) have an interaction [Fig. 2.5 (b)]. LSIC brings the equilibrium energy closer to PBE energy. The implication is that the selected iso-orbital indicator behaves well for differentiating the single-orbital like regions and many-electron like regions.

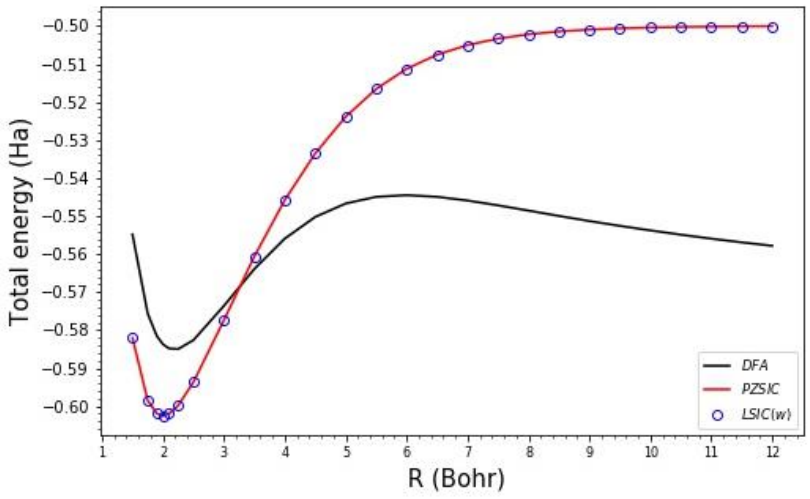

(a)

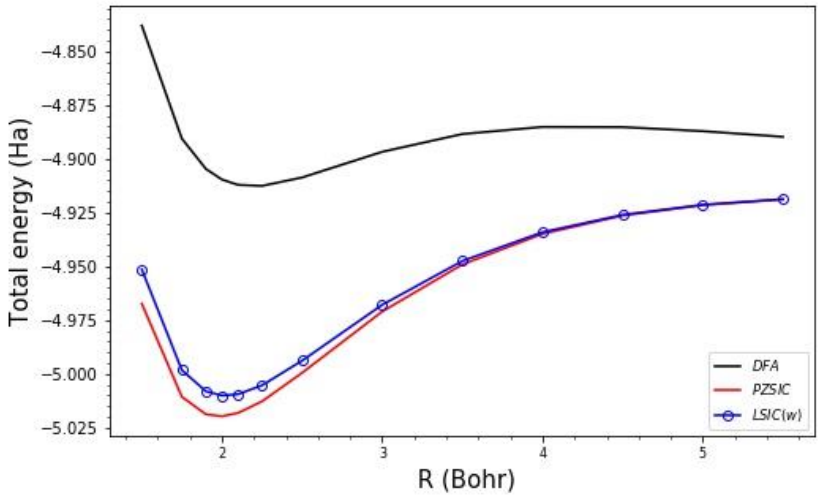

(b)

Fig. 2.5. Dissociation curves of (a) H_2^+ and (b) He_2^+.

2.5 DISCUSSION

LSIC(w) uses $w_{i\sigma} = \rho_{i\sigma}/\rho_\sigma$ as the iso-orbital indicator in the LSIC method. The motivation to used this simpler indicator was inspired from the work of Vydrov *et al*. [32]. The calculation of $w_{i\sigma}$ is slightly inexpensive and easier to obtain than z_σ, and its simpler form may help us understand better about why the LSIC method works well in many electronic structure properties. Also, this indicator may accelerate the development of the variational LSIC implementation.

A study done by Santra and Perdew [107] showed that, although semilocal DFA functionals are designed to satisfy the uniform electron gas limit, this exact condition is no longer satisfied when PZSIC is applied to the functionals. There has been efforts to restore the condition to the PZSIC-DFA, but simply restoring the condition was not enough to resolve all of the poor performance in PZSIC. Nevertheless, it is a good indication if the method and iso-orbital indicator recover the broken exact condition. Santra and Perdew computed the exchange energies of noble gas atoms and extrapolated using the large-Z expansion of E_X as a fitting function. The calculations were

performed to obtain the exchange energy (E_X) of LSIC(w)-LSDA for Ne, Ar, Kr, and Xe atoms. Then the obtained set of E_X's were fitted into a curve using the fitting function,

$$\frac{E_X^{approx} - E_X^{exact}}{E_X^{exact}} \cdot 100\% = a + bx^2 + cx^3 \tag{2.13}$$

where $x = Z^{-1/3}$ and a, b and c are fitting parameters. The obtained extrapolation curves are shown in Fig. 2.6. In the large-Z limit, the percentage error of LSIC(w) is 0.4 %, the correct limit within uncertainty.

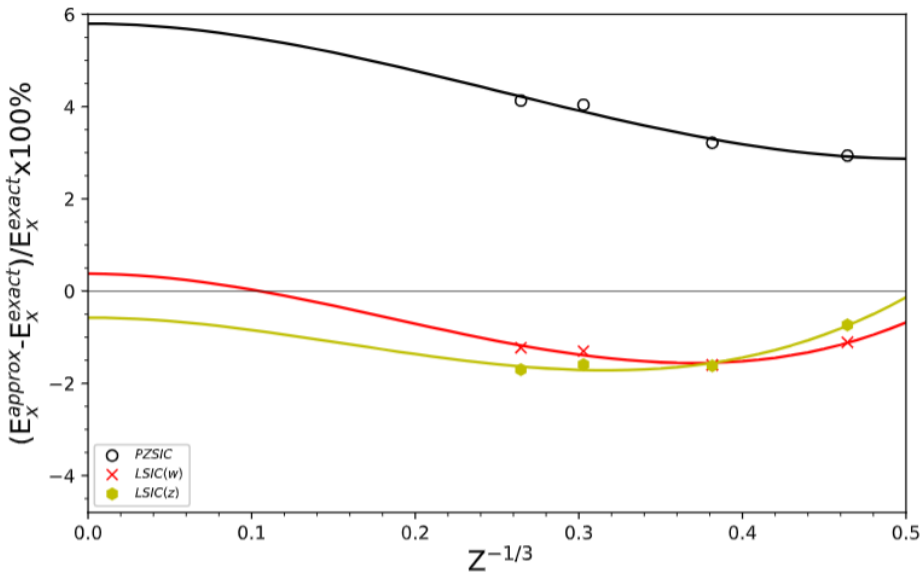

Fig. 2.6. Plot of percentage error of the approximated exchange energy compared to the exact exchange energy as a function of $Z^{-1/3}$.

2.6 CONCLUSIONS

We investigated the performance of LSIC with a simple iso-orbital indicator that only depends on local and total densities. This alternative iso-orbital indicator used with LSIC method gives performance comparable or slightly worse in comparison to the LSIC with z_σ for almost all cases. We also compared the performance of $w_{i\sigma}$ for LSIC against OSIC.

2.7 ACKNOWLEDGEMENT

Authors acknowledge Drs. Jorge Vargas and Luis Basurto and Mr. Carlos M. Diaz for discussions and technical supports. This work was supported by the US Department of Energy, Office of Science, Office of Basic Energy Sciences, as part of the Computational Chemical Sciences Program under Award No. DE-SC0018331. The work of R.R.Z. was supported in part by the US Department of Energy, Office of Science, Office of Basic Energy Sciences, under Award No. DE-SC0006818. Support for computational time at the Texas Advanced Computing Center through NSF Grant No. TG-DMR090071, and at NERSC is gratefully acknowledged.

CHAPTER 3: IMPROVEMENTS IN THE ORBITALWISE SCALING DOWN OF PERDEW–ZUNGER SELF-INTERACTION CORRECTION IN MANY-ELECTRON REGIONS

"Reproduced from Yoh Yamamoto, Selim Romero, Tunna Baruah, and Rajendra R. Zope. Improvements in the orbitalwise scaling down of Perdew–Zunger self-interaction correction in many-electron regions, J. Chem. Phys. 152, 174112 (2020); https://doi.org/10.1063/5.0004738 with permission of AIP Publishing"

3.1 ABSTRACT

The Perdew–Zunger (PZ) method provides a way to remove the self-interaction (SI) error from density functional approximations on an orbital by orbital basis. The PZ method provides significant improvements for the properties such as barrier heights or dissociation energies but results in over-correcting the properties well described by SI-uncorrected semi-local functional. One cure to rectify the over-correcting tendency is to scale down the magnitude of SI-correction of each orbital in the many-electron region. We have implemented the orbitalwise scaled down SI-correction (OSIC) scheme of Vydrov et al. [J. Chem. Phys. 124, 094108 (2006)] using the Fermi–Löwdin SI-correction method. After validating the OSIC implementation with previously reported OSIC-LSDA results, we examine its performance with the most successful non-empirical SCAN meta-GGA functional. Using different forms of scaling factors to identify one-electron regions, we assess the performance of OSIC-SCAN for a wide range of properties: total energies, ionization potentials and electron affinities for atoms, atomization energies, dissociation and reaction energies, and reaction barrier heights of molecules. Our results show that OSIC-SCAN provides superior results than the previously reported OSIC-LSDA, -PBE, and -TPSS results. Furthermore, we propose selective scaling of OSIC (SOSIC) to remove its major shortcoming that destroys the $-1/r$ asymptotic behavior of the potentials. The SOSIC method gives the highest occupied orbital eigenvalues practically identical to those in PZSIC and unlike OSIC provides bound atomic anions even with larger powers of scaling factors. SOSIC compared to PZSIC or OSIC provides a more balanced description of total energies and barrier heights.

3.2 INTRODUCTION

The Kohn–Sham (KS) formulation [1,2], of the density functional theory (DFT) is formally an exact approach to obtain the ground state energy of a many-electron system. It is by far the most widely used method for obtaining the electronic and structural properties of molecules and solids. Its practical applications require an approximation to the exact exchange-correlation functional that is representative of the non-classical energy contributions. There is no systematic way to construct the functional, and a large number of approximate functionals have been proposed and widely used. The exchange-correlation functional approximations are classified by Perdew and Schmidt [3] using an analogy to Jacob's ladder wherein the functional approximation corresponds to the rungs of a ladder. The earliest functional approximation is the celebrated local spin density approximation (LSDA) [4] that forms the first rung of the ladder. The functionals with more complex ingredients such as density gradients, density Laplacians, or Kohn–Sham orbitals belong to the higher rungs. Thus, the generalized-gradient approximation (GGA) [5,6], goes beyond the LSDA by capturing non-homogeneity of density using density gradients, corresponding to the second rung. Likewise, the third rung of the ladder corresponds to the meta-GGAs that use kinetic energy densities or density Laplacians, while the fourth one corresponds to the hyper-GGA functionals, examples of which are the hybrid functionals [7] that include certain percentages of the Hartree–Fock (HF) exchange in the functional approximation. The functionals from the second to fourth rungs (GGAs, meta-GGAs, and hyper-GGAs) are widely used today in the molecular physics, solid state physics, and materials science. These functionals can describe many physical properties with sufficient accuracy. Their efficient numerical implementations, available in a large number of easy-to-use codes, have led to a proliferation of density functional based studies. One shortcoming of the majority of the density functional approximations (DFAs) mentioned above is that these approximations suffer from the self-interaction error (SIE), which arises due to incomplete cancellation of the classical Coulomb interaction of an electron with itself by the approximate exchange-correlation term in the energy functional. In general, the modern semi-local functionals are sophisticated enough to provide a fairly accurate description of the equilibrium properties such as atomization energies, but they fail to describe the properties such as transition states in chemical reactions, charge-transfer excitations, binding of an electron in some anions, and dissociation of molecules. The SIE in these functionals is considered to be responsible for

these failures.[8,9] Indeed, the SIE is recognized to be a major limitation of DFAs that limits their universal usage [10-14] In 1981, Perdew and Zunger [9] (PZ) proposed a method to eliminate SIE on an orbital by orbital basis. They applied this self-interaction correction (SIC) scheme to the LSDA that was the only known approximation at that time and found significant improvements in atomic properties. Their scheme later came to be known as PZSIC. Subsequent calculations on molecules in the mid-1980s by the Wisconsin group [15-17] used localized orbitals to compute the self-interaction (SI) energies of molecules. Since then, a number of studies have used SIC implementations [8,18-59] to study atoms, molecules, and solids. It has been found in a number of studies that the PZSIC when used to compute thermochemical properties such as enthalpies of formation provides improvement over the LSDA functional, but the results are still not as accurate as those obtained using the GGAs. In particular, PZSIC when used with GGAs and meta-GGAs often worsens the results for thermochemical properties. It, however, does provide significantly improved results for properties such as reaction barriers and barrier heights where chemical bonds are stretched. This improvement is observed for all the DFAs (LSDA, GGA, and metaGGAs). This conflicting performance of PZSIC for thermochemical properties and barrier heights is called the *paradox of PZSIC* [68], resolution of which was recently suggested by using the local scaling of the exchange-correlation and Coulomb energy densities [69]. A few schemes to rectify the over-correcting tendency of PZSIC have been proposed and examined. Klüpfel and co-workers [70] scaled down the entire SIC contribution by 50% and reported improved performance in atomization energy. They also reported that using complex orbitals can improve the performance, especially in the case of LSDA. In 2006, Vydrov *et al.* [30] proposed a method that scales down SIC in the many-electron region using an iso-orbital indicator weighted by the density of the local orbital. To distinguish from the constant (*global*) scaling approach of Jónsson and co-workers, we shall hereafter call the orbital dependent scaling approach by Vydrov and co-workers the *orbital scaling* method. Vydrov and co-workers examined in detail the performance of various powers of scaling factors for correcting the SIE in the LSDA, Perdew, Burke, and Ernzerhof (PBE) [5]; Tao, Perdew, Staroverov, and Scuseria (TPSS) [71]; and a hybrid of PBE with 25% of exact exchange (PBEh) [72,73] functionals. Subsequently, they also employed the orbital scaling to SIC to study the effect of scaled down SIC on the dissociation curves of H_2^+ , He_2^+ , LiH^+, and Ne_2^+ [74] . They found that only the unscaled PZSIC consistently yielded qualitatively correct curves for all four systems [74]. Their orbital scaling approach to PZSIC is free from exact one- and nearly exact

two-electron SI but still suffers many-electron SIE [74]. Thus, the benefit of the orbital scaling was primarily limited to equilibrium properties.

Since the report of the work by Vydrov and co-workers, a number of advances in the functional development have been reported. One important advance at the meta-GGA level is the development of *strongly constrained and appropriately normed* (SCAN) semilocal functional [75]. SCAN satisfies all 17 known exact constraints that a meta-GGA functional can satisfy. A number of studies reported in the literature show that the SCAN functional provides improvement over other functionals for a wide variety of solid-state and molecular properties [76-78]. Recently, we investigated the performance of the SCAN functional and self-interaction corrected SCAN functional for a wide array of molecular properties and found that eliminating self-interaction errors improves the performance of SCAN for dissociation energies and barrier heights, but it worsens the atomization energies [79]. The goal of the present work is multifold. We first want to examine the performance of orbital scaling when used with SCAN meta-GGA functionals for various electronic properties such as total atomic energies, ionization potentials (IP), electron affinities (EA), molecules atomization energies, reaction barrier heights, and dissociation and reaction energies. We also want to explore the use of alternative scaling factors in order to see if they provide any improvement over the scaling factor used by Vyrdov and co-workers. Finally, we want to explore if the orbital scaling approach can be modified by differentially scaling the SIC for orbitals to obtain even better all-around performance. We illustrate this idea by proposing a new orbital scaling scheme that preserves correct -1/*r* asymptotic behavior of the potentials for atoms. We also show that this new scaling scheme leads to significant improvements over the original orbital scaling approach for a number of properties.

3.2 THEORY

The PZSIC method removes the SIE in the approximate density functionals by means of orbital-dependent corrections to the approximate functional as follows:

$$E_{XC}^{PZSIC-DFA} = E_{XC}^{DFA}[\rho_{\uparrow}, \rho_{\downarrow}] - \sum_{i\sigma}^{occ}\{U[\rho_{i\sigma}] + E_{XC}^{DFA}[\rho_{i\sigma}, 0]\}. \quad (3.1)$$

Here, $\rho_{i\sigma}$ is the density of the ith orbital of spin σ, and $U[\rho_{i\sigma}]$ and $E_{XC}^{DFA}[\rho_{i\sigma}]$ are the self-Coulomb and the self-exchange-correlation energies, respectively. In their 1981 work, Perdew and Zunger [9] presented SIC calculations on atoms using the orbital densities obtained from the KS orbitals. They also noted that the delocalized nature of KS orbitals for extended systems will make the SIC non-size-extensive. Subsequently, Pederson, Heaton, and Lin [16,17] implemented PZSIC using local orbitals and performed the first SIC calculation on molecules. These localized orbitals are obtained from the unitary transformation of the KS orbitals by minimizing the energy, which results in the Pederson localization equation,

$$\langle \phi_{i\sigma} | V_{i\sigma}^{SIC} - V_{j\sigma}^{SIC} | \phi_{j\sigma} \rangle = 0. \tag{3.2}$$

Fermi–Löwdin orbital SIC (FLOSIC) [80] is a recently proposed approach to remove the SIE using the PZSIC methodology. In the FLOSIC, the optimal local orbitals, called Fermi–Löwdin orbitals (FLOs), are obtained by a unitary transformation that depends on position-like variables such that the unitary invariance of the total energy is ensured. The Fermi orbitals are constructed by introducing the Fermi orbital descriptor (FOD) positions [81-83]. Using the FOD positions $\boldsymbol{a}_j$, the KS orbitals ψ_i are transformed into the Fermi orbitals ϕ_j as follows:

$$\phi_i(\vec{r}) = \sum_j^{N_{occu}} \frac{\psi_j(\vec{a_i})\psi_j(\vec{r})}{\sqrt{\rho_i(\vec{a_i})}}. \tag{3.3}$$

here, N is the number of occupied orbitals. The localized Fermi orbitals $\{\phi_i\}$ are subsequently orthogonalized using Löwdin orthogonalization to obtain the FLOs. By finding the optimal FOD positions that minimize the total energy, we can find the solution of Eq. (3.1). The optimal positions of the FODs are obtained by minimizing the energy using either the conjugate-gradient method or the L-BFGS algorithm [84].

As mentioned in Sec. 3.1, the application of PZSIC worsens the description of equilibrium properties when used with semilocal functionals. To rectify the overcorrecting tendency of PZSIC, Vydrov and co-workers [30] scaled down the SIC in the many-electron region using an orbital dependent scaling factor, $X_{i\sigma}^k = \int z_\sigma^k(\vec{r})\rho_{i\sigma}(\vec{r})d\vec{r}$. Here, k is an integer and $z_\sigma(\vec{r}) = \tau_\sigma^W(\vec{r})/\tau_\sigma(\vec{r})$, where $\tau_\sigma(\vec{r}) = \frac{1}{2}\sum_i |\nabla\psi_{i\sigma}(\vec{r})|^2$, is the non-interacting kinetic energy density, and

τ_σ^W is the von Weizsäcker kinetic energy density. The iso-orbital indicator z_σ is a function of position in space and interpolates between the uniform density region ($z_\sigma = 0$) and one-electron region, $z_\sigma = 1$. Vydrov *et al.* [30] recommended $k \geq 3$ for the TPSS meta-GGA to preserve the correct fourth-order expansion in the limit of slow varying density. The same consideration should apply to SCAN meta-GGA. This way of scaling down PZSIC with an orbital dependent scaling factor will be hereafter referred to as OSIC.

The SIC energy in the OSIC approach of Vydrov *et al.* [30] is given by

$$E^{OSIC} = -\sum_{i\sigma}^{OCC} X_{i\sigma}^{k}(U[\rho_{i\sigma}] + E_{XC}^{DFA}[\rho_{i\sigma}, 0]). \tag{3.4}$$

it is evident that OSIC reduces to PZSIC for $k = 0$. In the $k \to \infty$ limit, Eq. (3.4) becomes zero with an exception of one-electron system. For the one-electron systems, the scaling factor will be 1 for any integer k. The scaling factor $z\sigma(\vec{r}) = \tau_\sigma^W(\vec{r})/\tau_\sigma(\vec{r})$ has the advantage that it vanishes in the uniform electron gas limit. It is not the only choice for the scaling factor in OSIC. A number of alternative choices can be made. Vydrov and Scuseria subsequently used the ratio of the orbital density to the total-spin density [32]. This does not require kinetic-energy densities and gave results comparable to those obtained using $z_\sigma(\vec{r}) = \tau_\sigma^W(\vec{r})/\tau_\sigma(\vec{r})$. In this work, we also explore the use of two other scaling factors. The first one is the electron localization function (ELF) introduced by Becke and Edgecombe [85]. The ELF is commonly used for classifying chemical bonds and is defined as follows:

$$ELF = \frac{1}{1+\alpha^2} \tag{3.5}$$

where $\alpha = (\tau - \tau^W)/\tau^{unif}$ and $\tau^{unif} = \left(\frac{3}{10}\right)(3\pi^2)^{2/3}\rho^{5/3}$ is τ in the uniform-density limit. Using ELF in place of z_σ partially satisfies the correct limits of the OSIC scaling factor. Although $ELF = 1$ for the single orbital limit, $ELF = 0.5$ in the uniform gas limit. Additionally, we also use β, another iso-orbital indicator defined as

$$\beta = \frac{\tau-\tau^W}{\tau-\tau^{unif}} \tag{3.6}$$

which has been used recently in the construction of meta-GGA functionals [86]. Following how β is used in the functional design, we use $1-(2\beta)^2$ as the alternative for z_σ in $X_{i\sigma}^k$. Although this form can become negative, we included it nonetheless for comparison since it has the correct interpolation between the single orbital limit, $\lim_{\tau\to\tau^W}\{1-(2\beta)^2\}=1$, and uniform-gas limit, $\lim_{|\nabla\rho|\to 0,\tau\to\tau^{unif}}\{1-(2\beta)2\}=0$, since τ^W becomes 0. Thus, OSIC with this scaling factor also recovers the uniform gas limit as the SI-correction vanishes in this limit and OSIC reduces to the DFA.

Appraisal of the orbital scaling factor for various electronic properties [30] showed that orbital scaling requires different values of k for different properties to obtain improved results. For example, excellent atomic energies are obtained for $k=4$, but $k=1$ or less is needed to obtain good estimates of reaction barrier heights. The orbitalwise scaling down of PZSIC leads to violation of some exact constraints satisfied in PZSIC. One such consequence is that it destroys the desirable correct $-1/r$ behavior of the exchange-correlation potential of the PZSIC. The orbital scaling of Eq. (3.4) also provides poor performance for many-electron SIC [74] compared to the original PZSIC. As the asymptotic behavior is important in many physical processes such as electron delocalization or in an accurate description of the charge transfer process, a new scaling approach that preserves $-1/r$ asymptotic of the potential can be formulated. We refer to this approach as selective-scaling-OSIC (SOSIC). The SOSIC correction to the energy in this approach is given by

$$E^{SOSIC}=-\sum_{i\sigma}^{M}X_{i\sigma}^{k}\left(U[\rho_{i\sigma}]+E_{XC}^{DFA}[\rho_{i\sigma},0]\right)-\sum_{i\sigma}^{P}Y_{i\sigma}\left(U[\rho_{i\sigma}]+E_{XC}^{DFA}[\rho_{i\sigma},0]\right), \tag{3.7}$$

where $M=N-P$, with N being the total number of occupied electrons. P is the number of local orbitals corresponding to the electrons in the highest occupied orbital (HOO) shell. For example, for an Ar atom, $P=8$ as there are six electrons in the degenerate HOO shell that project onto 8 sp^3 local orbitals. We set $Y_{i\sigma}=1$ to maintain the accurate asymptotic description of the

exchange-correlation potential. We shall show later that this SOSIC essentially preserves the accuracy of unscaled PZSIC HOO eigenvalues and leads to overall improvements of electronic properties in both the equilibrium cases as well as in stretched bond situations. The application of SOSIC requires identifying the FODs or FLOs that correspond to the HOO. This can be accomplished by finding the FLO that has a maximal overlap with the KS HOO. We note that even though we used $Y_{i\sigma}$ as unity, its value can be adjusted so that the negative of HOO eigenvalue matches with the exact experimental ionization potential. Adjusting the potential so that the magnitude of the HOO eigenvalue agrees with the first ionization potential has been done previously in the context of fully analytic (grid free) Slater–Roothaan method [87]. In recent years, a similar procedure has been used to obtain the range separation parameters in many applications of the range separated hybrid method [88–92].

We implemented the OSIC and SOSIC method in the FLOSIC code [93,94] that is based on UTEP-NRLMOL. The Porezag–Pederson NRLMOL basis set [95], which is roughly similar to quadruple zeta quality basis, was used. FLOSIC uses a variational mesh [96] that provides efficient numerical integration. The SCAN meta-GGA [75] was recently implemented [79] in the FLOSIC code. We used very dense mesh tailored for SCAN that provides energy convergence with respect to the radial mesh within 10-8 hartree accuracy [79]. For calculations of anions, in addition to NRLMOL extra basis sets, long range s, p, and d single Gaussian orbitals are used here their exponents (β) are extrapolated from the Nth basis of a given system using a relation as $\beta(N)2/\beta(N-1)$. This inclusion of additional diffuse exponents was suggested by Withanage *et al.* [97] for giving better descriptions of the extended nature of the anions. The full Hamiltonian in the OSIC is given by

$$H_i = -\frac{1}{2}\nabla^2 + v(\vec{r}) + \int \frac{\rho(\overrightarrow{r'})}{|\vec{r} - \overrightarrow{r'}|} d\overrightarrow{r'} + v_{XC}^{DFA}([\rho_\uparrow, \rho_\downarrow], \vec{r})$$
$$- X_i^k \left(\int \frac{\rho(\overrightarrow{r'})}{|\vec{r} - \overrightarrow{r'}|} d\overrightarrow{r'} + v_{XC}^{DFA}([\rho_\uparrow, 0], \vec{r}) \right)$$
$$- z_\sigma^k(\vec{r})(U[\rho_{i\sigma}] + E_{XC}^{DFA}[\rho_{i\sigma}, 0])$$
$$- \sum_m (U[\rho_{i\sigma}] + E_{XC}^{DFA}[\rho_{i\sigma}, 0]) \frac{\partial X_m^k}{\partial \rho(\vec{r})}. \quad (3.8)$$

in the present implementation, we ignore the last two terms that arise due to the variation of scaling factors in constructing the Hamiltonian. The calculations are performed self-consistently using Jacobi updates [98] similar to earlier reported FLOSIC calculations [57–59,63–65,67,79,97], but they are not full variational due to the neglected terms. We assessed the importance of the neglected terms by comparing our OSIC results with those of Vydrov and co-workers for the LSDA functional and obtained essentially the same results for various electronic properties studied here. For instance, using the OSIC-LSDA with $k = 1$, mean absolute error (MAE) per electron of total energies for Li–Ar is 0.004 hartree in both methods, and MAEs for AE6 and BH6 are 18.0 kcal/mol and 3.3 kcal/mol with our implementation, whereas Vydrov *et al.* obtained 21.0 kcal/mol and 3.5 kcal/mol, respectively. The small differences can arise from the different choice of the basis sets used to obtain these MAEs. These results also indicate that variations in the scaling factor are not too crucial for the properties studied here. Full variational calculation will be implemented in the future. Thus, the orbital SIC energies are scaled down as Eqs. (3.4) or (3.7), and self-interaction correction to the Hamiltonian matrix elements of *i*th orbital is scaled down accordingly as Eq. (3.8) by ignoring the last two terms.

The orbital scaling calculations performed this way has comparable computational cost as PZSIC. The only additional cost is the calculation of the scaling factor, which is not significant. For SCAN calculations, the FODs used in this study were optimized at the FLOSIC-SCAN level of theory where a convergence tolerance of at least 10-6 hartree was used. For all orbital scaling calculations, the FOD positions and electron densities optimized at the FLOSIC-SCAN level of theory were used as a starting point for a given system. For the AE6, BH6, SIE4 × 4, and SIE11 calculations,

we used the geometries from the test sets as provided. The SIE4 × 4 calculations required us to use simple mixing with a larger mixing parameter α = 0.15–0.35 to achieve SCF convergence. OSIC-LSDA calculations were performed self-consistently in a similar fashion where we used FLOSIC-LSDA FODs and densities as a starting point.

Fig. 3.1 shows the values of the scaling factors $X_{i\sigma}^{k}$ for the Kr atom and benzene within OSIC-SCAN calculations. In both cases, core orbitals tend to have a larger value than the rest. For the case of benzene, the factors for C–C σ bonds and π bonds have the values less than 0.5. The actual values of the OSIC scaling factor depend on two elements: (i) compactness of the local orbital and (ii) size of the single orbital regions identified from the iso-orbital indicator. For instance, the scaling factor of core orbitals in benzene is larger than that of the 1s orbital in the Kr atom, as shown in the contour maps of the scaling factors in Fig. 3.2.

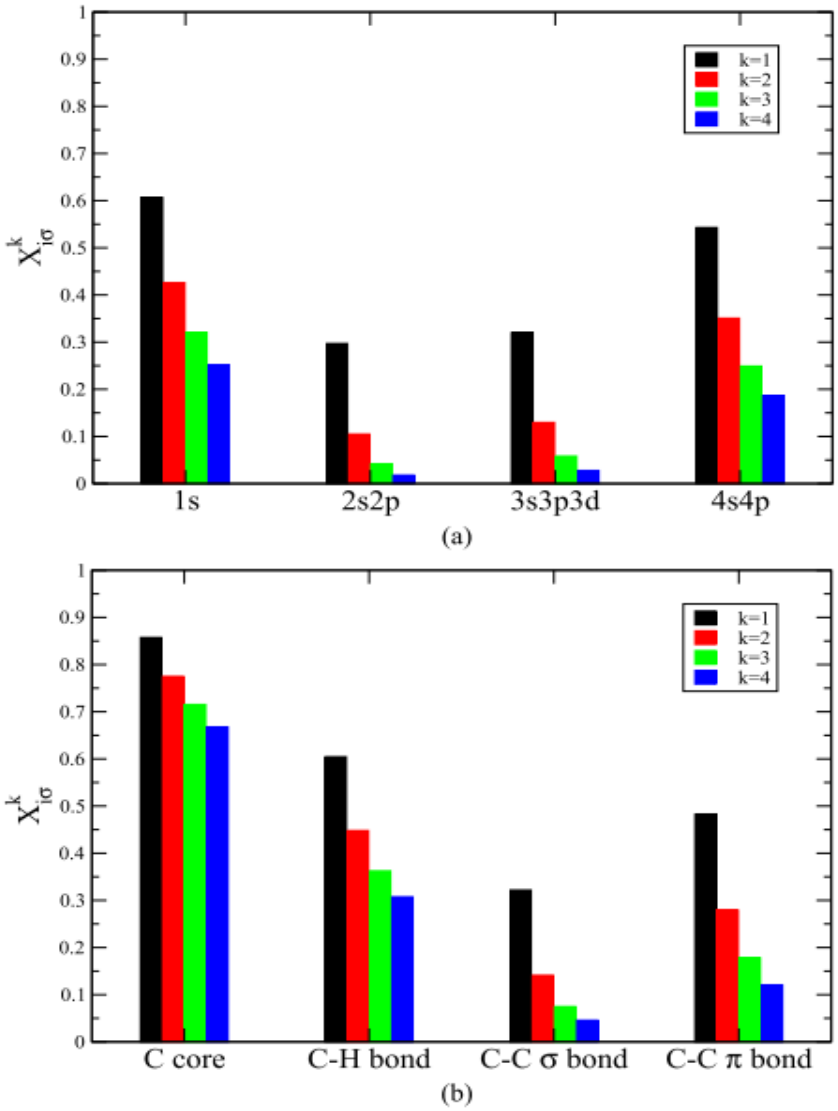

Fig. 3.1. Scaling factors $X_{i\sigma}^{k}$ with $z_{\sigma}(\vec{r}) = \tau_{\sigma}^{W}(\vec{r})/\tau_{\sigma}(\vec{r})$ and varying values of k: (a) the averaged values for each electron shell of the Kr atom and (b) the average values for each bond type of benzene.

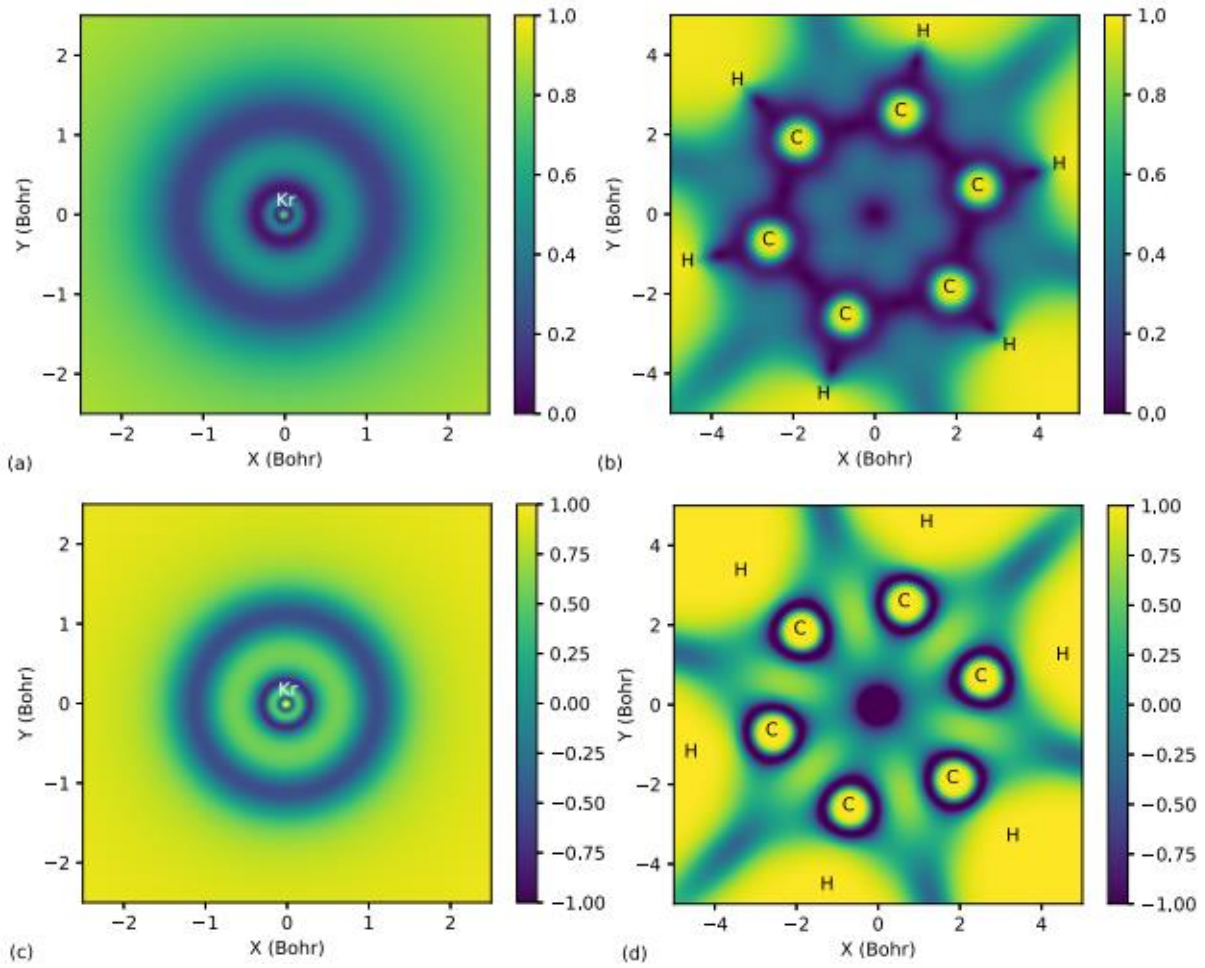

Fig. 3.2. The contour map of $z_\sigma(\vec{r}) = \tau_\sigma^W(\vec{r})/\tau_\sigma(\vec{r})$ for (a) the Kr atom and (b) benzene in OSIC-SCAN ($k = 1$) calculations. Similarly, $1 - (2\beta)^2$ is shown for the (c) Kr atom and (d) benzene. $z_\sigma(\vec{r}) = 1$ for the single orbital regions, and $z_\sigma(\vec{r}) = 1$ for the uniform density regions. For simplicity, only the spin-up kinetic energy density ratio is shown.

3.3 RESULTS

3.3.1 ATOMS: TOTAL ENERGIES, IONIZATION POTENTIALS, AND ELECTRON AFFINITIES

We studied atoms $Z = 1$–18 and compared the total energies using different scaling powers on PZSIC and OSIC with accurate non-relativistic calculated reference values obtained by

Chakravorty *et al.* [99] The total energy differences with respect to reference values are shown in Fig. 3.3 for various values of k. The PZSIC corresponds to $k = 0$, and all $k \geq 1$ results shown are with the OSIC method. We include the recently reported DFA-SCAN and PZSIC-SCAN results79] here for comparison. DFA-SCAN shows a small MAE of 0.019 hartree, and correcting for self-interaction results in significantly over-corrected total energies (MAE 0.147 hartree) with a systematic increase in error with an increase in the number of electrons. For Ar, the SI-correction is ~ 0.46 hartree. We note that the application of OSIC reduces the MAE, and as the k values increase, the MAE becomes smaller. The results for different scaling powers are summarized in Table 3.1. OSIC-SCAN with $k = 1$ reduces the MAE from 0.147 hartree to 0.069 hartree, whereas $k = 3$ shows comparable performance with DFA-SCAN. The best total energies are obtained with $k = 4$ with an MAE of only 0.012 hartree. These results are consistent with earlier reports [30] that increasing value of k results in better total energies. A comparison with previously reported results shows that OSIC-SCAN with $k = 4$ gives atomic energies that are better than the previously reported OSIC-LSDA, OSIC-PBE, or OSIC-TPSS. The MAE per electron of atoms Li to Ar for OSIC-SCAN $k = 4$ is 0.002 Hartree, whereas the reported best MAEs for OSIC-LSDA $k = 1$, OSIC-PBE $k = 3$, and OSIC-TPSS $k = 3$ are 0.004 hartree, 0.007 hartree, and 0.003 hartree, respectively.

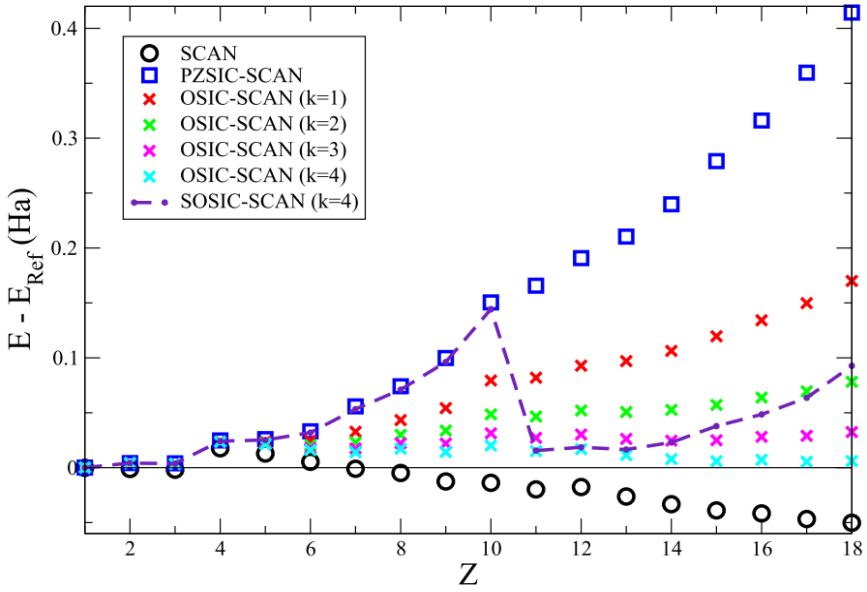

Fig. 3.3. Total energy difference (in Hartree) of atoms Z = 1–18 with respect to exact energies in various methods.

Table 3.1. The mean absolute error (MAE) of total atomic energies in various methods. These MAEs are in Hartree atomic unit.

Method	LSDA	SCAN	PBE[a,b]	TPSS[a,b]
DFA	0.726 (0.822)[a,b]	0.019	0.101	0.022
PZSIC	0.380 (0.420)[a,b]	0.147	0.183	0.278
OSIC ($k = 1$)	0.035 (0.037)[a,b]	0.069	0.118	0.131
OSIC ($k = 2$)	(0.205)[a,b]	0.038	0.095	0.073
OSIC ($k = 3$)	(0.316)[a,b]	0.021	0.085	0.042
OSIC ($k = 4$)		0.012		
SOSIC ($k = 4$)		0.043		
OSIC (z_σ = ELF, $k = 1$)	0.037	0.069		
OSIC [$z_\sigma = 1 - (2\beta)^2$, $k = 1$]	0.062	0.063		
LSIC	0.041[c]			

[a]Reference 30.
[b]MAE reported in the reference is for atom Z = 3–18.
[c]Reference 69.

IONIZATION POTENTIAL

Ionization potentials (IP's) and electron affinities (EA's) are determined by processes that involve electron removal and electron addition, respectively. These processes are therefore sensitive to the asymptotic structure of the effective potential. One would therefore expect that removal of self-interaction in DFAs would result in significant improvement in the quality of these quantities. In general, however, it has been found that these quantities calculated as the difference of total energies of neutral and charge systems are fairly accurately predicted by many DFAs. The calculation of IPs (EAs) from the self-consistent total energy differences of atoms and their cation (anion) is called the ΔSCF method [100]. We calculated the IPs for atoms from hydrogen through krypton using the ΔSCF method and compared them against the experimentally reported values from Ref. 101 in Table 3.2. To facilitate a direct comparison with the values reported by Vydrov et al., we also present results for a subset of atoms, from hydrogen through argon. For this smaller subset of atoms $Z = 2-18$, the MAEs are 0.175 eV and 0.274 eV for SCAN and PZSIC-SCAN, respectively. The OSIC-SCAN results for various k values have similar performance with MAEs within $0.178-0.181$ eV. Vydrov *et al.* [30] reported that the OSIC with $k = 2$ and 3 improves IPs of atoms $Z = 1-18$ for LSDA, PBE, TPSS, and PBEh functionals. A similar trend was also observed in the present OSIC-SCAN ionization potentials for the subset of atoms. For this subset, the DFA already performs well and OSIC lowers the larger errors produced by PZSIC bringing the resultant errors close to those in DFA and in some cases improves them further. However, if one extends the dataset to include a larger number of atoms ($Z = 2-36$), then a different trend is observed. In this case, PZSIC-SCAN (MAE of 0.259 eV) shows better performance than DFA-SCAN (MAE of 0.273 eV). The OSIC-SCAN results have MAEs ranging $0.304-0.349$ eV, and these errors are larger than those of both DFA and PZSIC. This result suggests that full SIC treatment is needed to obtain accurate estimates of IPs of heavier atoms. All OSIC results for the complete set ($Z = 2-36$) studied here have similar errors as we have seen for the smaller subset ($Z = 2-18$), but there is a slight but noticeable decrease in errors as the value of k increases.

Table 3.2. The mean absolute error (in eV) of ΔSCF ionization potentials computed in various methods.

	SCAN		PBE[a]	TPSS[a]
Method	Z = 2–18 (17 IPs)	Z = 2–36 (35 IPs)	Z = 1–18 (18 IPs)	Z = 1–18 (18 IPs)
DFA	0.175	0.273	0.15	0.12
PZSIC	0.274	0.259	0.39	0.34
OSIC (k = 1)	0.181	0.342	0.22	0.17
OSIC (k = 2)	0.178	0.322	0.15	0.12
OSIC (k = 3)	0.178	0.304	0.12	0.11
OSIC (k = 4)	0.183	0.294		
	LSDA			
Method	Z = 2–18 (17 IPs)	Z = 2–36 (35 IPs)		
LSIC[b]	0.206	0.170		

[a]Reference 30.
[b]Reference 69.

ELECTRON AFFINITY

We studied EAs of 20 atoms, specifically H, Li, B, C, O, F, Na, Al, Si, P, S, Cl, K, Ti, Cu, Ga, Ge, As, Se, and Br atoms. These 20 atoms are experimentally shown to bind an extra electron, and their experimental EAs are found in the NIST database in Ref. 101. Similar to the IP calculations, EAs were obtained using the ΔSCF approach.

In Table 3.3, we present results for a subset of 12 EAs for the first three rows of periodic table and the third column shows the results that include the fourth row in addition to the 12 EAs, resulting in 20 EAs. For the 12 EAs, DFA-SCAN shows the smallest error, but it has the problem of positive HOO eigenvalues. Correcting for SIE results in binding of the electron, and PZSIC-SCAN shows the MAE of 0.364 eV for ΔSCF EAs. The OSIC-SCAN with $k = 4$ improves the EAs to an MAE of 0.125 eV. For the larger set of 20 EAs, MAEs are 0.148 eV and 0.341 eV for SCAN and PZSIC-SCAN in the respective order. The OSIC-SCAN gives performance improvement, especially when $k = 2$ is used. The error in this case is the smallest with an MAE of 0.128 eV. Thus, OSIC-SCAN provides better performance for the EAs than the PZSIC-SCAN. We note that although the ΔSCF approach yields positive EAs for the DFAs, the eigenvalue corresponding to the added electron becomes positive in all DFA anion calculations, indicating that the extra

electron is not actually bound in the complete basis set limit. This problem is due to the incorrect asymptotic form of the potential in the DFA calculations. SIC fixes this [9], leading to bound states for the HOO in the anions. As mentioned in the Introduction, the OSIC has an undesirable effect on the asymptotic potential. In OSIC, the correct $-1/r$ behavior of asymptotic potential in PZSIC is replaced by $-X_{HO}/r$, where X_{HO} is the scaling factor for the electronic shell to which HOO belongs. In Fig. 3.4, we compared the HOO eigenvalues for PZSIC and OSIC calculations along with the experimental electron affinity. PZSIC gives negative HOO eigenvalues for all systems, indicating that the HOO electrons are bound to those atoms. It is evident from Fig. 3.4 that the absolute HOO eigenvalue in PZSIC overestimates the electron affinity. Applying OSIC shifts the eigenvalues upward. This upward shift for $k = 1$ reduces the overestimation of absolute HOO as seen in PZSIC and brings it closer to the experimental electron affinities. However, the shift systemically increases with the scaling factor as k increases. As a consequence, the sign of the eigenvalue eventually changes for some systems and the electron in HOO becomes unbound as the asymptotic potential becomes too shallow to provide sufficient attractive potential for the electron. This behavior was not noted earlier in the OSIC calculations of Vydrov and co-workers, but it was expected as scaling down SIC by larger factors brings OSIC results closer to those of DFAs. The OSIC with $k = 4$ has a drawback that several atomic anions are unbound in this model. Exceptions are alkali metals and halogens that maintained negative eigenvalues with OSIC unless very large scaling power k is applied. These exceptions occur as halogens have larger electron affinities and because the scaled down factor for the HOO of alkali anions is large (e.g., 0.83 for Li- and 0.71 for Na-) even for $k = 4$. For the rest of the atom families, anion HOO eigenvalues become positive with a scaling power of 2–3. This is not too surprising considering OSIC recovers DFA performance in the $k \to \infty$ limit.

Table 3.3. The mean absolute error (in eV) of ΔSCF electron affinities computed in various methods.

	SCAN		PBE[a]	TPSS[a]
Method	12 EAs	20 EAs	12 EAs	12 EAs
DFA[b]	0.115	0.148	0.13	0.05
PZSIC	0.364	0.341	0.57	0.47
OSIC ($k = 1$)	0.198	0.151	0.29	0.24
OSIC ($k = 2$)	0.143	0.128	0.15	0.12
OSIC ($k = 3$)	0.126	0.134	0.10	0.08
OSIC ($k = 4$)	0.125	0.143		
	LSDA			
Method	12 EAs	20 EAs		
LSIC[c]	0.097	0.102		

[a]Reference 30.
[b]DFA results are based on ΔSCF. The eigenvalue of an extra electron becomes positive (see the text for details).
[c]Reference 69.

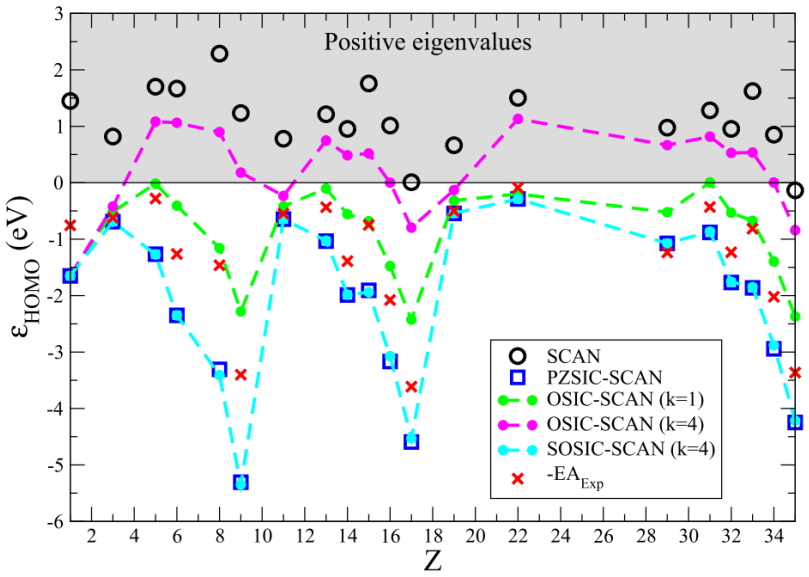

Fig. 3.4. The HOO eigenvalue of 20 atoms within various models along with the negative of experimental EA values (in eV).

3.3.2 ATOMIZATION ENERGIES

The AE6 benchmark set [102] was used to study the performance of the OSIC approach in atomization energies. This set includes six molecules: SiH_4, SiO, S_2, propyne (C_3H_4), glyoxal ($C_2H_2O_2$), and cyclobutane (C_4H_8), and it is a good representation of the larger main group atomization energy (MGAE109) set [103]. The geometries and reference values are obtained at the QCISD/MG3 level of theory. The atomization energy (AE) of a molecule is obtained with

$$AE = \sum_i^N E_i - E_{mol} > 0, \tag{3.9}$$

where E_i is the energy of the atom, E_{mol} is the energy of a given molecule, and N is the number of atoms in the molecule. AEs were compared against the non-spin-orbit coupling reference values reported in Ref. [103]. The results are summarized in Table 3.4. The DFA-SCAN provides quite accurate estimates of AE with an MAE of only 2.85 kcal/mol. However, correcting for SIE worsens AEs. PZSIC-LSDA FODs were used for the MAE reported in Ref. [69]. It is found that relaxation of FODs within PZSIC-SCAN increases the error (MAE 26.52 kcal/mol) using the data extracted from Ref. [79]. We observed that scaling down PZSIC improves the performance as the value of k increases with $k = 4$, yielding the best MAE of 4.10 kcal/mol; although this error is larger in comparison with that of DFA-SCAN, the value is six times smaller compared to the PZSIC-SCAN result. PZSIC-SCAN tends to overestimate total energies, especially for molecules, and this leads to a large discrepancy in atomization energies. Scaling down PZSIC helps reduce the overestimation and improves prediction of atomization energies. This result shows that DFA-SCAN is better for predicting atomization energies without the self-interaction correction. Atomization energy calculations involve equilibrium molecular structure where the SCAN functional performs well.

Table 3.4. The mean absolute and mean absolute percentage errors of AE6 set of molecules in various methods.

	LSDA		SCAN		PBE[a]		TPSS[a]	
Method	MAE (kcal/mol)	MAPE (%)	MAE (kcal/mol)	MAPE (%)	MAE (kcal/mol)	MAPE (%)	MAE (kcal/mol)	MAPE (%)
DFA	74.26 (77.3)[a]	15.93 (17.27)[a]	2.85	1.15	15.5	4.43	5.9	2.43
PZSIC	57.97 (60.3)[a]	9.37 (10.61)[a]	26.52	7.35	17.0	5.54	34.7	9.29
OSIC ($k = 1$)	18.93 (21.0)[a]	3.96 (5.12)[a]	8.67	2.78	12.6	4.21	9.9	4.01
OSIC ($k = 2$)	(8.6)[a]	(3.56)[a]	4.86	2.12	16.0	4.76	11.3	4.09
OSIC ($k = 3$)	(7.2)[a]	(3.41)[a]	4.18	1.93	17.2	5.20	12.4	4.10
OSIC ($k = 4$)			4.10	1.85				
OSIC (z_σ = ELF, $k = 1$)	23.21	4.85	9.04	2.68				
OSIC [$z_\sigma = 1 - (2\beta)^2$, $k = 1$]	11.66	2.92	6.73	2.96				
LSIC[b]	9.95	3.20						

[a]Reference 30.
[b]Reference 69.

3.3.3 REACTION BARRIER HEIGHTS

The BH6 benchmark set [102] was used to study the scaling down performance in the reaction barrier. The BH6 set consists of three hydrogen transfer reactions ($OH + CH_4 \rightarrow CH_3 + H_2O, H + OH \rightarrow O + H_2, and\, H + H_2S \rightarrow H_2 + HS$). Total energies for the leftand right-hand sides and saddle-point of a given reaction formula were calculated, and the barrier heights of forward (f) and reverse (r) reactions were obtained from the energy differences of these three points. Errors are summarized in Table 3.5.

Table 3.5. The mean and mean absolute errors (in kcal/mol) in barrier heights of BH6 set of molecules.

Method	LSDA		SCAN		PBE[a]		TPSS[a]	
	ME	MAE	ME	MAE	ME	MAE	ME	MAE
DFA	−17.62 (−17.9)[a]	17.62 (17.9)[a]	−7.86	7.86	−9.5	9.5	−8.5	8.5
PZSIC	−4.88 (−5.2)[a]	4.88 (5.2)[a]	−0.81	2.96	−0.1	4.2	−0.2	5.7
OSIC ($k = 1$)	−2.95 (−3.2)[a]	3.31 (3.5)[a]	−3.96	3.96	−4.2	4.3	−4.6	5.0
OSIC ($k = 2$)	(−2.8)[a]	(4.7)[a]	−5.45	5.45	−6.5	6.5	−6.8	6.8
OSIC ($k = 3$)	(−2.9)[a]	(5.7)[a]	−6.22	6.22	−7.7	7.7	−7.9	7.9
OSIC ($k = 4$)			−6.66	6.66				
SOSIC ($k = 4$)[b]			−0.75	1.92				
OSIC (z_σ = ELF, $k = 1$)	−3.08	3.15	−4.25	4.25				
OSIC [$z_\sigma = 1 - (2\beta)^2$, $k = 1$]	−1.88	2.28	−4.87	4.87				
LSIC[c]	0.7	1.3						

[a]Reference 30.
[b]Full PZSIC was applied on H-transfer FLOs (see the text for details.).
[c]Reference 69.

Many DFA functionals including SCAN do not give a correct picture of the chemical reaction because in most cases, the saddle point energies are underestimated. These are the cases where self-interaction correction becomes important. From Table 3.5, it can be seen that PZSIC corrects the shortcoming of DFA in this situation. The full SIC treatment with $k = 0$ reduces both ME and MAE. When orbital scaling is applied to PZSIC, i.e., OSIC with $k = 1$, the MAE increases to 3.96 kcal/mol from the PZSIC's 2.96 kcal/mol. The MAE systematically increases with higher powers of the scaling factor. In all cases of OSIC, the reaction barriers are underestimated for all six reactions as can be seen from the MEs and MAEs in Table 3.5. For the saddle-point calculations with stretched bonds, one needs full SIC correction. The increase in the value of k results in larger percent of SIC correction being scaled down, which leads to poor estimates of barrier heights. Note that for $k = 4$, the error is comparable to the DFA error. A further discussion is presented in Sec. 3.5.

3.3.4 SIE BENCHMARK SETS

The SIE11 sets consist of five cationic and six neutral chemical reactions that are very sensitive to self-interaction errors [104]. The SIE4×4 sets consist of dissociation energy

calculations of positively charged dimers at four different distances R from their equilibrium distances Re: $R/Re = 1.0$, 1.25, 1.5, and 1.75 Ref. [105]. Reaction energies for SIE11 and dissociation energies for SIE4×4 were computed and compared against the reference values. The dissociation energies and reaction energies are obtained from the energy difference between left- and right-hand sides of a given chemical reaction formula. The reference values provided in Ref. [104] obtained at the coupled-cluster single double and perturbative triple [CCSD(T)]/CBS level of theory are used for comparison with our values. The results are presented in Table 3.6.

Table 3.6. The mean absolute error (in kcal/mol) of SIE4 × 4 and SIE11 sets of molecules.

Method	SIE4 × 4	SIE11	SIE11, 5 cationic	SIE11, 6 neutral
SCAN	17.9	10.1	10.4	9.9
PZSIC-SCAN	2.2	5.7	5.1	6.2
OSIC-SCAN ($k = 1$)	2.9	14.7	6.5	21.5
OSIC-SCAN ($k = 2$)	5.2	13.4	7.6	18.2
OSIC-SCAN ($k = 3$)	6.5	7.4	7.7	7.0
OSIC-SCAN ($k = 4$)	7.4	8.5	7.7	9.2
OSIC-LSDA ($z_\sigma = \tau^W/\tau, k = 1$)	4.7	15.4	9.4	20.4
OSIC-LSDA (z_σ = ELF, $k = 1$)	7.3	18.0	11.8	23.1
OSIC-LSDA [$z_\sigma = 1 - (2\beta)^2, k = 1$]	4.6	5.9	5.0	6.7
OSIC-SCAN (z_σ = ELF, $k = 1$)	5.0	7.3	6.4	7.9
OSIC-SCAN [$z_\sigma = 1 - (2\beta)^2, k = 1$]	4.5	15.3	9.6	20.1
LSIC-LSDA[a]	2.6	4.5	2.3	6.3

[a]Reference 69.

From SCAN to PZSIC-SCAN, there is a substantial decrease in errors: for SIE4×4, the MAE is decreased from 17.9 kcal/mol to 2.2 kcal/mol. Similar performance improvements are also seen in the SIE11 test set where the MAEs decrease from 10.4 kcal/mol to 5.1 kcal/mol for the cationic reactions and from 9.9 kcal/mol to 6.2 kcal/mol for the neutral reactions. On the other hand, all of the OSIC results show larger errors compared to PZSIC-SCAN. Especially, for SIE4×4 and SIE11 cationic reactions, larger MAEs are seen for higher k. For the SIE11 neutral systems, however, the error decreases for larger values of k although it is still larger than that of the PZSIC-SCAN. In

our previous study [69], we used a pointwise local scaling approach on PZSIC-LSDA for the SIE sets. We found MAEs of 2.6 kcal/mol, 2.31 kcal/mol, and 6.31 kcal/mol for SIE4×4, SIE11 cationic, and SIE11 neutral reactions, respectively. In all three cases, deviations were decreased from PZSIC-LSDA. In contrast, our OSIC results in Table 3.6 show an increase in errors going from PZSIC-SCAN to OSIC-SCAN. We find that orbital scaling does not perform well for the SIE4×4 and SIE11 calculations, while LSIC [69], which is an interior scaling approach, does not experience the same performance degradation. The ideas to improve upon these shortcomings are discussed in Sec. 3.5.

3.4 PERFORMANCE OF DIFFERENT SCALLING FACTORS

In Table 3.1, we compare the results of OSIC-LSDA with different iso-orbital indicators. For this comparison, we used $k = 1$. We used ELF and $1 - (2\beta)^2$ as alternatives for the scaling factor in OSIC. We investigated the effect of these scaling factors in OSIC-LSDA and OSIC-SCAN on four different properties: total energies of atoms, atomization energies (AE6), barrier heights (BH6), and SIE sets of reactions. With OSIC-LSDA, $1 - (2\beta)^2$ produces a larger MAE of 0.062 hartree in the total energies of atoms compared to ELF (0.037 hartree) and τ^W/τ (0.035 hartree). However, for the other properties, $1 - (2\beta)^2$ shows better performance than the others. For atomization energies, the factor $1 - (2\beta)^2$ yields an MAE of 11.7 kcal/mol compared to the MAE of 23.2 kcal/mol and 18.9 kcal/mol for ELF and τ^W/τ, respectively. Similarly, for barrier heights, $1 - (2\beta)^2$ (MAE of 2.3 kcal/mol) shows better performance than ELF (MAE of 3.2 kcal/mol) and τ^W/τ (MAE of 3.3 kcal/mol). A large difference can be seen for SIE11 where MAE is 5.9 kcal/mol for $1 - (2\beta)^2$. This is almost half of PZSIC-LSDA MAE of 11.7 kcal/mol, whereas the other two scaling factors show larger error than PZSIC-LSDA.

In addition to OSIC-LSDA, we also studied the effect of alternative scaling factors with OSIC-SCAN. For OSIC-SCAN, all three scaling factors have comparable performance in atomic total energies, AE6, and BH6. There are some differences for the SIE sets where ELF is similar to τ^W/τ ($k = 3$) and $1 - (2\beta)^2$ is similar to τ^W/τ ($k = 2$) in performance. Overall, the performance of PZSIC is best for the SIE sets of reactions.

3.5 DISCUSSION AND IMPROVEMENTS TO THE OSIC

Applications of OSIC in the present work to the SCAN functional show that the OSIC can overcome the worsening effects of the PZSIC results for equilibrium properties such as atomization energies or total energies if higher values of k are used. For example, OSIC-SCAN with $k = 4$ gives good total energies and atomization energies. On the other hand, the OSIC-SCAN with the same $k = 4$ results in deterioration of barrier heights or dissociation energies where the bonds are stretched. In this case, unscaled PZSIC (OSIC with $k = 0$) works better than all scaled down PZSIC studied herein. Thus, no single value of k is sufficient to obtain good results for all properties. These results are consistent with earlier scaled down PZSIC calculations of Vydrov and co-workers. The explanation as to why PZSIC does not perform well for semi-local functionals has been understood in terms of the orbital densities. It was shown that noded orbital densities produce large errors when used to estimate the self-interaction correction using the Perdew–Zunger method [30,106]. It was found that these errors can be reduced but not eliminated using nodeless densities of complex orbitals. Another source of error in PZSIC is that its application to a semilocal functional causes appropriate norm that are built in to the functional to be violated [107]. With OSIC, the loss of the uniform electron gas limit depends on the form of the scaling factor used to identify the many-electron region. As discussed in Sec. 3.2, except for the ELF scaling factor used in this work, the OSIC has the correct uniform electron gas limit. The OSIC approach shows behavior that is opposite to the paradoxical behavior of the original PZSIC. It improves some properties (equilibrium properties) at the cost of worsening the barrier heights where the bonds are stretched. The recent interior local scaling LSIC approach that corrects for the self-interaction in the single-orbital region by scaling energy densities does not suffer from such conflicting behavior [69]. The OSIC thus has limited usefulness over PZSIC unless the property dependent choice of k (powers of scaling factor) is made. The external scaling form of OSIC [Eq. (3.4)] offers unique ways to apply the SIC [Eq. (3.7)]. For example, the paradoxical behavior of OSIC can be mitigated by selectively applying the orbital scaling factor used in each local orbital. That is, one can apply the scaling with $k = 4$ for most orbitals (core and part of valence states) and keep the full PZSIC correction for the orbitals that require full SIC treatment. We considered a few cases to demonstrate the potential of this approach, which are discussed below.

3.5.1 HOO EIGENVALUES

One known shortcoming of orbital scaling is that the magnitude of the highest occupied eigenvalues (ϵ_{HO}) becomes underestimated. In exact DFT, the highest occupied eigenvalue equals the negative of the ionization potential [108-112]. This relationship does not strictly hold for approximate density functionals, and in most DFAs, the absolute value of the HOO eigenvalue substantially underestimates the first ionization potential due to SIE. In Table 3.7, we compared MAEs of the HOO eigenvalues of atoms $Z = 1-36$ against the experimental IPs [101] using several different methods. PZSIC shows the smallest MAE of 0.606 eV as expected from the PZSIC's correct asymptotic potential shape, and the OSIC (scaled down PZSIC with $k > 0$) generally shows larger deviations. This arises due to scaling down the correction for the highest occupied orbital. The correct asymptotic behavior can be preserved if Eq. (3.7) is used instead of Eq. (3.4). To illustrate this, we applied the orbital scaling to PZSIC, except for the local orbitals on the electron shell that belong to the outermost electrons. The full PZSIC is used for these outermost orbitals. A comparison of the HOO eigenvalues of atoms so obtained are compared against experimental IPs [101] for a smaller subset of atoms with $Z = 1-18$ presented in Fig. 3.5. For this set, the OSIC with $k = 4$ has an MAE of 2.414 eV, which is significantly larger compared to that of the PZSIC (MAE of 0.763 eV). On the other hand, SOSIC has an MAE of only 0.754 eV, which shows that SOSIC can provide the $-\epsilon_{HO}$ of the same quality as the PZSIC. It is interesting to see how the SOSIC affects total energies. We have shown this for atoms in Fig. 3.3 [SOSIC-SCAN ($k = 4$)]. Since orbitals other than those belonging to the HOO shell are scaled, the total energy in SOSIC would lie between OSIC $k = 4$ and PZSIC total energies. Thus, lighter atoms for which most of the orbitals belong to the HOO shell have total energies closer to PZSIC. For benefiting both accuracy of PZSIC's $-\epsilon_{HO}$ and improved total energies from the orbital scaling, the best case is when a small fraction of local orbitals is mapped to HOO and is treated with full PZSIC. This is the case for the alkali metal atoms. In the worst case, SOSIC recovers the PZSIC energies. Halogens and noble gas atoms are the examples of such cases (see Fig. 3.3).

Table 3.7. The mean absolute errors (in eV) in the highest occupied eigenvalues ($-\epsilon_{HO}$) for atoms hydrogen through argon and hydrogen through krypton.

Method	Z = 1–18 MAE	Z = 1–36 MAE
SCAN	4.549	3.880
PZSIC-SCAN	0.763	0.606
OSIC-SCAN (k = 1)	1.051	1.045
OSIC-SCAN (k = 2)	1.750	1.644
OSIC-SCAN (k = 3)	2.151	1.981
OSIC-SCAN (k = 4)	2.414	2.205
SOSIC-SCAN (k = 4)	0.754	

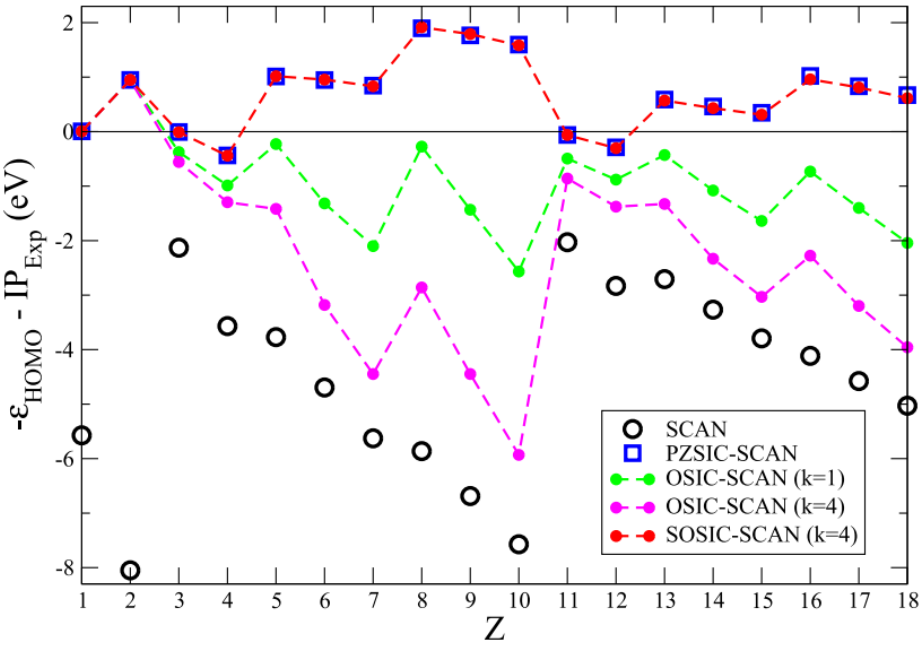

Fig. 3.5. The difference in HOO eigenvalue of atoms Z = 1–18 with respect to experimental IP (in eV). Note that, unlike OSIC eigenvalues, SOSIC eigenvalues closely mimic PZSIC eigenvalues.

3.5.2 BARRIER HEIGHT

Barrier height is another property that can benefit from selective scaling in OSIC. From Sec. 3.3, we know that OSIC with $k = 4$ gives good atomization energies but poor barrier heights. The calculations of saddle points with stretched bonds are responsible for the increased discrepancies in the BH6 benchmark result. To see if barrier height estimates can be improved using selective scaling, we calculated the BH6 barrier heights using the following approach. Since we know that exterior scaling works well for the local orbitals in an equilibrium state, we applied the scaled down PZSIC ($k = 4$) for these orbitals while using full PZSIC for the orbital corresponding to the hydrogen transfer. With this selective scaling, we obtained an MAE of 1.92 kcal/mol and ME of -0.75 kcal/mol. Curiously, this error is even smaller than the MAE of 2.96 kcal/mol with PZSIC. This finding suggests that good results for barrier height calculation using the OSIC method can be achieved if scaling factors for certain orbitals are chosen according to the characteristics of orbitals as the spirit of SOSIC.

Finally, we comment on the possible effect of SOSIC on the dissociation energy curves. As mentioned in the Introduction, Ruzsinszky and co-workers have studied the dissociation energy curves of H_2^+ , He_2^+ , LiH^+, and Ne_2^+ using OSIC and have noted that unlike PZSIC, OSIC does not provide qualitatively correct curves for all four systems [74]. The SOSIC may correct this failure of OSIC as it provides the correct asymptotic description of the potential. Our attempts to compute the dissociation curves for LiH^+, and Ne_2^+ were not successful due to difficulties in obtaining convergence in the far stretched regime using the Jacobi scheme of Ref. [98]. A new method with a single SIC Hamiltonian is being developed [113], which shows promise in handling dissociating fractions with correct charge. We will study dissociation with SOSIC in the future.

3.6 CONCLUSIONS

We have implemented the orbitalwise scaling down of PZSIC using the FLOSIC methodology. The OSIC method is used in combination with the SCAN meta-GGA functional to assess its performance for a wide array of properties—for atoms: total energies, ionization potential, electron affinities, and for molecules: atomization energies, reaction barrier heights, and

dissociation energies. We find that for equilibrium properties, the OSIC with $k = 4$ works well, and it recovers the performance of the uncorrected SCAN. For non-equilibrium properties, we observed that full PZSIC treatment is necessary in many situations. The comparison of present OSIC-SCAN results with earlier reported OSIC-PBE and OSIC-TPSS meta-GGA [30] indicates superior performance of OSIC-SCAN over the OSIC-PBE and OSIC-TPSS. We also show that by selectively scaling down and applying full PZSIC correction on active or outermost orbitals, the inconsistencies of OSIC can be mitigated or eliminated and its performance can be improved beyond equilibrium properties. Thus, the selective scaling down approach presented here can provide a good description of equilibrium properties, estimates of ionization energies from the HOO eigenvalues, stable atomic anions, and reaction barrier heights. The SOSIC thus provides major improvement over the OSIC formalism. It is interesting to compare the SOSIC approach with the LSIC method that we recently proposed [69]. The LSIC method removes the self-interaction selectively in the spatial region where the correction is necessary and resolves the paradoxical behavior of PZSIC. It provides good results for both equilibrium properties and for properties where bonds are stretched. The SOSIC approach, though not as elegant as LSIC [69], accomplishes this goal by choosing the scaling factors according to the characteristic of orbitals. We hope that the present results along with our recent results [69,79] provide a more sanguine future of SIC-DFA that has broader applicability than the standard DFAs.

3.7 ACKNOWLEDGMENTS

The authors acknowledge Professors Koblar Jackson, Adrienn Ruzsinszky, Mark Pederson, and John Perdew for comments on the manuscript. Discussions with Mr. Carlos Diaz and Dr. Luis Basurto are gratefully acknowledged. R.R.Z. is grateful to Prof. Rajeev K. Pathak for introducing him to self-interaction-corrected density functional theory. This work was supported by the U.S. Department of Energy, Office of Science, Office of Basic Energy Sciences, as part of the Computational Chemical Sciences Program under Award No. DE-SC0018331. Support for computational time at the Texas Advanced Computing Center through NSF Grant No. TG-DMR090071 and at NERSC is gratefully acknowledged.

REFERENCES

[1] W. Kohn and L. J. Sham, "Self-consistent equations including exchange and correlation effects," Phys. Rev. 140, A1133 (1965).

[2] P. Hohenberg and W. Kohn, "Inhomogeneous electron gas," Phys. Rev. 136, B864 (1964).

[3] J. P. Perdew and K. Schmidt, "Jacob's ladder of density functional approximations for the exchange-correlation energy," AIP Conf. Proc. 577, 1–20 (2001).

[4] J. P. Perdew and Y. Wang, "Accurate and simple analytic representation of the electron-gas correlation energy," Phys. Rev. B 45, 13244 (1992).

[5] J. P. Perdew, K. Burke, and M. Ernzerhof, "Generalized gradient approximation made simple," Phys. Rev. Lett. 77, 3865 (1996).

[6] J. P. Perdew, K. Burke, and M. Ernzerhof, "Generalized gradient approximation made simple [Phys. Rev. Lett. 77, 3865 (1996)]," Phys. Rev. Lett. 78, 1396 (1997).

[7] A. D. Becke, "A new mixing of Hartree-Fock and local density-functional theories," J. Chem. Phys. 98, 1372 (1993).

[8] J. Gräfenstein, E. Kraka, and D. Cremer, "The impact of the self-interaction error on the density functional theory description of dissociating radical cations: Ionic and covalent dissociation limits," J. Chem. Phys. 120, 524 (2004).

[9] J. P. Perdew and A. Zunger, "Self-interaction correction to density-functional approximations for many-electron systems," Phys. Rev. B 23, 5048 (1981).

[10] Y. Zhang and W. Yang, "A challenge for density functionals: Self-interaction error increases for systems with a non-integer number of electrons," J. Chem. Phys. 109, 2604 (1998).

[11] A. J. Cohen, P. Mori-Sánchez, and W. Yang, "Development of exchange-correlation functionals with minimal many-electron self-interaction error," J. Chem. Phys. 126, 191109 (2007).

[12] D. S. Ranasinghe, J. T. Margraf, Y. Jin, and R. J. Bartlett, "Does the ionization potential condition employed in QTP functionals mitigate the self-interaction error?," J. Chem. Phys. 146, 034102 (2017).

[13] P. Klüpfel, P. M. Dinh, P.-G. Reinhard, and E. Suraud, "Koopmans' condition in self-interaction-corrected density-functional theory," Phys. Rev. A 88, 052501 (2013).

[14] N. I. Gidopoulos and N. N. Lathiotakis, "Constraining density functional approximations to

yield self-interaction free potentials," J. Chem. Phys. 136, 224109 (2012).
[15] R. A. Heaton, J. G. Harrison, and C. C. Lin, "Self-interaction correction for density-functional theory of electronic energy bands of solids," Phys. Rev. B 28, 5992 (1983).
[16] M. R. Pederson, R. A. Heaton, and C. C. Lin, "Local-density Hartree-Fock theory of electronic states of molecules with self-interaction correction," J. Chem. Phys. 80, 1972 (1984).
[17] M. R. Pederson, R. A. Heaton, and C. C. Lin, "Density-functional theory with self-interaction correction: Application to the lithium molecule," J. Chem. Phys. 82, 2688 (1985).
[18] J. Garza, J. A. Nichols, and D. A. Dixon, "The optimized effective potential and the self-interaction correction in density functional theory: Application to molecules," J. Chem. Phys. 112, 7880 (2000).
[19] J. Garza, R. Vargas, J. A. Nichols, and D. A. Dixon, "Orbital energy analysis with respect to LDA and self-interaction corrected exchange-only potentials," J. Chem. Phys. 114, 639 (2001).
[20] S. Patchkovskii, J. Autschbach, and T. Ziegler, "Curing difficult cases in magnetic properties prediction with self-interaction corrected density functional theory," J. Chem. Phys. 115, 26 (2001).
[21] M. K. Harbola, "Theoretical investigation of the polarizability of small metal clusters," Solid State Commun. 98, 629 (1996).
[22] S. Patchkovskii and T. Ziegler, "Improving difficult reaction barriers with self-interaction corrected density functional theory," J. Chem. Phys. 116, 7806 (2002).
[23] S. Patchkovskii and T. Ziegler, "Phosphorus NMR chemical shifts with self-interaction free, gradient-corrected DFT," J. Phys. Chem. A 106, 1088 (2002).
[24] S. Goedecker and C. J. Umrigar, "Critical assessment of the self-interaction corrected–local-density-functional method and its algorithmic implementation," Phys. Rev. A 55, 1765 (1997).
[25] V. Polo, E. Kraka, and D. Cremer, "Electron correlation and the self-interaction error of density functional theory," Mol. Phys. 100, 1771 (2002).
[26] V. Polo, J. Gräfenstein, E. Kraka, and D. Cremer, "Long-range and short-range Coulomb correlation effects as simulated by Hartree–Fock, local density approximation, and generalized gradient approximation exchange functionals," Theor. Chim. Acta 109, 22 (2003).
[27] J. Gräfenstein, E. Kraka, and D. Cremer, "Effect of the self-interaction error for three-electron bonds: On the development of new exchange-correlation functionals," Phys. Chem. Chem. Phys. 6, 1096 (2004).

[28] O. A. Vydrov and G. E. Scuseria, “Effect of the Perdew-Zunger self-interaction correction on the thermochemical performance of approximate density functionals,” J. Chem. Phys. 121, 8187 (2004).
[29] O. A. Vydrov and G. E. Scuseria, “Ionization potentials and electron affinities in the Perdew-Zunger self-interaction corrected density-functional theory,” J. Chem. Phys. 122, 184107 (2005).
[30] O. A. Vydrov, G. E. Scuseria, J. P. Perdew, A. Ruzsinszky, and G. I. Csonka, “Scaling down the Perdew-Zunger self-interaction correction in many-electron regions,” J. Chem. Phys. 124, 094108 (2006).
[31] R. R. Zope, M. K. Harbola, and R. K. Pathak, “Atomic Compton profiles within different exchange-only theories,” Eur. Phys. J. D 7, 151 (1999).
[32] O. A. Vydrov and G. E. Scuseria, “A simple method to selectively scale down the self-interaction correction,” J. Chem. Phys. 124, 191101 (2006).
[33] T. Tsuneda, M. Kamiya, and K. Hirao, “Regional self-interaction correction of density functional theory,” J. Chem. Phys. 24, 1592 (2003).
[34] J. B. Krieger, Y. Li, and G. J. Iafrate, “Construction and application of an accurate local spin-polarized Kohn-Sham potential with integer discontinuity: Exchange-only theory,” Phys. Rev. A 45, 101 (1992).
[35] J. B. Krieger, Y. Li, and G. J. Iafrate, “Systematic approximations to the optimized effective potential: Application to orbital-density-functional theory,” Phys.Rev. A 46, 5453 (1992).
[36] U. Lundin and O. Eriksson, “Novel method of self-interaction corrections in density functional calculations,” Int. J. Quantum Chem. 81, 247 (2001).
[37] Y. Li, J. B. Krieger, and G. J. Iafrate, “Self-consistent calculations of atomic properties using self-interaction-free exchange-only Kohn-Sham potentials,” Phys. Rev. A 47, 165 (1993).
[38] S. Lehtola, M. Head-Gordon, and H. Jónsson, “Complex orbitals, multiple local minima, and symmetry breaking in Perdew-Zunger self-interaction corrected density functional theory calculations,” J. Chem. Theory Comput. 12, 3195 (2016).
[39] G. I. Csonka and B. G. Johnson, “Inclusion of exact exchange for self-interaction corrected H3 density functional potential energy surface,” Theor. Chim. Acta 99, 158 (1998).
[40] L. Petit, A. Svane, M. Lüders, Z. Szotek, G. Vaitheeswaran, V. Kanchana, and W. M. Temmerman, “Phase transitions in rare earth tellurides under pressure,” J. Phys. Cond. Matter 26, 274213 (2014).

[41] S. Kümmel and L. Kronik, “Orbital-dependent density functionals: Theory and applications,” Rev. Mod. Phys. 80, 3 (2008).
[42] T. Schmidt, E. Kraisler, L. Kronik, and S. Kümmel, “One-electron self-interaction and the asymptotics of the Kohn–Sham potential: An impaired relation,” Phys. Chem. Chem. Phys. 16, 14357 (2014).
[43] D.-y. Kao, M. Pederson, T. Hahn, T. Baruah, S. Liebing, and J. Kortus, “The role of self-interaction corrections, vibrations, and spin-orbit in determining the ground spin state in a simple heme,” Magnetochemistry 3, 31 (2017).
[44] S. Schwalbe, T. Hahn, S. Liebing, K. Trepte, and J. Kortus, “Fermi-Löwdin orbital self-interaction corrected density functional theory: Ionization potentials and enthalpies of formation,” J. Comput. Chem. 39, 2463 (2018).
[45] H. Jónsson, K. Tsemekhman, and E. J. Bylaska, “Accurate self-interaction correction to semilocal density functionals,” in Abstracts of Papers of the American Chemical Society (American Chemical Society, Washington, USA, 2007), Vol. 233, p. 120.
[46] M. M. Rieger and P. Vogl, “Self-interaction corrections in semiconductors,” Phys. Rev. B 52, 16567 (1995).
[47] W. Temmerman, A. Svane, Z. Szotek, H. Winter, and S. Beiden, “On the implementation of the self-interaction corrected local spin density approximation for d-and f-electron systems,” in Electronic Structure and Physical Properties of Solids (Springer, 1999), pp. 286–312.
[48] M. Daene, M. Lueders, A. Ernst, D. Ködderitzsch, W. M. Temmerman, Z. Szotek, and W. Hergert, “Self-interaction correction in multiple scattering theory: Application to transition metal oxides,” J. Phys.: Condens. Matter 21, 045604 (2009).
[49] Z. Szotek, W. M. Temmerman, and H. Winter, “Self-interaction correction of localized bands within the LMTO-ASA band structure method,” Physica B 172, 19 (1991).
[50] J. Messud, P. M. Dinh, P.-G. Reinhard, and E. Suraud, “Time-dependent density-functional theory with a self-interaction correction,” Phys. Rev. Lett. 101, 096404 (2008).
[51] J. Messud, P. M. Dinh, P.-G. Reinhard, and E. Suraud, “Improved slater approximation to SIC–OEP,” Chem. Phys. Lett. 461, 316 (2008).
[52] M. Lundberg and P. E. M. Siegbahn, “Quantifying the effects of the self-interaction error in DFT: When do the delocalized states appear?,” J. Chem. Phys. 122, 224103 (2005).
[53] T. Körzdörfer, M. Mundt, and S. Kümmel, “Electrical response of molecular systems: The

power of self-interaction corrected Kohn-Sham theory," Phys. Rev. Lett. 100, 133004 (2008).
[54] T. Körzdörfer, S. Kümmel, and M. Mundt, "Self-interaction correction and the optimized effective potential," J. Chem. Phys. 129, 014110 (2008).
[55] I. Ciofini, C. Adamo, and H. Chermette, "Self-interaction error in density functional theory: A mean-field correction for molecules and large systems," Chem. Phys. 309, 67 (2005).
[56] T. Baruah, R. R. Zope, A. Kshirsagar, and R. K. Pathak, "Positron binding: A positron-density viewpoint," Phys. Rev. A 50, 2191 (1994).
[57] A. I. Johnson, K. P. K. Withanage, K. Sharkas, Y. Yamamoto, T. Baruah, R. R. Zope, J. E. Peralta, and K. A. Jackson, "The effect of self-interaction error on electrostatic dipoles calculated using density functional theory," J. Chem. Phys. 151, 174106 (2019).
[58] J. Vargas, P. Ufondu, T. Baruah, Y. Yamamoto, K. A. Jackson, and R. R. Zope, "Importance of self-interaction-error removal in density functional calculations on water cluster anions," Phys. Chem. Chem. Phys. 22, 3789 (2020).
[59] K. Trepte, S. Schwalbe, T. Hahn, J. Kortus, D.-Y. Kao, Y. Yamamoto, T. Baruah, R. R. Zope, K. P. K. Withanage, J. E. Peralta, and K. A. Jackson, "Analytic atomic gradients in the Fermi-Löwdin orbital self-interaction correction," J. Comput. Chem. 40, 820 (2019).
[60] K. P. K. Withanage, K. Trepte, J. E. Peralta, T. Baruah, R. Zope, and K. A. Jackson, "On the question of the total energy in the Fermi-Löwdin orbital self-interaction correction method," J. Chem. Theory Comput. 14, 4122 (2018).
[61] M. R. Pederson, T. Baruah, D.-y. Kao, and L. Basurto, "Self-interaction corrections applied to Mg-porphyrin, C60, and pentacene molecules," J. Chem. Phys. 144, 164117 (2016).
[62] S. Schwalbe, L. Fiedler, T. Hahn, K. Trepte, J. Kraus, and J. Kortus, "PyFLOSIC—Python based Fermi-Löwdin orbital self-interaction correction," arXiv:1905.02631 [physics.comp-ph] (2019).
[63] D.-y. Kao, K. Withanage, T. Hahn, J. Batool, J. Kortus, and K. Jackson, "Self-consistent self-interaction corrected density functional theory calculations for atoms using Fermi-Löwdin orbitals: Optimized Fermi-orbital descriptors for Li–Kr," J. Chem. Phys. 147, 164107 (2017).
[64] R. P. Joshi, K. Trepte, K. P. K. Withanage, K. Sharkas, Y. Yamamoto, L. Basurto, R. R. Zope, T. Baruah, K. A. Jackson, and J. E. Peralta, "Fermi-Löwdin orbital self-interaction correction to magnetic exchange couplings," J. Chem. Phys. 149, 164101 (2018).
[65] K. Sharkas, L. Li, K. Trepte, K. P. K. Withanage, R. P. Joshi, R. R. Zope, T. Baruah, J. K.

Johnson, K. A. Jackson, and J. E. Peralta, “Shrinking self-interaction errors with the Fermi–Löwdin orbital self-interaction-corrected density functional approximation,” J. Phys. Chem. A 122, 9307 (2018).
[66] K. A. Jackson, J. E. Peralta, R. P. Joshi, K. P. Withanage, K. Trepte, K. Sharkas, and A. I. Johnson, “Towards efficient density functional theory calculations without self-interaction: The Fermi-Löwdin orbital self-interaction correction,” J. Phys.: Conf. Ser. 1290, 012002 (2019).
[67] K. Sharkas, K. Wagle, B. Santra, S. Akter, R. R. Zope, T. Baruah, K. A. Jackson, J. P. Perdew, and J. E. Peralta, “Self-interaction error overbinds water clusters but cancels in structural energy differences,” Proceedings of the National Academy of Sciences117,11283–11288 (2020), https://www.pnas.org/content/117/21/11283.full.pdf
[68] J. P. Perdew, A. Ruzsinszky, J. Sun, and M. R. Pederson, “Paradox of self-interaction correction: How can anything so right be so wrong?,” in Advances in Atomic, Molecular, and Optical Physics (Academic Press, 2015), Vol. 64, Chap. I, pp. 1–14.
[69] R. R. Zope, Y. Yamamoto, C. M. Diaz, T. Baruah, J. E. Peralta, K. A. Jackson, B. Santra, and J. P. Perdew, “A step in the direction of resolving the paradox of Perdew-Zunger self-interaction correction,” J. Chem. Phys. 151, 214108 (2019).
[70] S. Klüpfel, P. Klüpfel, and H. Jónsson, “The effect of the Perdew-Zunger self-interaction correction to density functionals on the energetics of small molecules,” J. Chem. Phys. 137, 124102 (2012).
[71] J. Tao, J. P. Perdew, V. N. Staroverov, and G. E. Scuseria, “Climbing the density functional ladder: Nonempirical meta–generalized gradient approximation designed for molecules and solids,” Phys. Rev. Lett. 91, 146401 (2003).
[72] C. Adamo and V. Barone, “Toward reliable density functional methods without adjustable parameters: The PBE0 model,” J. Chem. Phys. 110, 6158 (1999).
[73] M. Ernzerhof and G. E. Scuseria, “Assessment of the Perdew-Burke-Ernzerhof exchange-correlation functional,” J. Chem. Phys. 110, 5029 (1999).
[74] A. Ruzsinszky, J. P. Perdew, G. I. Csonka, O. A. Vydrov, and G. E. Scuseria, “Density functionals that are one- and two- are not always many-electron self-interaction-free, as shown for H+ 2 , He+ 2 , LiH+, and Ne+ 2 ,” J. Chem. Phys. 126, 104102 (2007).
[75] J. Sun, A. Ruzsinszky, and J. P. Perdew, “Strongly constrained and appropriately normed semilocal density functional,” Phys. Rev. Lett. 115, 036402 (2015).

[76] Y. Fu and D. J. Singh, "Applicability of the strongly constrained and appropriately normed density functional to transition-metal magnetism," Phys. Rev. Lett. 121, 207201 (2018).
[77] M. Chen, H.-Y. Ko, R. C. Remsing, M. F. C. Andrade, B. Santra, Z. Sun, A. Selloni, R. Car, M. L. Klein, J. P. Perdew et al., "Ab initio theory and modeling of water," Proc. Natl. Acad. Sci. U. S. A. 114, 10846 (2017).
[78] A. Paul, J. Sun, J. P. Perdew, and U. V. Waghmare, "Accuracy of first-principles interatomic interactions and predictions of ferroelectric phase transitions in perovskite oxides: Energy functional and effective Hamiltonian," Phys. Rev. B 95, 054111 (2017).
[79] Y. Yamamoto, C. M. Diaz, L. Basurto, K. A. Jackson, T. Baruah, and R. R. Zope, "Fermi-Löwdin orbital self-interaction correction using the strongly constrained and appropriately normed meta-GGA functional," J. Chem. Phys. 151, 154105 (2019).
[80] M. R. Pederson, A. Ruzsinszky, and J. P. Perdew, "Communication: Self-interaction correction with unitary invariance in density functional theory," J. Chem. Phys. 140, 121103 (2014).
[81] W. L. Luken and D. N. Beratan, "Localized orbitals and the Fermi hole," Theor. Chem. Acc. 61, 265 (1982).
[82] W. L. Luken and J. C. Culberson, "Localized orbitals based on the Fermi hole," Theor. Chem. Acc. 66, 279 (1984).
[83] J. M. Leonard and W. L. Luken, "Quadratically convergent calculation of localized molecular orbitals," Theor. Chem. Acc. 62, 107 (1982).
[84] D. C. Liu and J. Nocedal, "On the limited memory BFGS method for large scale optimization," Math. Program. 45, 503 (1989).
[85] A. D. Becke and K. E. Edgecombe, "A simple measure of electron localization in atomic and molecular systems," J. Chem. Phys. 92, 5397 (1990).
[86] J. W. Furness and J. Sun, "Enhancing the efficiency of density functionals with an improved iso-orbital indicator," Phys. Rev. B 99, 041119 (2019).
[87] R. R. Zope and B. I. Dunlap, "Slater's exchange parameters α for analytic and variational Xα calculations," J. Chem. Theory Comput. 1, 1193 (2005).
[88] E. Livshits and R. Baer, "A well-tempered density functional theory of electrons in molecules," Phys. Chem. Chem. Phys. 9, 2932 (2007).
[89] R. Baer, E. Livshits, and U. Salzner, "Tuned range-separated hybrids in density functional

theory," Annu. Rev. Phys. Chem. 61, 85 (2010).
[90] L. Kronik, T. Stein, S. Refaely-Abramson, and R. Baer, "Excitation gaps of finite sized systems from optimally tuned range-separated hybrid functionals," J. Chem. Theory Comput. 8, 1515 (2012).
[91] M. E. Foster and B. M. Wong, "Nonempirically tuned range-separated DFT accurately predicts both fundamental and excitation gaps in dna and rna nucleobases," J. Chem. Theory Comput. 8, 2682 (2012).
[92] H. Sun and J. Autschbach, "Influence of the delocalization error and applicability of optimal functional tuning in density functional calculations of nonlinear optical properties of organic donor–acceptor chromophores," ChemPhysChem 14, 2450 (2013).
[93] R. R. Zope, T. Baruah, Y. Yamamoto, L. Basurto, C. Diaz, J. Peralta, and K. A. Jackson, FLOSIC 0.1.2, based on the NRLMOL code of M. R. Pederson.
[94] Y. Yamamoto, L. Basurto, C. M. Diaz, R. R. Zope, and T. Baruah, "Self-interaction correction to density functional approximations using Fermi-Löwdin orbitals: Methodology and parallelization" (unpublished).
[95] D. Porezag and M. R. Pederson, "Optimization of Gaussian basis sets for density-functional calculations," Phys. Rev. A 60, 2840 (1999).
[96] M. R. Pederson and K. A. Jackson, "Variational mesh for quantum-mechanical simulations," Phys. Rev. B 41, 7453 (1990).
[97] K. P. K. Withanage, S. Akter, C. Shahi, R. P. Joshi, C. Diaz, Y. Yamamoto, R. Zope, T. Baruah, J. P. Perdew, J. E. Peralta, and K. A. Jackson, "Self-interaction free electric dipole polarizabilities for atoms and their ions using the Fermi-Löwdin self-interaction correction," Phys. Rev. A 100, 012505 (2019).
[98] Z.-h. Yang, M. R. Pederson, and J. P. Perdew, "Full self-consistency in the Fermi-orbital self-interaction correction," Phys. Rev. A 95, 052505 (2017).
[99] S. J. Chakravorty, S. R. Gwaltney, E. R. Davidson, F. A. Parpia, and C. F. Fischer, "Ground-state correlation energies for atomic ions with 3 to 18 electrons," Phys. Rev. A 47, 3649 (1993).
[100] O. Gunnarsson and B. I. Lundqvist, "Exchange and correlation in atoms, molecules, and solids by the spin-density-functional formalism," Phys. Rev. B 13, 4274 (1976).
[101] National Institute of Standards and Technology, NIST Computational Chemistry Comparison and Benchmark Database NIST Standard Reference Database Number 101 Release

19, April 2018, edited by R. D. Johnson III, http://cccbdb.nist.gov/.
[102] B. J. Lynch and D. G. Truhlar, "Small representative benchmarks for thermochemical calculations," J. Phys. Chem. A 107, 8996 (2003).
[103] R. Peverati and D. G. Truhlar, "Communication: A global hybrid generalized gradient approximation to the exchange-correlation functional that satisfies the second-order density-gradient constraint and has broad applicability in chemistry," J. Chem. Phys. 135, 191102 (2011).
[104] L. Goerigk and S. Grimme, "A general database for main group thermochemistry, kinetics, and noncovalent interactions—Assessment of common and reparameterized (meta-)GGA density functionals," J. Chem. Theory Comput. 6, 107 (2010).
[105] L. Goerigk, A. Hansen, C. Bauer, S. Ehrlich, A. Najibi, and S. Grimme, Phys. Chem. Chem. Phys. 19, 32184 (2017).
[106] C. Shahi, P. Bhattarai, K. Wagle, B. Santra, S. Schwalbe, T. Hahn, J. Kortus, K. A. Jackson, J. E. Peralta, K. Trepte, S. Lehtola, N. K. Nepal, H. Myneni, B. Neupane, S. Adhikari, A. Ruzsinszky, Y. Yamamoto, T. Baruah, R. R. Zope, and J. P. Perdew, "Stretched or noded orbital densities and self-interaction correction in density functional theory," J. Chem. Phys. 150, 174102 (2019).
[107] B. Santra and J. P. Perdew, "Perdew-Zunger self-interaction correction: How wrong for uniform densities and large-Z atoms?," J. Chem. Phys. 150, 174106 (2019).
[108] J. P. Perdew, R. G. Parr, M. Levy, and J. L. Balduz, Jr., "Density-functional theory for fractional particle number: Derivative discontinuities of the energy," Phys. Rev. Lett. 49, 1691 (1982).
[109] M. Levy, J. P. Perdew, and V. Sahni, "Exact differential equation for the density and ionization energy of a many-particle system," Phys. Rev. A 30, 2745 (1984).
[110] C.-O. Almbladh and U. von Barth, "Exact results for the charge and spin densities, exchange-correlation potentials, and density-functional eigenvalues," Phys. Rev. B 31, 3231 (1985).
[111] J. P. Perdew and M. Levy, "Comment on "Significance of the highest occupied Kohn-Sham eigenvalue"," Phys. Rev. B 56, 16021 (1997).
[112] M. K. Harbola, "Relationship between the highest occupied Kohn-Sham orbital eigenvalue and ionization energy," Phys. Rev. B 60, 4545 (1999).
[113] M. R. Pederson and T. Baruah, "Single Hamiltonian for self-interaction corrected DFT with Fermi-Löwdin orbitals" (unpublished)

[114] A. Dal Corso, “A pseudopotential plane waves program (pwscf) and some case studies,” in Quantum-Mechanical Ab-initio Calculation of the Properties of Crystalline Materials, edited by C. Pisani (Springer Berlin Heidelberg, Berlin, Heidelberg, 1996) pp. 155–178.
[115] A. Szabo, and N. Ostlund, Modern Quantum Chemistry: Introduction to Advanced Electronic Structure Theory (Macmillan, 1982)
[116] “A brief review of elementary quantum chemistry,” http://vergil.chemistry.gatech.edu/notes/, accessed: 2020-06-24.
[117] John P Perdew, Stefan Kurth, Aleˇs Zupan, and Peter Blaha. “Accurate density functional with correct formal properties: A step beyond the generalized gradient approximation,” Physical review letters, 82(12):2544, 1999.
[118] John P Perdew, Jianmin Tao, Viktor N Staroverov, and Gustavo E Scuseria. ”Meta-generalized gradient approximation: Explanation of a realistic nonempirical density functional,” The Journal of chemical physics, 120(15):6898{6911, 2004.
[119] Adrienn Ruzsinszky, Jianwei Sun, Bing Xiao, and Gbor I. Csonka. “A meta-gga made free of the order of limits anomaly,” Journal of Chemical Theory and Computation, 8(6):2078{2087, 2012. PMID: 26593840.
[120] Jianwei Sun, Bing Xiao, and Adrienn Ruzsinszky. “Communication: Effect of the orbital-overlap dependence in the meta generalized gradient approximation,”2012.
[121] Jianwei Sun, Robin Haunschild, Bing Xiao, Ireneusz W Bulik, Gustavo E Scuseria, and John P Perdew. “Semilocal and hybrid meta-generalized gradient approximations based on the understanding of the kinetic-energy-density dependence,” The Journal of chemical physics, 138(4):044113, 2013.
[122] Jianwei Sun, John P Perdew, and Adrienn Ruzsinszky. “Semilocal density functional obeying a strongly tightened bound for exchange,” Proceedings of the National Academy of Sciences, 112(3):685-689, 2015.
[123] Axel D Becke. “Density-functional exchange-energy approximation with correct asymptotic behavior,” Physical review A, 38(6):3098, 1988.
[124] Axel D Becke. “Density functional calculations of molecular bond energies,” The Journal of Chemical Physics, 84(8):4524-4529, 1986.
[125] David C Langreth and MJ Mehl. “Beyond the local-density approximation in calculations of ground-state electronic properties,” Physical Review B, 28(4):1809,

1983.
[126] John P Perdew and Wang Yue. “Accurate and simple density functional for the electronic exchange energy: Generalized gradient approximation,” Physical review B, 33(12):8800, 1986.
[127] Axel D Becke. “Density functional calculations of molecular bond energies,” The Journal of Chemical Physics, 84(8):4524-4529, 1986.
[128] D. M. Ceperley and B. J. Alder, “Ground state of the electron gas by a stochastic method,” Phys. Rev. Lett.45, 566–569 (1980).
[129] C. Kittel, Introduction to Solid State Physics, 6th ed. (John Wiley & Sons, Inc., New York,1986).
[130] F. Giustino: Materials Modeling using Density Functional Theory (Oxford university press,2014).
[131] D. Griffiths: Introduction to quantum mechanics (Prentice Hall, 1995).
[132] P. Hohenberg and W. Kohn, “Inhomogeneous electron gas,” Phys. Rev.136, B864–B871(1964).
[133] R. O. Jones and O. Gunnarsson, “The density functional formalism, its applications and prospects,” Rev. Mod. Phys.61, 689–746 (1989).
[134] R. O. Jones, “Density functional theory: Its origins, rise to prominence, and future,” Rev.Mod. Phys.87, 897 (2015).
[135] Y. Zhao and D. G. Truhlar, “A new local density functional for main-group thermochemistry, transition metal bonding, thermochemical kinetics, and noncovalent interactions,” J.Chem. Phys.125, 194101 (2006), https://doi.org/10.1063/1.2370993.
[136] J. Jaramillo, G. E. Scuseria, and M. Ernzerhof, “Local hybrid functionals,” J. Comp. Phys.118, 1068–1073 (2003).
[137] J. Sun, R. C. Remsing, Y. Zhang, Z. Sun, A. Ruzsinszky, H. Peng, Z. Yang, A. Paul, U. Waghmare, X. Wu, et al., “Accurate first-principles structures and energies of diversely bonded systems from an efficient density functional,” Nat. Chem.8, 831 (2016).
[138] E. R. Johnson, P. Mori-Sánchez, A. J. Cohen, and W. Yang, “Delocalization errors in density functionals and implications for main-group thermochemistry,” The Journal of Chemical Physics129, 204112 (2008), https://doi.org/10.1063/1.3021474.

[139] E. R. Johnson, A. Otero-de-la Roza, and S. G. Dale, "Extreme density-driven delocalization error for a model solvated-electron system," The Journal of Chemical Physics139,184116 (2013), https://doi.org/10.1063/1.4829642.

[140] M. R. Pederson and T. Baruah, "Chapter eight - self-interaction corrections within the fermi-orbital-based formalism," (Academic Press, 2015) pp. 153 – 180.

[141] R. P. Joshi, J. J. Phillips, and J. E. Peralta, "Magnetic exchange couplings in heterodinuclear complexes based on differential local spin rotations," Journal of Chemical Theory and Computation12, 1728–1734 (2016), pMID: 26953521,https://doi.org/10.1021/acs.jctc.6b00112.

[142] R. R. Zope, T. Baruah, and K. A. Jackson, "FLOSIC 0.2," Based on the NRLMOL code of M. R. Pederson.

[143] Y. Yamamoto, S. Romero, T. Baruah, and R. R. Zope, "Improvements in the orbital wise scaling down of Perdew-Zunger self-interaction correction in many-electron regions," The Journal of Chemical Physics152, 174112 (2020), https://doi.org/10.1063/5.0004738.

[144] S. Klüpfel, P. Klüpfel, and H. Jónsson, "Importance of complex orbitals in calculating the self-interaction-corrected ground state of atoms," Phys. Rev. A84, 050501 (2011).

[145] J. P. Perdew, A. Ruzsinszky, J. Sun, and M. R. Pederson, "Chapter one - paradox of self-interaction correction: How can anything so right be so wrong?" in Advances In Atomic, Molecular, and Optical Physics, Vol. 64 (Academic Press, 2015) pp. 1 – 14.

[146] A. Ruzsinszky, J. P. Perdew, G. I. Csonka, O. A. Vydrov, and G. E. Scuseria, "Spurious fractional charge on dissociated atoms: Pervasive and resilient self-interaction error of common density functionals," J. Chem. Phys.125, 194112 (2006),https://doi.org/10.1063/1.2387954.

[147] P. Bhattarai, K. Wagle, C. Shahi, Y. Yamamoto, S. Romero, B. Santra, R. R. Zope, J. E. Peralta, K. A. Jackson, and J. P. Perdew, "A step in the direction of resolving the paradox of perdew–zunger self-interaction correction. ii. gauge consistency of the energy density at three levels of approximation," The Journal of Chemical Physics152, 214109(2020), https://doi.org/10.1063/5.0010375.

[148] O. A. Vydrov and G. E. Scuseria, "A simple method to selectively scale down the self-interaction correction," J. Chem. Phys.124, 191101 (2006),https://doi.org/10.1063/1.2204599.

[149] L. A. Curtiss, K. Raghavachari, G. W. Trucks, and J. A. Pople, "Gaussian-2 theory for molecular energies of first- and second-row compounds," J. Chem. Phys.94, 7221–7230(1991), https://doi.org/10.1063/1.460205.

[150] L. Goerigk, A. Hansen, C. Bauer, S. Ehrlich, A. Najibi, and S. Grimme, "A look at the density functional theory zoo with the advanced GMTKN55 database for general main group thermochemistry, kinetics and noncovalent interactions," Phys. Chem. Chem. Phys.19, 32184–32215 (2017).

[151] A. Ruzsinszky, J. P. Perdew, and G. I. Csonka, "Binding energy curves from nonempirical density functionals. i. covalent bonds in closed-shell and radical molecules," The Journal of Physical Chemistry A109, 11006–11014 (2005), pMID: 16331944,https://doi.org/10.1021/jp0534479.

[152] M. Chen, H.-Y. Ko, R. C. Remsing, M. F. Calegari Andrade, B. Santra, Z. Sun,A. Selloni, R. Car, M. L. Klein, J. P. Perdew, and X. Wu, "Ab initio theoryand modeling of water," Proc. Natl. Acad. Sci. (2017), 10.1073/pnas.1712499114, https://www.pnas.org/content/early/2017/09/19/1712499114.full.pdf.

[153] R. C. Remsing, M. L. Klein, and J. Sun, "Dependence of the structure and dynamics of liquid silicon on the choice of density functional approximation," Phys. Rev. B96, 024203(2017).

[154] Sun, J., Remsing, R., Zhang, Y. et al. "Accurate first-principles structures and energies of diversely bonded systems from an efficient density functional." Nature Chem 8, 831–836 (2016). https://doi.org/10.1038/nchem.2535

APPENDIX

LIST OF PUBLICATIONS

1) Improvements in the orbitalwise scaling down of Perdew–Zunger self-interaction correction in many-electron regions, Yoh Yamamoto, **Selim Romero**, Tunna Baruah, and Rajendra R. Zope,
   J. Chem. Phys. 152, 174112 (2020); https://doi.org/10.1063/5.0004738
2) A step in the direction of resolving the paradox of Perdew–Zunger self-interaction correction. II. Gauge consistency of the energy density at three levels of approximation, P. Bhattarai, Kamal Wagle, Chandra Shahi, Yoh Yamamoto, **Selim Romero,** Biswajit Santra, Rajendra R. Zope, Juan E. Peralta, Koblar A. Jackson, and John P. Perdew,
   J. Chem. Phys. 152, 214109 (2020); https://doi.org/10.1063/5.0010375.
3) *Local self-interaction corrected density functional method with simple scaling factor*, **Selim Romero**, Yoh Yamamoto, Tunna Baruah, and Rajendra R. Zope (to be submitted to J. Chem. Phys.)

Permission of "Improvements in the orbitalwise scaling down of Perdew–Zunger self-interaction correction in many-electron regions"

Dear Dr. Romero:

You are permitted to include your published article in your thesis, provided you also include a credit line referencing the original publication.

Our preferred format is (please fill in the citation information):

"Reproduced from [FULL CITATION], with the permission of AIP Publishing."

If the thesis will be available electronically, please include a link to the version of record on AIP Publishing's site.

Please let us know if you have any questions.

Sincerely,
Susann LoFaso
Manager, Rights & Permissions

AIP Publishing
1305 Walt Whitman Road | Suite 300 | Melville NY 11747-4300 | USA
t +1.516.576.2268
rights@aip.org | publishing.aip.org

VITA

My name is Selim Romero, a UTEP student since 2016, I obtained my M.S. in Physics in 2018 with the work "GEANT4 STUDY OF A GAMMA RAY COLLIMATOR FOR PROTON THERAPY." Currently, I am part of the Computational Science (CPS) Program since August 2018 – present. The work presented here is to accomplish the degree of M.S. in CPS and to obtain my Ph.D. candidacy. This thesis entitled "DEVELOPMENT AND ASSESMENT OF LOCAL SCALED SELF-INTERACTION CORRECTED DENSITY FUNCTIONAL METHOD WITH SIMPLE SCALING FACTOR", presents two papers: "PERFORMANCE OF LOCAL SELF-INTERACTION CORRECTION METHOD WITH SIMPLE SCALING FACTOR" not published yet and "IMPROVEMENTS IN THE ORBITALWISE SCALING DOWN OF PERDEW–ZUNGER SELF-INTERACTION CORRECTION IN MANY-ELECTRON REGIONS" published in the Journal of Chemical Physics. I received my Bachelor of physics (2015) at Autonomous University of Ciudad Juarez, Juarez City, Chihuahua, Mexico. I attended Joint Fall 2017 Meeting of the Texas Section of the APS, Texas Section of the AAPT, and Zone 13 of the Society of Physics Students, The University of Texas Dallas, Richardson, Texas, 21 October 2017. My academic employment was as graduate Teaching Assistant, Department of physics, University of Texas at El Paso, August 2016 to 2019. My responsibilities included: assist professors with the preparation and presentation of material for undergraduate courses, proctoring and tutoring. I am a Research Assistant since 2019 to present working under supervision of Dr. Rajendra Zope.

Contact Information: ssromerogon@miners.utep.edu